

Voltage Coordination in Multi-Area Power Systems
via Distributed Model Predictive Control

Spanningscoördinatie in multi-zone-energienetten
via gedistribueerde modelgebaseerde voorspellende regelaars

Mohammad Moradzadeh

Promotoren: ereprof. dr. ir. R. Boel, prof. dr. ir. L. Vandevelde
Proefschrift ingediend tot het behalen van de graad van
Doctor in de Ingenieurswetenschappen: Elektrotechniek

Vakgroep Elektrische Energie, Systemen en Automatisering
Voorzitter: prof. dr. ir. J. Melkebeek
Faculteit Ingenieurswetenschappen en Architectuur
Academiejaar 2012 - 2013



ISBN 978-90-8578-567-5
NUR 959
Wettelijk depot: D/2012/10.500/93

Acknowledgements

I take this opportunity to express my profound sense of gratitude to all those who helped me throughout my PhD studies over the last four years.

First and foremost, I would like to sincerely thank my promotor prof. René Boel for providing me with the great opportunity to perform my doctoral studies in SYSTeMS research group, department of Electrical Energy, Systems and Automation (EESA) in University of Ghent (UGent). This work certainly would not have been possible without his careful guidance, encouragement, great understanding, and most importantly his friendship. He encouraged me to not only grow as power-control engineer but also as an independent intellectual thinker.

I am heartily grateful to my (co)promoter prof. Lieven Vandeveldel for his inspiring discussions and continuous support. His insights to power system dynamics and stability is second to none. I appreciate the freedom I was given by him in pursuing my own choices in the research.

I am particularly grateful to all jury members for their rigorous reading and constructive comments to further improve this dissertation.

I especially wish to thank prof. Dirk Aeyels and prof. Gert de Cooman for their competent support and invaluable advices during the tough moments of the duration of this dissertation. I very much appreciate prof. Mia Loccufier for her attentiveness and careful advices for my post doctoral careers.

My sincere appreciation goes to prof. Jan H. van Schuppen from whom I have learnt a lot about coordination control, control of hybrid and discrete-event systems in the framework of two EU FP7 projects namely C4C and DISC.

I was given the opportunity to serve as a mentor to two students, Varun and Lokesh, for their BSc internship. Undoubtedly working with them was enjoyable and fruitful. Many thanks also go to ir. Fortunato Villella from Tractebel Engineering for some inspiring discussions on modeling issues.

I am indebted to all those many colleagues and visitors of the SYSTeMS research group who created a pleasant and enjoyable atmosphere, that made it for four years my home far away from my home in Iran. I especially thank Erik, for always staying helpful for me when dealing with annoying computer issues, and for his brilliant \LaTeX advices.

Last but certainly not least, I would like to thank my family, particularly my parents, for always standing by my side, being a constant source of unwavering love and support. Without them, I would never have gotten to where I am today.

Ghent, December 2012
Mohammad Moradzadeh

Table of Contents

List of Figures	vii
List of Tables	ix
List of Acronyms	xi
Nederlandse samenvatting	xiii
English summary	xvii
1 Introduction	1-1
1.1 Classification of power system stability	1-3
1.1.1 Rotor angle stability	1-4
1.1.2 Frequency stability	1-4
1.1.3 Voltage stability	1-4
1.1.3.1 Voltage stability of a simple ∞ -bus and isolated- load system	1-5
1.1.3.2 Short-term versus long-term voltage instability .	1-8
1.1.3.3 Normal and emergency voltage control	1-8
1.1.3.4 Countermeasures against voltage instability . . .	1-9
1.1.3.5 Hierarchical voltage control	1-11
1.1.3.6 Steady-state and dynamic voltage instability analy- sis	1-12
1.2 Steady-state voltage stability analysis	1-13
1.2.1 PV curve	1-14
1.2.2 VQ curve	1-15
1.3 Historical review of notable voltage instability incidents	1-15
1.4 Research motivation	1-17
1.4.1 Hybrid modeling framework	1-17
1.4.2 Real-time communication-based voltage controller	1-19
1.5 Thesis outline	1-21
1.6 List of publications	1-23

2	Modeling and simulation	2-1
2.1	Introduction	2-1
2.2	Modelica [®] and Dymola	2-1
2.2.1	Acausal modeling	2-2
2.2.2	Hybrid modeling	2-3
2.3	Hybrid automaton (HA)	2-4
2.4	Hybrid automaton component models for power system	2-5
2.4.1	∞ -bus	2-6
2.4.2	Transmission line	2-6
2.4.3	Capacitor bank (CB)	2-6
2.4.4	Synchronous generator equipped with AVR and OXL	2-6
2.4.5	LTC	2-10
2.4.6	Load	2-11
2.4.6.1	Static load models	2-12
2.4.6.2	Dynamic load models	2-13
2.5	Conclusions	2-14
3	The need for coordination	3-1
3.1	Introduction	3-1
3.2	Example illustrating the need for coordination	3-3
3.3	Trial and error coordination	3-3
3.3.1	Case study 1	3-4
3.3.1.1	Uncoordinated deadband control	3-5
3.3.1.2	CB switching	3-6
3.3.1.3	Load shedding	3-6
3.3.1.4	Coordinated action of LTC and CB	3-7
3.3.2	Case study 2	3-8
3.3.2.1	Uncoordinated deadband control	3-10
3.3.2.2	LTC setpoint reduction	3-10
3.3.2.3	A coordinated application of (one step) CB switching, LTC setpoint reduction and (one step) load shedding	3-10
3.4	Main trends in development of coordination schemes	3-13
3.4.1	Centralized coordination schemes	3-13
3.4.2	Decentralized schemes (no coordination)	3-15
3.4.3	Distributed coordination schemes	3-15
3.5	Measurements and communication	3-16
3.6	Abstraction	3-17
3.6.1	Reduction-based approaches	3-19
3.6.2	Identification-based approaches	3-19
3.7	Conclusions	3-20

4	Distributed neighbor-to-neighbor coordination control	4-1
4.1	Introduction	4-1
4.2	Model Predictive Control (MPC)	4-2
4.3	Networks of MPC-based voltage controllers	4-4
4.3.1	Decentralized MPC	4-5
4.3.2	Centralized MPC	4-5
4.4	Distributed Communication-based Model Predictive Control (DCMPC)	4-6
4.4.1	Basic assumptions	4-7
4.4.2	Decomposition criterion	4-8
4.4.3	Modeling framework	4-10
4.4.4	Notation	4-11
4.4.5	Principle of the proposed coordination scheme	4-11
4.4.6	Control problem formulation	4-13
4.4.7	Optimization algorithm	4-14
4.4.8	On the choice of signal to communicate	4-15
4.5	Conclusions	4-17
5	Simulation Results	5-1
5.1	ABB 12-bus test system	5-1
5.1.1	Case 1: response with the decentralized deadband control	5-2
5.1.2	Case 1: response with the DCMPC	5-3
5.1.3	Case 2: response with the decentralized deadband control	5-4
5.1.4	Case 2: response with the DCMPC	5-5
5.2	Nordic32 test system	5-6
5.2.1	Case 1: Outage of Line 4032-4044	5-8
5.2.2	Case 2: Outage of Line 4011-4021	5-16
5.2.3	Computational Burden	5-16
5.2.4	Robustness analysis	5-22
5.3	Conclusions	5-25
6	Conclusions and future work	6-1
6.1	Future work	6-3
6.1.1	Extension of the DCMPC	6-3
6.1.2	Application to microgrids	6-4
6.1.3	Towards the practical implementation	6-5
A	Steady-state voltage characteristic of a synchronous generator	A-1
B	An example of Modelica code	B-1
	Bibliography	C-1

List of Figures

1.1	A traditional power system	1-2
1.2	A simple 2-bus power system	1-6
1.3	The PQV surface	1-7
1.4	Different voltage control regimes associated with different operating states	1-10
1.5	A generic hierarchical voltage control structure	1-11
1.6	The PV curves	1-14
1.7	The VQ curve	1-15
2.1	A simple hybrid automaton	2-5
2.2	S_{OXL} : An HA representation of an OXL with inverse-time delay S_a and integral action S_b	2-7
2.3	S_{ACL} : An HA representation of a simple ACL with fixed $I_{\text{arm}(\text{lim})}$ and fixed T_{arm}	2-8
2.4	$S_{\text{LTC-DB}}$: An HA representation of an LTC in the classical uncoordinated fashion	2-12
2.5	$S_{\text{LTC-C}}$: An HA representation of an LTC in the distributed operation fashion	2-12
3.1	On-line diagram of a 12-bus power system	3-3
3.2	Bus voltages and the corresponding LTC actions	3-4
3.3	Case study 1: one-line diagram of a 4-bus power system	3-5
3.4	Case study 1: uncoordinated deadband control	3-6
3.5	Case study 1: CB switching	3-7
3.6	Case study 1: load shedding	3-8
3.7	Case study 1: coordinated control actions	3-9
3.8	Case study 2: one-line diagram of a 12-bus power system	3-9
3.9	Case study 2: uncoordinated deadband control	3-11
3.10	Case study 2: LTC setpoint reduction	3-12
3.11	Case study 2: coordinated application of CB switching, LTC setpoint reduction and load shedding	3-14
4.1	MPC concept	4-3
4.2	A system controlled by MPC	4-3
4.3	A simple quadratic cost function	4-8

4.4	A multi-area power system	4-9
4.5	Distributed MPC with neighbor-to-neighbor communication	4-12
4.6	A simple 2-area interacting power system	4-15
5.1	ABB 12-bus, case 1: response with the decentralized deadband control	5-2
5.2	ABB 12-bus, case 1: response with the DCMPC	5-3
5.3	ABB 12-bus, case 2: response with the decentralized deadband control	5-4
5.4	ABB 12-bus, case 2: response with the DCMPC	5-5
5.5	One-line digram of Nordic32 test system	5-7
5.6	Nordic32 partitioned interconnected test system	5-8
5.7	Case 1: Transmission bus voltages, and distributed coordinated LTC moves	5-9
5.8	Case 1: Inverse-characteristic timer x_t and OXL signal of g_7	5-10
5.9	Case 1: Bus voltages and uncoordinated deadband LTC moves	5-12
5.10	Case 1: Timer signals x_t and OXL signals in the deadband control approach	5-13
5.11	Case 1: Bus voltages and uncoordinated LTC moves in the decentralized MPC approach	5-14
5.12	Case 1: timer signals x_t and OXL signals in the decentralized MPC approach	5-15
5.13	Case 2: Bus voltages and uncoordinated deadband LTC moves	5-17
5.14	Case 2: timer signals x_t and OXL signals in the deadband control approach	5-18
5.15	Case 2: Bus voltages, coordinated LTC moves, and OXL signals	5-19
5.16	Case 2: Bus voltages and uncoordinated LTC moves in the decentralized MPC approach	5-20
5.17	Case 2: x_t and OXL signals in the decentralized MPC approach	5-21
5.18	Case 1: Bus voltages and coordinated LTC moves, with 10% increase in the load at bus 4043	5-23
5.19	Case 1: Timer x_t and OXL signal of g_7 , with 10% increase in the load at bus 4043	5-24
6.1	A basic microgrid architecture	6-5

List of Tables

1.1	Power system stability classification	1-3
1.2	Major Blackouts worldwide	1-16
2.1	Block-oriented versus object-oriented tools	2-3
2.2	Different steady-state operating conditions of generator for voltage control	2-9

List of Acronyms

TSO	Transmission System Operator
ENTSO-E	European Network of Transmission System Operators for Electricity
CA	Control Agent
LTC	Load Tap Changing transformer
OXL	Over eXcitation Limiter
MPC	Model Predictive Control
QSS	Quasi Steady-State
DAE	Differential-Algebraic Equation
AVR	Automatic Voltage Regulator
ACL	Armature Current Limiter
SC	Synchronous Condenser
FACTS	Flexible Alternating Current Transmission System
SVC	Static VAR Compensator
STATCOM	Static Synchronous Compensator
OPF	Optimal Power Flow
PVC	Primary Voltage Control
SVC	Secondary Voltage Control
TVC	Tertiary Voltage Control
RPR	Reactive Power Reserve
DG	Distributed Generation
DMPC	Distributed Model Predictive Control
DCMPC	Distributed Communication-based Model Predictive Control

Nederlandse samenvatting

–Summary in Dutch–

Recente technische, economische en juridische ontwikkelingen maken de betrouwbare en duurzame sturing van het geïntegreerde elektrisch vermogensnet tot een uitdagend onderzoeksonderwerp. Dit samenhangende elektrische vermogensnet, waarbij de energieproductie gestuurd wordt door verschillende TSOs (Transmission System Operator), is één van de grootste en meest complexe systemen ooit gebouwd. Het Europese geïnterconnecteerde elektrisch vermogensnet omvat ongeveer 4300 knooppunten, 6300 transmissielijnen en 1100 transformatoren, samen met de eraan verbonden distributienetten en hun belasting, en met de duizenden generatoren.

Betrouwbare regeling van een dergelijk groot systeem is zeer moeilijk als gevolg van de ingewikkelde interacties tussen allerlei, zowel continue als discrete, dynamische verschijnselen. De grootte van het systeem vereist de ontbinding van het systeem in verscheidene componenten, waarbij één component vaak overeenstemt met het gebied gestuurd door één TSO. Plaatselijke storingen in één gebied veroorzaken vaak lokale regelacties die niet enkel het lokale gedrag corrigeren maar die ook effecten hebben in naburige gebieden, effecten die op hun beurt gecorrigeerd worden door regelacties in die naburige gebieden, wat dan weer leidt tot nieuwe acties in nog andere gebieden inclusief het gebied dat eerst verstoord werd. Deze ketting van reacties kan leiden tot ongewenst gedrag, en uiteindelijk tot falen van het volledige systeem (blackout). Dit falen kan grote sociale en maatschappelijke kosten veroorzaken.

Een belangrijke klasse instabiliteiten die aanleiding geven tot blackouts betreft spanningsstoringen die het resultaat zijn van een tijdelijke verstoring van het evenwicht tussen het reactieve vermogen dat gegenereerd kan worden enerzijds en het instantane reactieve vermogen dat vereist is voor de dynamisch evoluerende spannings-afhankelijke lasten anderzijds. Aangezien spanning een lokale veranderlijke is (in tegenstelling tot frequentie) kunnen spanningsstoringen in één gebied, indien ze niet op een correcte manier worden bijgestuurd, aanleiding geven tot een ingewikkelde opeenvolging van gebeurtenissen in andere gebieden (zoals wijzigingen in de tap positie van transformatoren, of afschakeling van lasten wegens te hoge of te lage spanning), met als uiteindelijk resultaat een blackout of het opsplitsen van het net in afzonderlijke niet-gesynchroniseerde deelgebieden.

In deze thesis wordt de lange-termijn spanningsregeling bestudeerd. Spanningsinstabiliteiten over tijdsintervallen van de orde van minuten worden hoofd-

zakelijk veroorzaakt door de evolutie van het vermogen verbruikt door spanningsafhankelijke dynamische lasten die trachten om het vermogen van voor de storing te herstellen, maar ook door de ingewikkelde interacties met de lokale regelmechanismen. Op een tijdsschaal van tientallen seconden proberen LTCs (Load Tap Changing transformer) de spanning van elk onderstation te herstellen naar het oorspronkelijke niveau door hun tappositie aan te passen. Als gevolg daarvan kunnen de generatoren echter limieten bereiken van het maximale reactieve vermogen dat ze kunnen produceren, door het activeren van de OXL (Over eXcitation Limiter), of kunnen transmissielijnen begrenzingsniveaus bereiken van het maximale vermogen dat ze kunnen transporteren. Goede lokale regelaars moeten rekening houden met het risico dat dergelijke begrenzingsniveaus in de toekomst geactiveerd kunnen worden, door het toekomstige gedrag te voorspellen.

De analyse van het systeemgedrag dat aanleiding kan geven tot lange-termijn spanningsinstabiliteit wordt nog ingewikkelder gemaakt door de interacties tussen verschillende gebieden, gecontroleerd door verschillende TSOs, waarbij b.v. een wijziging in de tappositie in één gebied aanleiding geeft tot ongewenste veranderingen in tappositie, of het activeren van een OXL in een naburig gebied, wat op zijn beurt aanleiding kan zijn voor nieuwe ongewenste wijzigingen in de tappositie van LTCs in nog andere gebieden of in het gebied waar de storing begon. Dergelijke globale interacties kunnen een ineenstorting van het spanningsniveau van het gehele net veroorzaken. Om dit te vermijden moeten de regelacties van regelagenten (TSOs in het jargon van vermogensnetten) voor naburige gebieden met elkaar gecoördineerd worden. Deze coördinatie vereist uiteraard communicatie tussen naburige regelagenten. In dit proefschrift wordt een terugkoppelparadigma - gedistribueerde modelvoorspellende regelaars - voorgesteld dat “anticipatie” en “coördinatie” combineert (Distributed Communication-based Model Predictive Control (DCMPC)). De communicatie vereist voor de DCMPC die in deze thesis wordt ingevoerd beperkt zich tot het versturen naar naburige regelagenten (typisch TSOs) van de regelacties die gepland zijn tot en met de regelhorizon van de modelvoorspellende regelaar.

De anticipatie vereist voor de modelvoorspellende regelaar maakt gebruik van een simulator van het elektrische vermogensnet die veel sneller is dan reële tijd. Het vermogensnet evolueert onder invloed van zowel continue differentiaal-algebraïsche (DAE) vergelijkingen als onder invloed van gebeurtenissen gegenereerd volgens een automatenmodel (zowel voor de logica die aan de basis ligt van het LTC gedrag als voor de logica van de regelaars). Modelica, een gratis beschikbare object georiënteerde computertaal, bleek geschikt om efficiënt dergelijke hybride automatenmodellen van vermogensnetten te implementeren. De object-georiënteerde opbouw van Modelica laat ook toe om de compositionaliteit van het vermogensnet op een natuurlijke wijze te gebruiken in de simulatieprogramma's.

De lokale model-voorspellende spanningsregelaar vergelijkt de trajectoriën gegenereerd als antwoord van het systeemmodel op verschillende mogelijke discrete regelacties (in deze thesis wordt enkel als regelactie beschouwd het al of niet wijzigen op verschillende tijdstippen tijdens de regelhorizon van tapposities van LTCs), startend in de huidige toestand van het systeem. De model-voorspellende rege-

laar selecteert gedurende de regelhorizon die sequentie regelacties die de beste trajectorie genereert, met kleinst mogelijke afwijkingen t.o.v. de referentiespanning, met zo weinig mogelijk veranderingen van tappositie en zo dat spanningen steeds binnen de gewenste grenzen blijven (en eventueel ook zo dat zo weinig mogelijk generatoren een OXL activeren). Dit vereist dat de lokale regelaar een model van het dynamisch gedrag in zijn eigen gebied kent, en dat een benaderend model beschikbaar is voor het gedrag van andere gebieden (b.v. een QSS (Quasi Steady-State) model voor burens, en een PV (regime vermogen versus spanning) curve voor niet-naburige componenten). De regelagent voert dan uit als regelactie de keuze tijdens het eerste tijdsinterval van de beste regelsequentie. Aan het einde van dit eerste tijdsinterval wordt deze bovenstaande berekening herhaald, en als gevolg van de afwijkingen tussen model en werkelijkheid kan een andere sequentie regelacties in de met één tijdsstap vooruitgerolde voorspellingshorizon geselecteerd worden als beste. In het tweede interval wordt dan de eerste stap van die nieuwe beste sequentie regelacties geïmplementeerd. Dit procedé wordt voortdurend herhaald door de model voorspellende regelaar.

De voorspellingen van de lokale MPCs (Model Predictive Control) worden onnauwkeurig omdat geen gebruik gemaakt wordt van gedetailleerde kennis van het model van naburige componenten (en deze kennis is vaak moeilijk op een betrouwbare manier te bekomen) en door het feit dat de geplande regelacties van de naburige regelagenten niet gekend zijn. Dit gebrek aan coördinatie kan verholpen worden als elke regelagent via een communicatienetwerk geïnformeerd wordt over de geplande regelacties van naburige regelagenten, en als de lokale regelagent deze informatie benut in zijn anticipatie. Het gedistribueerde coördinerende modelvoorspellende regelparadigma dat in deze thesis wordt voorgesteld gebruikt dus de uitwisseling van tijdens de regelhorizon geplande regelacties om de voorspellingen die lokaal gebruikt worden in de greedy optimisator te verbeteren.

Het goede gedrag van deze DCMPC wordt in deze thesis aangetoond voor verschillende voorbeelden van vermogensnetten. Het ingewikkeldste geval dat beschouwd wordt betreft het klassieke, vrij realistische, Nordic32 test systeem, waarop allerlei verstoringen kunnen worden gesimuleerd. Via simulatie kan zo de robuustheid van DCMPC worden nagegaan. De simulatieresultaten tonen aan dat anticipatie gebaseerd op lokale MPC regelaars een aantal gevallen kan stabiliseren waar de klassieke deadband regelaars voor LTCs leiden tot falen van het systeem. In een aantal andere gevallen met nog ergere storingen faalt lokale anticipatie, maar blijkt dat het systeem kan gestabiliseerd worden met behulp van de coördinatie (gebruik makend van communicatie van geplande regelsequenties) volgens het in deze thesis voorgestelde DCMPC paradigma.

English summary

Power systems are nowadays becoming more and more interconnected, and controlled by several TSOs (Transmission System Operators), in order to ensure a reliable and economical supply and distribution of electric power. These (interconnected) electrical power networks are often considered as the most complex man-made dynamical systems ever. For example, according to the dataset provided by the ENTSO-E (European Network of Transmission System Operators for Electricity) for static studies (calculation of the AC load flow), the European interconnected power grid consists of approximately 4300 buses, 6300 lines and 1100 transformers together with their loads, distribution systems and generations in-feeds (in different voltage levels of 380 kV, 220 kV and 150 kV).

The proper control of such a large-scale interconnected power system is a very challenging problem due to the various continuous and discrete dynamics evolving in the system and their complicated interactions. Each local control agent (CA), corresponding to an area operated by one TSO, tries to achieve local improvement. However, it happens frequently that a local initiating disturbance in one area triggers some local control actions in its own area which in turn triggers further disturbances in the neighboring areas causing some undesirable control actions by their neighbors, and eventually a cascade of possibly wrong control actions lead the overall system to a final collapse.

One important class of power system instability is voltage instability, which actually arises from the inability of combined generation-transmission systems to deliver the power requested by (dynamical recovery) voltage-dependent loads. Such a voltage instability, if not corrected properly, due to a cascade of events, can eventually lead to voltage collapse (abnormally low voltages in a major portion of the system) often resulting in blackouts or separation of the system into separate unsynchronized islands. The societal impacts and financial costs/losses caused by blackouts are significantly huge.

The voltage in electrical power systems is, in nature, a “local” variable unlike frequency being a “global” variable. This means that, in multi-area power systems, only areas that are electrically close together interact with each other for voltage, and there is no need to involve distant areas with negligible common interest in solving a local optimization problem. The latter promotes the decomposition approaches for voltage control, where the voltage control still remains a prerogative of the local utilities.

This thesis focuses on long-term voltage instability - in the order of several minutes after a major disturbance. The driving force of such instability, following

a disturbance, is the process of load restoration, where the dynamics of recovering loads directly as well as some control mechanism such as LTCs (Load Tap Changing transformers) indirectly (by restoring the distribution-side voltages of the corresponding voltage-dependent loads), try to locally restore the load powers to the pre-disturbance values. The long-term voltage instability often occurs when LTCs try to restore the distribution side voltages of the connected buses, while the maximum power that the transmission system can provide to loads is reduced by the reactive power capability limits of generators, mainly enforced by OXLs (Over eXcitation Limiters). It seems rather intuitive, then, to seek some way of anticipating what will be the future behavior of a power system, by employing controllers which can look ahead in time. The long-term voltage control becomes even a more complex and harder problem in large-scale multi-area power system, each controlled by an independent TSO. The reason is that, for example, an arbitrary LTC move in one area can trigger undesirable LTC move(s), OXL activations in other areas, and such complicated global interactions may eventually lead to a blackout in the form of a voltage collapse. In order to avoid such a collapse in large-scale multi-area power systems, the local control actions taken by each CA, must be coordinated with those of (adjacent) neighbors. This coordination requires communications between neighboring CAs.

This thesis proposes an efficient distributed Model Predictive Control (MPC) paradigm which combines two concepts of “looking-ahead” and “coordination”. The proposed MPC-based control scheme relies on the communication of planned local control actions among neighboring CAs, each possibly operated by an independent TSO.

Modelica[®], a free of charge object-oriented language, is used to develop a much-faster-than-real-time simulator, providing an hybrid framework for effectively modeling and simulating power systems. Modelica facilitates the development of tools to generate very efficient codes for modeling of compositional physical systems such as electrical power networks, by relaxing the causality constraint of components, and focusing only on the topology of the overall system. In this thesis, the dynamic models for anticipation, are derived by considering each area as a hybrid dynamical system, using DAEs to describe piecewise continuous dynamics, and the set of events of hybrid automata representing the discrete logical controllers. This hybrid modeling framework captures the complex interactions between continuous and discrete dynamics.

The “looking-ahead” voltage controller can anticipate, within the prediction horizon window, for example, the activation of OXLs, moving towards reaching the maximum physical tap limits for LTCs, and deviating too much from the prescribed voltage bounds for buses. The controller will then efficiently use these anticipations, by selecting a control sequence that does not cause the above-mentioned constraint violations. The first input of the best control sequence selected by each local MPC, at each discrete time instant, will be applied to the local system until the next time instant, where the local optimization repeats again selecting the new best control action.

Each CA, knowing a local model of its own area, as well as a reduced-order

Quasi Steady-State (QSS) models of its immediate neighboring areas, and assuming a simpler equivalent PV model for the distant areas, performs a greedy local optimization over a finite window in time, communicating its planned control input sequence to its immediate neighbors only.

The “communicating” voltage controller enables each CA to coordinate its own local action with what its immediate neighbors are planning to do, assuming a QSS model for predicting how control actions of neighbors influence the interacting variables.

The good performance of the proposed real-time model-based feedback coordinating controller, following major disturbances, is illustrated using time-domain simulation of the well-known realistic Nordic32 test system, assuming worst-case conditions. Robustness of the proposed method against measurement inaccuracies, modeling errors as well as the uncertainty of the load behavior has also been illustrated.

This thesis considers two cases where, in the first reasonably sized network, a local CA, knows the complete model of the overall system, while, in the second realistic sized system, it employs reduced-order QSS models for immediate neighbors, and assumes a simpler equivalent PV model for the distant areas.

Simulation results illustrates the significant achievements obtained when the proposed model-based coordinating control is applied to different systems under some severe disturbances.

This thesis compares the above-mentioned simulation results with scenarios where a purely decentralized uncoordinated deadband control, as the current practice for LTCs, is applied, or where a decentralized uncoordinated MPC approach with no communication is applied. In this way it becomes possible to identify the two afore-mentioned distinct contributions of the proposed model-based coordinating approach namely “looking-ahead” and “communication”, since the decentralized deadband approach lacks both anticipation and coordination, and the decentralized MPC approach ignores the communications with neighbors.

1

Introduction

An electrical power system is a heterogeneous, geographically wide-spread network composed of numerous different components such as generators, transformers, transmission lines, protection devices and last but not least loads/consumers, all aiming at generating, transmitting and distributing electric power to the consumers.

Traditionally, electric power is generated in large central power plants such as thermal plants (e.g. fossil fuel-fired (burning) coal, natural gas or oil, or nuclear power plants) or hydro-electric power plants in the voltage level of up to 20 kV. This low voltage level is then, in transmission stage, increased to high voltage levels (up to 750 kV in Europe¹) in order to transmit the generated electricity through over-head transmission lines or under-ground cables minimizing the transmission ohmic losses. Finally, at distribution stage, these high voltages are reduced to lower levels (eventually down to 220 V in Europe) in order to feed the consumers. Note that in this conventional paradigm, as shown in Fig. 1.1, the power unidirectionally flows from generation sides to the distribution ends.

Large-scale power systems, by nature, are very likely to be subjected to unpredictable faults (disturbances). Faults may arise from tripping of some equipment such as generators or transmission lines due to natural calamities or even sometimes intentional hostile attack, or from mal-operation of some protection devices, human errors and short circuits.

Nearly all aspects of modern life, strongly depend on reliable electricity sup-

¹Ultra high voltage transmission voltage levels have been experimentally used at 1200 kV in the former Soviet Union and today in Kasachastan, and at 1100 kV in Japan.

ply. For instance, industry, household, telecommunication, transportation, banking, financial services, oil, water and gas infrastructures are highly dependent to electricity [1].

Moreover, a number of factors such as economical and ecological constraints on the expansion of the generation and transmission system, ever-increasing electricity demand (mainly for BRICS countries)², and the interdependency between electrical energy and other critical infrastructures stresses the power system more than ever to operate closer and closer to their safety and stability limits. It is noteworthy that it is becoming understandably ever more difficult to site new transmission lines, due to for example land use considerations, in densely populated areas where most electric power is consumed. Renewable energy resources, on the other hand, for which by nature their availability are not predictable, makes generated power even more unreliable in the modern power systems.

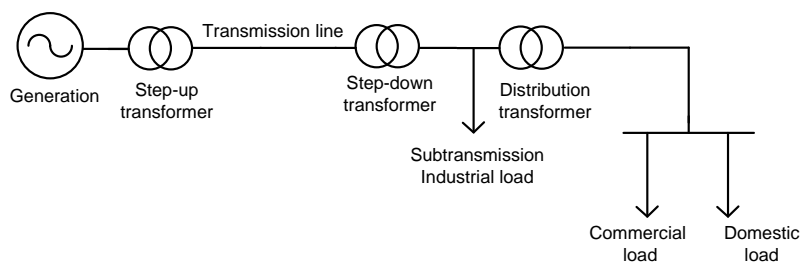


Figure 1.1: A traditional power system

One other important factor that places further stress on traditional power systems is the introduction of the competitive market into electricity industry, due to the deregulation and liberalization of electrical power systems, and the growing concern of ever-increasing internationalization in the electricity industry. This results in multi-area systems operated by several TSOs (Transmission System Operators). These areas are typically interconnected through power transmission corridors which carry heavy power flows in order to economically establish a common open electricity market and technically, hopefully, to ensure a greater security margin, through sharing of active/reactive power reserves. This interconnectedness, on the other hand, makes the large-scale power systems even more complex and harder to control making it more vulnerable to global collapse, initiated by a local fault.

Thus, secure, economical, and reliable operation of power systems is indispensably of great importance as consequences caused by failures in undertaking so,

²In economics and politics, BRICS refers to the countries of Brazil, Russia, India, China and South Africa, which are all deemed to be at a similar stage of newly advanced economic development.

could unpredictably affect the national and even international economy, security, health of citizens, and quality of life. Moreover the arguments above indicate that ensuring this reliable operation will require distributed control.

As a consequence of the aforementioned increasingly stressed conditions, a power system may experience a special class of instability in the form of sudden or progressive fall or rise of voltage in some buses. Such a voltage instability, if not corrected properly, due to a cascade of events, can lead to voltage collapse (abnormally low voltages in a major portion of the system causing circuit breakers to disconnect lines) often resulting in blackouts or separation of the system into separate unsynchronized islands.

Low voltages can cause damage to electrical motors and may lead to failures in electronic devices, and high voltages can, on the other hand, cause dangerous electric arcs (flashovers) by exceeding the insulation capabilities of electric devices [2]. Therefore, maintaining an acceptable voltage profile across a power system in both normal and emergency situations is a vital issue as system voltages vary continuously according to the electrical demand, control actions and emergency situations occurring in the system.

1.1 Classification of power system stability

The dynamic performance of a typical power system is often influenced by a wide array of devices (both equipments and controllers) with different dynamic response and characteristics. This makes it practically impossible to deal with the power system stability as a single problem. Therefore, the power system stability is often classified into different categories and sub-categories in order to better understand the underlying causes of the instability, and to devise the appropriate controls. Table 1.1 represents a possible classification based upon time scale (short-term (fast) or long-term (slow)), driving mechanism (generator-driven or load-driven) and the size of the disturbance (small disturbance or large-disturbance) [3]. A brief overview of this classification is described in the following subsections. A more detailed description may be found in [4, 5].

	Time scale	Driving mechanism	Size of disturbance
Rotor angle stability	Fast/Slow	Generator	Small/Large
Frequency stability	Slow	Generator	Large
Voltage stability	Fast/Slow	Load	Small/Large

Table 1.1: Power system stability classification

1.1.1 Rotor angle stability

Rotor angle stability refers to the ability of interconnected synchronous generators of a power system, for a given initial operating conditions, to remain in synchronism or colloquially “in step”, following a disturbance. According to the well-known swing equations of a synchronous generator, under steady-state conditions, the input mechanical torque and the output electrical torque of each machine is in equilibrium, and thus the speed remains constant. Obviously, following a disturbance, this equilibrium is perturbed, resulting in acceleration or deceleration of the rotors of some machines according to the highly nonlinear power-angle relationships (see equation (1.2)). Instability may occur due to the increasing angular swings of some generators leading to their loss of synchronism with other generators. This class of instability may occur due to small or large disturbances. The corresponding sub-classes are respectively called “steady-state or small-signal (small-disturbance)” and “transient or large-disturbance” stability. The time-scale of interest for the transient rotor angle stability analysis is in the order of 3 – 10 s, and 10 – 20 s for the steady-state analysis, after a disturbance.

1.1.2 Frequency stability

Frequency stability refers to the ability of power system to maintain its frequency within a prescribed bound around its nominal frequency, following a major disturbance resulting in a significant global generation-load imbalance. Note that frequency instability results from a global mismatch between generation and load in the overall system, as a result, frequency being a “global” variable. The frequency excursion is often a very slow phenomenon with the overall time scale of up to several minutes after disturbance, as it deals with the mechanical devices such as the boiler, prime mover and governor control. Often when dealing with modeling the voltage dynamics in computer simulations, the frequency regulation is assumed to be successfully performed through a single slack bus. However, in reality many generators (and not necessarily all) throughout the system participate in frequency control through, for example, well-known power-frequency droop control algorithm.

1.1.3 Voltage stability

Voltage stability, the main focus of this thesis, refers to the ability of a power system to maintain all its bus voltage magnitudes within a prescribed interval around the nominal bus voltages, even following a disturbance. In other words, voltage instability implies that the post-disturbance power system is unable to reach a new set of permissible steady-state voltages at some buses. A more formal definition of voltage instability is given in [6]:

“Voltage instability stems from the attempt of load dynamics to restore power consumption beyond the capability of the combined transmission and generation system.”

Voltage control, unlike the frequency control, is linked to electrical distance between generation and load, voltage being a “local” variable. Despite the recent prevailing trend of globalization/internationalization in the electricity industry, voltage control still remains a prerogative of the local utilities. The justification is that the inductive nature (and thus reactive characteristic) of a typical power transmission system is very dominant over its resistive one (and thus active characteristic) i.e. ($X \gg R$), which means reactive power (Q) is a more local quantity than active power (P).

One very important factor contributing to the voltage instability is the limited capability of transmission system for transferring (a large amount of) active and reactive power from generation centers to load centers. This happens because of voltage drops over the mainly inductive reactances of long transmission lines, or due to the maximum thermal loading limits of the lines. This (limited) power transfer capability may become even more restricted when some of the generators reach their limit of maximum reactive power generation. Therefore, the existence of a maximum deliverable power, referring to limited power transfer capabilities of combined generation and transmission system, may result in voltage instability and/or collapse. Loads are the main driving mechanism for voltage instability as the consumed load powers, following a disturbance, tend to be restored to their pre-disturbance values by the dynamics of recovery loads and/or indirectly by the action of Load Tap Changing transformers (LTCs).

Note that voltage collapse normally is not due to a single contingency but instead due to cascading failures. It is typically caused by an initiating disturbance e.g. transmission line or generator outage, or short circuit. The uncoordinated operation of protection relays to remove the faulted line/generator may lead to overloading of other transmission lines and/or generators. Subsequently, the newly overloaded lines and/or generators may be tripped by their undervoltage relays resulting in an even more drastic voltage decay. This further deteriorates the situation, and a partial or complete blackout may eventually be resulted from this cascade of unwanted events [7, 8].

1.1.3.1 Voltage stability of a simple ∞ -bus and isolated-load system

The fundamental concept of voltage instability can be analytically illustrated using a simple 2-bus system model, as shown in Fig. 1.2. The system consists of an infinite bus (with constant voltage magnitude E and frequency ω) feeding a single remote load through a purely inductive transmission line (jX).

Under steady-state conditions, the algebraic power (load) flow equations can be obtained using phasor quantities as follows [6, 9]:

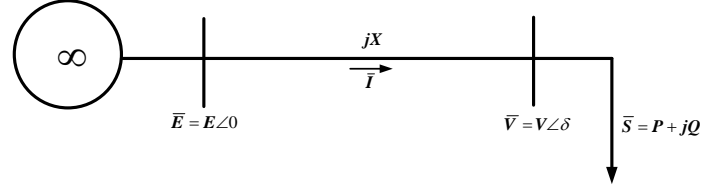


Figure 1.2: A simple 2-bus power system

$$\bar{S} = P + jQ = \bar{V}\bar{I}^* = V\angle\delta \left(\frac{E\angle 0 - V\angle\delta}{jX} \right)^* \quad (1.1)$$

and thus

$$P = \frac{-EV}{X} \sin \delta \quad (1.2)$$

$$Q = \frac{-V^2}{X} + \frac{EV}{X} \cos \delta = -\frac{V}{X}(V - E \cos \delta) \quad (1.3)$$

where P and Q are active and reactive power consumed by the load, respectively, V and δ voltage magnitude and phase angle (with reference to ∞ -bus) of the load bus.

Note that the systems's short-circuit level is $S_{sc} = (E)\left(\frac{E}{X}\right) = \frac{E^2}{X}$.

Normalizing equations (1.2) and (1.3) with $v = \frac{V}{E}$, $p = \frac{P}{S_{sc}} = \frac{PX}{E^2}$ and $q = \frac{Q}{S_{sc}} = \frac{QX}{E^2}$ yields:

$$p = -v \sin \delta \quad (1.4)$$

$$q = -v^2 + v \cos \delta \quad (1.5)$$

Eliminating δ from equations (1.4) and (1.5) gives the following quadratic equation with respect to v^2

$$v^4 + (2q - 1)v^2 + (p^2 + q^2) = 0 \quad (1.6)$$

The necessary condition to have at least one real solution ($v^2 \geq 0$) for equation (1.6) is that its discriminant is non-negative, i.e.

$$(2q - 1)^2 - 4(p^2 + q^2) \geq 0 \quad (1.7)$$

$$\text{or } 1 - 4q - 4p^2 \geq 0$$

This inequality represents the possible combinations of active and reactive power that the combined generation-transmission system of Fig. 1.2 can supply to the

load.

Solving equation (1.6) with respect to v , two positive real solutions are given by:

$$v_s = \sqrt{\frac{(1-2q) + \sqrt{1-4q-4p^2}}{2}}, \quad v_u = \sqrt{\frac{(1-2q) - \sqrt{1-4q-4p^2}}{2}} \quad (1.8)$$

Taking the inequality (1.7) into account, one can verify that both higher/lower voltages (associated with plus/minus signs) in the solution (1.8) are positive. For example for minus sign, we get a trivial inequality as below:

$$\frac{(1-2q) - \sqrt{1-4q-4p^2}}{2} \geq 0 \quad (1.9)$$

or, $(p^2 + q^2) \geq 0$

The 3-D graphs in $p v q$ -space in Fig. 1.3 illustrate, the solutions for load voltage v as a function of load active p and reactive q powers, for some different power factors $\tan \phi = \frac{q}{p}$.

As shown in Fig. 1.3, there exists a set of feasible combinations of load powers (p, q) , for which there are two positive solutions for voltages (v_s, v_u) , where v_s (higher voltage and lower current) is the stable solution representing the actual voltage of the load, and v_u (lower voltage and higher current) is the unstable solution as the dynamics there tend not to return perturbed states to the initial states.

Note that starting from an arbitrary operating point, any increase in the system loading (i.e. an increase in p, q or both) bring the system operating states closer to the maximum deliverable power point. Beyond this point, any increase in p, q or both makes the mechanism of the load restoration unstable.

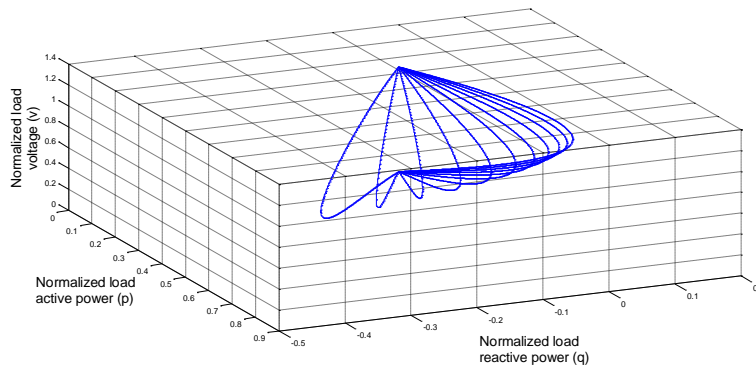


Figure 1.3: The PQV surface

1.1.3.2 Short-term versus long-term voltage instability

Depending on the mechanism of load power restoration, different voltage instability scenarios may evolve associated with the time scales lasting from a few seconds to several minutes, often referred to as their short-term (also sometimes called fast or transient) and long-term (also sometime called slow or mid-term or post-transient) voltage instabilities.

Short-term voltage instability is due to the tendency of fast-restoring stalling-prone induction motors to restore their consumed power (mechanical torque) in a time frame of typically one second after a voltage drop caused by a disturbance. If the post-disturbance system fails in providing the reactive power needed to maintain the voltage, the induction motors stall and short-term instability occurs due to loss of post-disturbance equilibrium. This class of voltage instability can also occur due to a slow fault clearing or delayed corrective control actions, where the system's trajectories have already evolved beyond the stable region of attraction, and thus are unable to be attracted by the stable post-disturbance equilibrium.

In long-term voltage instability, the short-term instability is assumed to have been survived following the initial disturbance (thanks to the assumed perfect available short-term voltage control e.g. generators' AVRs). The long-term dynamics, in the period of a couple of minutes after a major disturbance, is typically driven by LTCs trying to locally restore the distribution side voltages of the connected buses, and hence the corresponding voltage-dependent active/reactive powers of the dynamical recovery loads, while the Over eXcitation Limiter (OXL) of synchronous generators may be activated, restricting their maximum reactive power generation capability [6].

In this thesis, the long-term voltage instability - in the time scale of 1 s to several minutes after disturbance - will be tackled by designing a model-based coordinating control of LTCs, as the most likely control mechanism (together with the restoration process of dynamical loads) for driving the long-term voltage instability.

1.1.3.3 Normal and emergency voltage control

Voltage control is often also broadly categorized into two distinct "normal" and "emergency" state control modes, in accordance with normal and emergency operating states of a power system. The "preventive" and the "corrective" controls are two complementary lines of defence against voltage instability in these two control modes, respectively. The power system is initially assumed to operate in the normal operating state, and the associated normal state voltage control, following a disturbance that has (or has not) been considered in the operational planning stage of the system, aims at maintaining an acceptable voltage profile for all buses and/or minimizing the system losses, by taking some cheap preventive actions

such as switching of CBs, adjustments of generators' voltage setpoints and standard deadband LTC control [10].

Note that those preventive voltage control actions are designed in the planning stage of the system for a set of credible disturbances. They are applied to the pre-disturbance system in order to prevent the actual occurrence of the disturbance in the normal operating state, by increasing the security margins of the system with respect to that particular disturbance. These controls are normally costly as some of the credible disturbances for which preventive control actions have been designed, may not even occur in practice in the system.

If a sufficiently severe disturbance occurs such that the system cannot be timely stabilized by only applying a combination of some high-priority cheap preventive controls, the system then enters the emergency operating state. This enables the associated emergency voltage control, which makes use of full range of available controls (including undesirable expensive corrective actions) such as load reduction either by direct shedding or indirectly through emergency/modified control of LTCs, (fast) generation rescheduling and cross-border flow management. Fig. 1.4 illustrates these two operating states of a typical power system and their corresponding voltage control regimes. Note that some other operating states are considered in [4], but are not represented here as they are not of primary interest for our research.

Note that small disturbances such as small variations in load and generation occur continually in the power systems, while large disturbances are often due to faults (e.g. a three-phase short-circuit), or the outage of a transmission line or a large generator.

This thesis develops a model-based coordinating controller for LTCs in order to mitigate the long-term voltage instability. The proposed controller always acts on the real-time voltage deviations regardless when and where exactly a disturbance occurs. Thus it does not generally require to distinguish between normal and emergency operating modes, covering both normal and emergency state voltage control. This simplification is important as the current existing feedback voltage controllers require accurate mode detectors to identify the operating state of the system in order to take the appropriate control actions, accordingly.

1.1.3.4 Countermeasures against voltage instability

Voltage instabilities commonly occur due to reactive power deficiency in electric transmission networks. Thus for voltage control, a proper provision of the fast/slow reactive power resources is required to provide sufficient Reactive Power Reserve (RPR)³ in the system. The RPR is the remaining reactive power capability (of the available reactive power resources such as generators, CBs and FACTS

³Regarding voltage control, the more RPR means the more voltage-secure system.

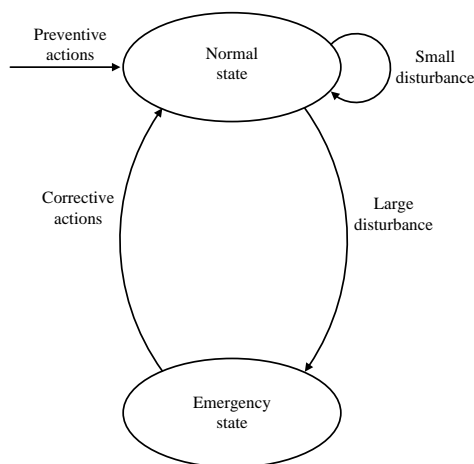


Figure 1.4: Different voltage control regimes associated with different operating states

devices) that the system can provide (to produce/absorb reactive power) when a disturbance occur that influences the voltage profile. Fast countermeasures to react against rapid short-term voltage variations include adjustment of voltage set-points of generators, synchronous condensers (SCs), SVCs, automatic (thyristor-controlled) CBs, and ultimately (fast) load shedding. The voltage support provided by generators are commonly preferred to CBs. This is thanks to the much faster response time of the generators' AVRs (electric (and not mechanical) control of the field current), more accurate response (feedback setpoint tracking of AVRs), and larger reactive capability range of the generators. More importantly, unlike CBs,⁴ the reactive support of generators does not lose effectiveness at low voltages.

On the other hand, the long-term voltage instabilities, traditionally, are tackled by several control actions such as manual switching of (mechanically switched) CBs, generation rescheduling, (emergency/modified) LTC controls and undervoltage load shedding. In this thesis, based on the time scale of interest for designing the coordinating model-based voltage controller, only the action of LTCs are considered as the available control. However, the proposed control approach can be easily extended to accommodate other existing discrete controls such as automatic CB switching and load shedding, without loss of generality.

⁴The reactive power that a CB can produce is proportional to square of the voltage ($Q = \frac{V^2}{X_c}$). Thus their reactive support quadratically drop during low voltage conditions, losing effectiveness.

1.1.3.5 Hierarchical voltage control

The voltage control in electrical power system is commonly achieved in a hierarchical fashion, with typically three layers of control, namely Primary Voltage Control (PVC), Secondary Voltage Control (SVC) and Tertiary Voltage Control (TVC), as shown in Fig. 1.5. These three control loops operate at different system levels, and with different time scale of response. Furthermore, the geographical area covered by these control layers are also different, as the PVC operates only on the local particular (generator) bus, the SVC on the zonal/regional level (a set of buses), and the TVC on the global (national/international) system level [11–13].

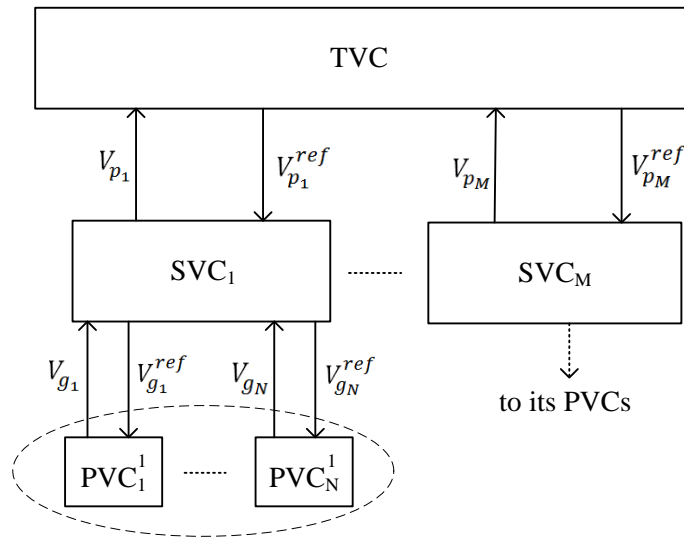


Figure 1.5: A generic hierarchical voltage control structure

- The PVC layer is the lowest, most local, level in the control hierarchy which directly acts on the physical components (mainly generator units), and has the fastest time response of a fraction of a second. It immediately responds to the local voltage deviations caused by, for example, load or generation changes, and ensures that the voltages track (remain close to) their setpoint values chosen by associated higher-level secondary controller. The primary voltage controller is often employed locally using only local measurements (as a simple feedback controller). In other words, in order to guarantee a *reliable operation*, it does not rely on communication and is thus expected to function even when communication fails. In a conventional synchronous generator, typically an Automatic Voltage Regulator (AVR) acts as the primary voltage controller by adjusting the generator field current in order to control its terminal voltage. However, other fast-reacting control-

lable devices such as SC or power electronic-based FACTS devices (such as Static VAR Compensator (SVC) or Static Synchronous Compensator (STATCOM)) can also be used in the primary voltage control layer [14].

- The SVC layer is the next higher level which provides setpoints for the local primary controllers within each zone, in order to mitigate longer term voltage deviations. In this layer, a pilot bus (not necessarily a generator bus) is selected for each given geographical zone such that the voltage magnitude of the pilot bus represents the voltage profile over the entire corresponding zone. Then the secondary controller utilizes the regional information from all participating (generator) buses in order to control the voltage of the pilot bus. In other words, this control level minimizes the average of all voltage deviations as measured by generation units by attempting to shift voltage deviations towards zero after every possible change of load or generation, and thus ensures the *power quality*. It operates on a slower time scale in the order of a minute, leaving enough time for primary controller to (possibly) reach its steady-state voltage values before the setpoints are updated.

- The TVC layer is the highest level in the control hierarchy and has the slowest time response of tens of minutes. This single control layer solves a centralized optimization problem (an Optimal Power Flow (OPF) program), utilizing the global information of the whole system, in order to calculate the optimal steady-state voltage setpoints for the pilot buses of the existing lower-level secondary controllers. This improves the *economical operation* of the overall power system. The tertiary voltage controller ultimately operates after the actions of the primary controllers to ensure power reliability and the secondary controllers to improve power quality.

Note that the difference in the speed of response and the time scale over which the aforementioned hierarchical control layers operate, makes it possible to clearly decompose those three control loops.

The time response of the coordinated control, developed in this thesis, is in the order of 10 s. This coordinating controller complements the conventional secondary voltage control, but does not deal with the economical operation of the power systems, nor with fast local voltage control. The research reported in this thesis does not take into account limited power flow in corridors, as this is strongly related to the economical operation.

1.1.3.6 Steady-state and dynamic voltage instability analysis

From another perspective, the analysis of voltage instability can be also broadly classified into two techniques, namely static (steady-state or load-flow) and dynamic (time-domain) analysis [15, 16].

Static analysis assumes constant frequency throughout the system, and that the

system moves smoothly from one operating point to another, associated with small and slow disturbances such as gradual load changes. Here, the power (load) flow equations, derived from Kirchhoff's law, are employed to investigate the existence of new equilibrium points of a given power system, following a large number of post-contingency scenarios. Therefore, the new equilibrium points, if any, are revealed, and the factors influencing voltage profile are identified. Consequently, the system stability margins are evaluated using different "security indices" which measure the proximity of an existing operating point to a bifurcation point at which voltage instability occurs. The static voltage instability analysis is typically employed to investigate the voltage stability at any given instant of time. Here, the system's equations are often linearized around the pre-disturbance operating point in order to get the qualitative picture of the system such as, at the given instant, how stressed the system is, or how close the system is to the point of instability.

On the other hand, in order to fully analyze the system's stability and getting a clear/detailed picture of the response of the system, associated with large disturbances such as outage of generators or lines, the nonlinear dynamic performance of the system has to be examined over a sufficiently long time interval after the disturbance. Therefore, unlike the static analysis, the main concern of dynamic analysis is not only the existence of a new stable post-disturbance equilibrium, but also to investigate the ability of the system to reach this new equilibrium. Here appropriate component models, with the required degree of accuracy at the expense of simulation speed, are typically used, and the system is simulated over a sufficiently long time interval after a large disturbance, in order to capture the possibly complicated interactions among the slowly-acting devices influencing long-term voltage instability.

The aim of this thesis is to design a dynamic real-time model-based coordinating voltage control, and thus the dynamic aspect of the voltage instability phenomenon is of primary interest. This dynamic analysis will be studied in the following chapters. However, in order to clearly distinguish between steady-state and dynamic voltage control, § 1.2 briefly discusses the steady-state analysis of the voltage instability.

1.2 Steady-state voltage stability analysis

The steady-state analysis is carried out for assessing the proximity of a given power system to the point of voltage instability. Some widely-used conventional steady-state methods are listed below, where each method employs a different "security index" to measure the proximity to the voltage instability point.

- PV curve: assesses the sensitivity of load bus voltage to variations in load active power.
- VQ curve: assesses the sensitivity of load bus voltage to variations in (injected) load reactive power.
- singularity-based method: uses the fact that power-flow Jacobian matrix becomes singular at the point of voltage instability.

The first two methods mentioned above, namely PV and VQ curves, are concisely explained below.

1.2.1 PV curve

In this analysis, the proximity to voltage instability is measured as the distance between the active power (in p.u.) at the operating point on the PV curve and the limit (nose of the same curve), revealing the available amount of active power margin before the point of voltage instability. For the simple 2-bus system shown in Fig. 1.2, a family of curves, referred to as PV curves, is shown in Fig. 1.6, each corresponding to a specific load power factor. Each curve is plotted by varying the load in steps at a constant power factor, and calculating the load bus voltage for that specific power factor.

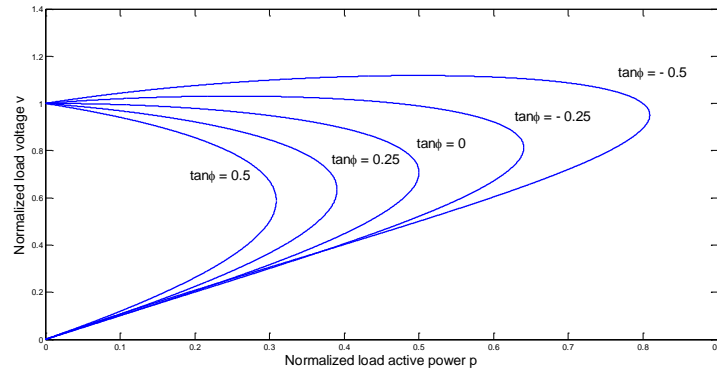


Figure 1.6: The PV curves

Assuming a constant power factor for load $q = p \tan \phi$, and substituting this in inequality (1.7) determines the maximum deliverable value for p for each $\tan \phi$ (nose of each curve).

$$p_{\max} = \frac{\sqrt{(1 + \tan^2 \phi)} - \tan \phi}{2} \quad (1.10)$$

1.2.2 VQ curve

In this analysis, the proximity to voltage instability is measured as the difference between the reactive power (in p.u.) at the operating point on the VQ curve and the limit (bottom of the same curve), revealing the available amount of reactive power support (reserve). For the simple 2-bus system shown in Fig. 1.2, a family of curves, referred to as VQ curves, is shown in Fig. 1.7, each corresponding to a specific constant load active power p .

A VQ curve is a plot of voltage at a given test/critical bus against reactive power reserve at that bus. A fictitious SC, with zero active power production but unlimited capability of reactive power generation, is connected to the test bus. The bus voltage is being smoothly varied and reactive power injection of the SC is recorded. The operating point corresponding to the zero reactive power reserve represents the situation with removed SC.

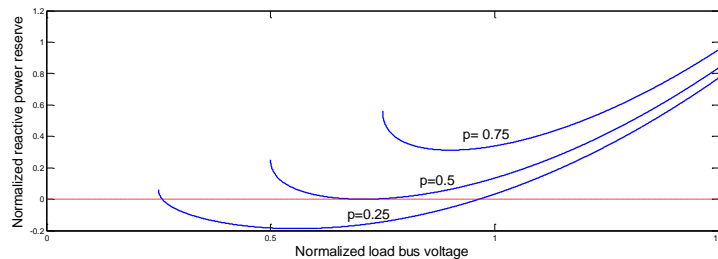


Figure 1.7: The VQ curve

1.3 Historical review of notable voltage instability incidents

As mentioned before, the classification of the power system instability into rotor angle, voltage and frequency analytically makes it convenient to identify the dominant initiating cause of instability, and facilitates the development of appropriate controls to mitigate the problem. However, when a power system undergoes system instability, there typically are several types of instabilities interacting. For example voltage instability and rotor angle instability often go hand in hand, meaning that unmitigated rotor angle instability may lead to voltage instability or vice versa [4, 17]. A blackout in the system, therefore, can occur either due to voltage collapse (as a calamitous result of unmitigated voltage instability), and/or due to frequency instability (caused by significant load/generation mismatch). However, over the past 40 years, since the late 1970s, more than 30 major blackouts worldwide were clearly attributed to voltage instability/collapse [18, 19].

Blackout	Affected people (Millions)	Average duration (Hours)	Cause
30 – 31/07/2012 India	710	up to 14	Excessive surging demand, partially due to low monsoon rains that reduced the capacity of hydroelectric power, and forced many farmers to turn to electric pumps to draw water from underground to their field, and also kept the temperature higher, further increasing the usage of air-conditioning units
10 – 11/11/2009 Central, south and southeastern Brazil and all Paraguay	87	4.5	Heavy rains and strong winds caused short circuit in the 3 transformers leading to loss of some transmission lines
18/08/2005 Indonesia, Java & Bali	100	6.5	Initial loss of one transmission line and subsequent outage of the overall 8 units of power plants
14 – 15/08/2003 North & north-eastern USA	55	≈ 18	Sequence of events initiated by a software bug causing failure in the alarm system of the control room, followed by some human error
28/09/2003 Italy	55	≈ 8	Initiated by tripping of a power line between Italy and Switzerland damaged by storm, followed by subsequent outage of two 400 kV power lines between Italy and France
11/03/1999 South & south-eastern Brazil	97	≈ 2	Lightning strike at a substation causing most of the 440 kV circuits to trip
09/11/1965 North & north-eastern USA	30	up to 12	Initiated by human error prior to blackout for incorrectly setting a protection relay on one transmission line, followed by tripping of the other lines

Table 1.2: Major Blackouts worldwide

Among them, at least 13 voltage-related blackouts have happened in the USA. Table 1.2 lists the largest and most wide-spread (not only voltage-related) blackouts, in terms of number of affected people, throughout the world, summarizing the cause and average duration of the disruption [20]. In particular, long-term voltage instability was the direct cause of the blackouts in the USA (13 – 14/08/2003), Italy (28/09/2003), Eastern Denmark and Southern Sweden (23/09/2003), Japan (23/07/1987), and Belgium (04/08/1982).

Talking about Europe, it is noteworthy to mention that the Europe's interconnected power grid experienced a serious incident on November 2006. This incident originated from Northern Germany, where a overhead high voltage 380 kV transmission line had to be tripped to allow a ship to pass safely underneath. This routine tripping led to overloading of the other lines, and eventually the Union for the Coordination of Transmission of Electricity (UCTE) network splitted into three islands operating with different frequencies. The final report released by UCTE, recently renamed to ENTSO-E (European Network of Transmission System Operators for Electricity), the coordinator of 41 TSOs in 34 European countries, identifies three main causes for this incident. Among which is poor inter-TSO coordination as the other European TSOs did not receive information on the control actions taken by German TSO E.ON Netz. However, thanks to the adequate performance of the automatic countermeasures in each individual TSO as well as additional quick manual actions by TSOs, a total blackout across the whole of Europe could be avoided, during that incident [21].

The societal costs and financial losses caused by those massive blackouts, and their impact on the society are believed to be significantly huge. For example, the economic cost of the August 2003 USA blackout is estimated to be in the range of \$(6 – 10) billions [1].

Accordingly, voltage control aiming at developing a design methodology to avoid voltage collapse, has become an active research topic, over the past few years, for power system researchers and planners.

1.4 Research motivation

The main research motivation (and thus the corresponding final contribution) of this thesis is twofold, as discussed in § 1.4.1 and § 1.4.2:

1.4.1 Hybrid modeling framework

Modeling and simulation of increasingly complex power systems is becoming more important for design, implementation and validation of on-line management of power systems.

Traditional special-purpose tools e.g. PSCAD/EMTDC as well as general-purpose block-oriented tools e.g. Matlab/Simulink, for modeling and simulation of power systems are computationally very efficient and reasonably user-friendly, but their closed architecture makes them very time-consuming and often practically impossible to examine or modify the encapsulated component models [22]. Dealing with physical systems (e.g. power systems) which are typically composed of many different components, the models of components should be as close as possible to the corresponding physical subsystems that make up the overall system. Causal modeling aims at representing each component with a single input-output block, and thus requires the underlying describing equations as an explicit input-output state-space form. This demands a huge amount of manual effort, or is often practically impossible when dealing with complicated compositional systems. Therefore, the actual topology of the physical system cannot always be reflected through block-diagram structure as some components cannot be represented as an individual block, inevitably being combined into the model of other components. As a consequence, the proper understanding of the interaction between components, each or some represented by one block, becomes very difficult [23]. Causal modeling is a fundamental limitation of block-oriented tools in which the blocks must have a unidirectional data flow from inputs to outputs. This is the reason why some components cannot be dealt with directly and if it is attempted to simulate the basic equations directly, there will be a loop which only contains algebraic equations. The latter is a well-known drawback of Matlab/Simulink which is not always able to handle the algebraic loops [24].

In order to overcome the above-mentioned drawback, general-purpose object-oriented tools have been proposed which are based on acausal modeling.

Particularly, speaking of power systems, beside the continuous dynamics which mostly arise from the physical laws at the system level, various discrete events may also occur in the system. The discrete events may be due to the operation of some equipment with logical controllers such as LTCs or Capacitor Banks (CBs), or may be in the form of thresholds influencing continuous dynamics reached by some devices such as OXL, or due to the faults (and thus the operation of the protection devices such as relays and switchgears). The introduction of these discrete events into continuous dynamics of a power system often involves an intrinsic strong coupling between those two dynamics, meaning that a power system represents a complicated nonlinear hybrid behavior. This occurs for example during voltage collapse phenomena when several discrete devices (either controllers or thresholds) switch on and off as a reaction to local measurements of currents and voltages that are influenced by local and global continuous dynamics of the system, and by the state of discrete devices [7].

On the other hand, according to the literature as illustrated in § 1.3, many voltage collapse incidents, over the past decades, have been caused by uncoordinated

interactions of local controllers following a major disturbance in electric power system operating closer and closer to their safety limits [2]. The first step in order to devise a model-based real-time coordinated voltage control, is to develop an appropriate much-faster-than-real-time simulator capable of effectively capturing those complicated interactions. Obviously the simulation speed is almost always compromised with the required accuracy.

To this end, this thesis proposes an efficient hybrid compositional framework for modeling and simulation of the power systems, which is very suitable for designing an on-line real-time voltage control. The proposed hybrid framework uses Modelica as a general-purpose object-oriented language. This modeling framework has been tested on different test systems. Simulation results show that the interaction between continuous dynamics of the power system and hybrid automata representing the discrete logical controllers and also nonlinear behavior of load dynamics can easily be studied in the proposed framework. On the other hand, the simulator is sufficiently fast to evaluate a model-based predictive control coordination strategy, serving as a real-time countermeasure to arrest voltage collapse [25].

1.4.2 Real-time communication-based voltage controller

Most existing control schemes against voltage collapse are rule-based, often using only local measurements. Their control actions are selected according to heuristic rules based on past experience of operators. However a power system normally is a very complex large-scale nonlinear hybrid system, and its operating conditions change as the system evolves in time.

Furthermore, as mentioned before, the deregulation, liberalization and globalization of the electrical power systems, on the one hand, and the larger and less predictable power flows due to the increased use of renewable energy recourses, on the other hand, have led to partitioning the traditional power systems into multiple areas each operated by an independent TSO acting on one/several control agents (CAs)⁵ [13,26]. The voltage and current values at boundary buses of the neighboring areas, and hence the flow of active and reactive powers over the corresponding interconnecting tie-lines depend on the control actions taken by those neighboring CAs (and indirectly by the neighbors of their neighbors). However CAs in practice only have accurate knowledge about their own local model but limited information about the neighboring areas, and may only observe active/reactive power flow and/or the voltage profile at interconnections. Thus, in the current practice, every CA takes some rule-based control actions locally according to heuristic rules based on the past experience of operators, often relying on local measurements only. However, due to the complex nonlinear hybrid nature of the geographically

⁵Note that although CAs are not necessarily the same as TSOs, and several CAs may be operated by a single TSO, however, hereafter throughout in this thesis, we assume that TSO and CA are interchangeable terms.

wide-spread large-scale multi-area power systems, the rule-based local control actions taken by one CA, as a result of a local disturbance, firstly may lead to an inefficient use of the grid and the controllers, and secondly a sequence of further undesirable perturbations and control actions might be triggered in the neighboring areas. Eventually, global complicated interactions may lead to collapse of the whole interacting power system [27].

Hence specifying some particular ad-hoc fixed rules in advance for each CA, using only local information and local anticipation, without taking coordination with neighboring CAs into account will not account for nonlinear interactions influencing the future behavior of the power system. These uncoordinated control actions, ignoring the influence of the control actions taken by the neighboring CAs, may endanger the power systems' security increasing the risk of unstable loops in the network of interacting controlled components (which for example can cause a blackout) [28,29]. Rule-based approaches are simple to design and implement, because the local information need not be communicated, but may not be applicable to systems with very complicated interactions.

In order to avoid such a collapse in large-scale multi-area power systems, there is a need for designing a real-time model-based system-wide coordinating feedback controller capable of properly coordinating local control actions taken by each independent CA, and accounting for nonlinear evolution of the system. Model-based approaches, obviously, require a lot of effort to design and implement, but have the potential to avoid voltage collapse under more severe conditions.

The commercial availability of the synchronized on-line real-time wide-area phasor measurement units and resilient high-speed communication, as well as the development of fast computation techniques are some enabling technologies to justify the design of such a model-based wide-area coordinating controller at the current time.

One of the most successful classes of closed-loop Model-based schemes is the Predictive Control paradigm (MPC), also called receding/moving horizon control. MPC relies on an estimate of the current system states at discrete time instant $t_k = k * T_c$ and an explicit *model* of the system in order to *predict* the future output behavior via simulation over a finite window $[t_k, \dots, t_{k+H}]$, for a set \mathcal{U} of allowable control sequences $\mathbf{u} = \{u(t_k), u(t_{k+1}), \dots, u(t_{k+N-1})\}$, where $\mathbf{u} \in \mathcal{U}$, $0 < N \leq H$. The corresponding performance criterion is calculated in each time instant t_k . This allows selection of the best sequence \mathbf{u}^* at that time t_k . The first element $u^*(t_k)$ of the selected best sequence \mathbf{u}^* at time t_k is then implemented at the present time instant t_k . All these calculations are repeated, using new observations, at the next time instant t_{k+1} , each time predicting performance over a shifted window with the size of $H * T_c$ [30–38].

To this end, this thesis, using a nonlinear hybrid model of the system, proposes

a coordination paradigm for long-term voltage control of large-scale multi-area power systems, by properly coordinating local control actions, taken by many communicating CAs. The proposed control scheme is inspired by distributed model predictive control (DMPC), and relies on the communication of planned local control actions among neighboring CAs, each possibly operated by an independent TSO. Each CA knows a local model of its own area as well as reduced-order Quasi Steady-State (QSS) models of its immediate neighboring areas, assuming simpler equivalent PV model for the distant areas. Local decisions are taken by using only local measurements including flow of power/current along interconnecting lines between areas, and the latest selected control sequences received from the neighboring CAs, by solving a greedy local optimization, taking only local constraints into account, over a finite window in time. The planned local control sequence is then communicated to the immediate neighboring CAs to be taken into account in their next optimization iteration.

The limited amount of exchanged information on the future control actions makes the approach more robust against communication failures. Furthermore, the fact of not requiring the complete and detailed knowledge of the overall system's model, provides enough robustness against lack of some system information.

The good performance of the proposed real-time model-based feedback coordinating controller, following major disturbances, is illustrated in this thesis using time-domain simulation of several test systems, among which is the well-known realistic Nordic32 test system, assuming worst case conditions [39,40].

1.5 Thesis outline

This thesis is organized in the following chapters:

Chapter 1: Introduction

This introductory chapter briefly discusses the general power system stability problem by classifying it into *rotor, frequency and voltage* stability problems. The voltage instability problem, as the main focus of this thesis, is then further elaborated from several perspectives. Short/long term voltage instability in normal/emergency states, hierarchical structure of the voltage control, and finally the steady-state and dynamic nature of the voltage control is discussed in more details. Research motivation is also provided, which highlights the need for a distributed communication-based model predictive control (DCMPC), the main contributions of the thesis. The remainder of the chapter outlines the content of the thesis, and lists the publications resulting from this research.

Chapter 2: Modeling and simulation

This chapter proposes an efficient hybrid framework for modeling and simulation of power systems, towards the ultimate goal of designing a well-performing real-time coordinating voltage control. Modelica[®], a general-purpose object-oriented language, is then introduced in order to build a fast simulator, and its two main features which makes it very suitable for study of voltage instability problem are discussed. Next, hybrid automata are defined in order to deal with the hybrid behavior of the power system, and to effectively capture interactions between continuous and discrete state variables. Using this hybrid framework, the model of the most relevant components to long-term voltage instability such as synchronous generator, LTC and load are then provided.

Chapter 3: The need for coordination

This chapter, employing a 12-bus meshed test system, illustrates the need for voltage coordination in electrical power systems, and demonstrates how local control actions in one CA may initiate other, possibly undesirable, control actions in the neighboring CAs. Next, this chapter considers two test systems to study the mechanisms involved in voltage instability. Simulation results are then provided, illustrating that, based on the proposed hybrid framework in chapter 2, and a proper coordination among different control actions, the system voltages can be effectively stabilized in circumstances where uncoordinated control actions leads to a final collapse. The coordination, in this chapter, is achieved by a manual, heuristic design approach, in a trial and error fashion, by carrying out many simulations. Next, the main trends in development of coordination schemes in electrical power networks are discussed and compared. The basic characteristics and also fundamental limitations of each scheme are briefly presented. Finally, the use of communication will be explained, and the problem of obtaining abstraction for component models will be discussed.

Chapter 4: Distributed neighbor-to-neighbor coordination control

This chapter proposes a coordination paradigm for properly coordinating local control actions, taken by many interacting CAs, in order to maintain multi-area power system voltages within acceptable bounds. The proposed control scheme is inspired by distributed model predictive control, and relies on communication among neighboring CAs. Initially, the main MPC approaches namely *decentralized*, *centralized* and *distributed* MPC to be applied in electrical power systems, are reviewed. Then, the basic assumptions about the voltage control problem and the modeling framework will be described. The principle of the proposed coordination scheme, the mathematical formulation of the control problem, and the underlying optimization algorithm will be finally discussed.

Chapter 5: Simulation Results

This chapter represents the time-domain simulation results on two test systems, in order for illustrating the good performances of the coordination scheme developed in chapter 4 by using the hybrid framework developed in chapter 2. The *ABB 3-area 12-bus* is the first reasonably-sized network, where for simulations we assumed that each CA knows the model of the entire network. The *Nordic32* is the second test system, where for simulations each CA knows a local model of its own area, as well as reduced-order QSS models of its immediate neighboring areas, and assumes a simpler equivalent PV model for the distant areas. Simulation results show that for both test systems, under limiting conditions for *ABB 3-area 12-bus*, and more generally for the *Nordic32*, the proposed DCMPC strategy can stabilize the system in cases when a completely decentralized deadband strategy, or a decentralized uncoordinated MPC approach, without any communications, leads to collapse. Simulation results illustrate that the significant improvement obtained when applying the proposed DCMPC approach, is thanks to both concepts of “anticipation” and “coordination”. Moreover, the robustness of the method against the noise (randomly changing load powers) and against the unmodeled dynamics (wrong parameters from the neighbors) has been illustrated.

Chapter 6: Conclusions and future work

This chapter provides the general conclusions and recommendations for further work on the topic.

1.6 List of publications

Most of findings from this thesis, have already been reported in the following articles:

- **M. Moradzadeh**, R. Boel and L. Vandeveldel, “Voltage Coordination in Multi-Area Power Systems via Distributed Model Predictive Control,” *IEEE Transactions on Power Systems*, In press, 2012, doi:10.1109/TPWRS.2012.2197028.
- **M. Moradzadeh** and R. Boel, “Voltage Coordination via Communication in Large-Scale Multi-Area Power Systems. Part I: Principal,” *Advanced Materials Research*, vol. 433-440, pp. 7175-7182, 2012.
- **M. Moradzadeh** and R. Boel, “Voltage Coordination via Communication in Large-Scale Multi-Area Power Systems. Part II: Simulation Results,” *Advanced Materials Research*, vol. 433 - 440, pp. 7183-7189, 2012.

- **M. Moradzadeh**, R. Boel and N. M. Tabatabaei, “Distributed Voltage Control in Electrical Power Systems,” In N. Bizon and N. M. Tabatabaei, editors, *Advances in Energy Research: Energy and Power Engineering*, Nova Science Publishers, USA, 2012.
- **M. Moradzadeh** and R. Boel, “Hybrid Modeling of Power Systems for Coordinated Voltage Control,” *International Journal on Technical and Physical Problems of Engineering (IJTPE)*, issue 5, no. 4, vol. 1, pp. 32-40, 2010.
- **M. Moradzadeh**, L. Bhojwani and R. Boel, “Coordinated Voltage Control via Distributed Model Predictive Control,” *In Proc. CCDC2011*, pp.1612-1618, China, 2011.
- **M. Moradzadeh** and R. Boel, “A Hybrid Framework for Coordinated Voltage Control of Power Systems,” *In Proc. IPEC2010*, pp.304-309, Singapore, 2010.
- **M. Moradzadeh**, M. Rajabzadeh and S. M. T. Bathaee, “A novel hybrid islanding detection method for distributed generations,” *In Proc. DRPT2008*, pp.2290-2295, China, 2008.

2

Modeling and simulation

2.1 Introduction

Modeling is normally the first interdisciplinary step to study a physical system, and to analyze its dynamic response to various disturbances. This often requires physical insights, hypotheses and simplifications in order to derive the appropriate mathematical equations to describe the system. The computer simulation is then employed to solve the set of derived equations either in a closed form or numerically, illustrating the dynamic performance of the system [41–43].

Towards the ultimate goal of the thesis to design a well-performing system-wide model-based coordinating voltage controller, providing an efficient modeling and simulation framework is essential. The proposed framework is needed to effectively capture the continuous and discrete dynamics of interest with sufficient accuracy for complicated networks of components, and to anticipate on the effect of control decisions that are planned.

2.2 Modelica[®] and Dymola

Modelica[®] is a free of charge non-proprietary and general-purpose object-oriented equation-based language, that has been designed to allow the development of tools to generate very efficient codes for modeling of compositional physical systems.¹

¹Modelica also contains an open-source standard library of component models in many different physical domains.

The modeling effort and complexity is considerably reduced in Modelica since the model of components can be reused, avoiding tedious and error-prone manual manipulations [24].

There exist several free as well as commercial tools based on the Modelica language e.g. OpenModelica from OSMC, MathModelica by MathCore, SimulationX by ITI, MapleSim by MapleSoft and Dymola by Dassault systems/Dynasim [44].

Dymola, Dynamic Modeling Laboratory, is a powerful commercial simulation environment with the ability of dealing with huge systems described by more than hundred thousand equations. The Modelica translator of Dymola serves to symbolically translate the Modelica equations generating C-code for simulation. Graph theory is used to identify the variables to be solved for in each equation and to find the minimal set of equations. The generated C-code can, via its convenient interfaces, be transformed into a Matlab/Simulink S-function C-mex file which can be simulated in Matlab/Simulink as an input/output block [23].

Modelica has two very important features which make it very suitable for modeling and simulation of power systems. These features are detailed below.

2.2.1 Acausal modeling

In order to derive reusable models of the components of a system, the underlying mathematical equations should be stated in a neutral form without considering a computational order, meaning that no input/output port necessarily has to be assigned a priori to the model's terminals [22, 24]. Speaking of power systems, causality may not be generally assigned, because an explicit input-output state-space set of equations is required to represent the corresponding causal block model [33]. Often several manual rewritings, including differentiation, are required to transform the equations into this form. The need for manual transformations implies that it is cumbersome to build modeling libraries for physical systems using the causal block-based tools like Matlab/Simulink.

Furthermore, it is often the case that causal modeling creates algebraic loops. They occur, for example in Matlab/Simulink, when an input port with direct feedthrough is driven by the output port of the same block, either directly, or by a feedback path through other blocks which have direct feedthrough. Matlab/Simulink built-in solvers try to efficiently detect such algebraic loops, and to find analytic solutions by sophisticated iterative algorithms. However the detection of (un)breakable loops cannot always be guaranteed. Manual efforts to resolve the situation include, for example the use of an *Initial Condition* block, or adding a small *delay* block (depending on the time scale of the dynamics) at the risk of adding unnecessary dynamics, and often require considerable modeling intuition.

Note that these algebraic loops often, and also in the long-term voltage instability analysis under consideration in this thesis, result from replacing fast dynamics by algebraic steady-state equations. However, other studies e.g. electro-magnetic transient studies may contain no algebraic loops at all.²

To resolve this drawback, acausal modeling tools have been proposed. The main aim of acausal modeling is to relax the causality constraint, by focusing only on the individual components, and on the way these components are connected to each other (i.e. the topology of the system) [45,46]. Modelica effectively supports acausal modeling. The fundamental difference in the form of the dynamic equations required in the block-oriented and object-oriented tools is shown in Table 2.1.

Block-oriented	Object-oriented
$\dot{x} = f(x, u)$	
$y = g(x, u)$	$f(\dot{x}, x, u, y) = 0$

Table 2.1: Block-oriented versus object-oriented tools

2.2.2 Hybrid modeling

The behavior of power systems, as mentioned before, is characterized by the complex interactions between continuous dynamics of the system and the discrete events, i.e. a power systems exhibits complex hybrid behavior. The model of a typical power system is conveniently expressed by the following set of mixed discrete-event continuous differential-algebraic equations:

$$f(\dot{x}(t), x(t), z(t), y(t)) = 0 \quad (2.1a)$$

$$z(T_e^+) = Z(x(T_e^-), z(T_e^-), y(T_e^-), u(T_e^-)) \quad (2.1b)$$

$$z(t) = z(T_e^+), T_e \leq t < T_{e+1}$$

$$g(x(t), z(t), y(t)) = 0 \quad (2.1c)$$

where x denotes dynamic continuous state variables of the synchronous generators, AVRs, OXs and load dynamics, z the discrete-event state variables typically arising from discrete control logic such as thresholds reached by OXs, LTC tap positions, switched CBs and disturbances, T_e the time at which a discrete event e occurs, $T_e^- = \lim_{\epsilon \rightarrow 0} T_e - \epsilon$ the pre-event time, $T_e^+ = \lim_{\epsilon \rightarrow 0} T_e + \epsilon$ the post-event time, y the local algebraic state variables e.g. network voltages and currents in the load flow equations, u the discrete control inputs. The functions f , Z and g represent

²Transient studies deal for example with high-frequency impulsive overcurrent/overvoltage surges induced by switching operations (opening/closing a switch/circuit breaker) and/or lightning strokes using the theory of traveling wave, in the time scale of 1 μ s – 1 ms.

the continuous differential equations, discrete-event dynamics and algebraic constraints, respectively.

Modelica provides algorithms for solving ordinary differential equations (ODEs) and differential-algebraic equations (DAEs) that describe mathematically the continuous time components' model. It also supports several formalisms e.g. hybrid automata for modeling the evolution of the times when events occur.

2.3 Hybrid automaton (HA)

An HA is a dynamical system describing the time evolution of a system involving the interaction of both continuous and discrete state variables. An HA, as shown in Fig. 2.1, typically consists of several discrete modes, each mode represented by one discrete state variable, in which different continuous dynamics are followed as long as the corresponding invariants of the mode are satisfied. As soon as a transition guard is activated, based on violation of invariants (forcing condition) or fulfilling some enabling conditions on continuous state variables (enabling condition), or due to external events (e.g. a fault that can occur at any time like a lightning strike), the system switches to another discrete mode, possibly resetting some continuous state variables [47].

The HA representation of an LTC in a distributed control fashion S_{LTC-C} in Fig. 2.5, is an example where an external control action, in this case u , enables discrete mode changes.

Various formal definitions for HA in different research communities have been proposed so far [7]. The following definition has been adopted from [48].

An HA H is a 9-ple:

$$H = [Q, X, W, f_q, Init, Inv, E, G, R]$$

where

- $Q = \{q_1, q_2, \dots\}$ is the set of all admissible discrete modes q .
- $X \subseteq \mathbb{R}^n$ is the set of continuous state variables x .
- $W \subseteq \mathbb{R}^{m+p}$ is the set of external variables $\omega = [u \ y]$ appending input variables $u \in U \subseteq \mathbb{R}^m$ and output algebraic variables $y \in Y \subseteq \mathbb{R}^p$.
- $f_q(x, \dot{x}, \omega) : X \times X \times W \rightarrow \mathbb{R}^n$ represents the DAEs.
- $Init \subseteq Q \times X$ is the set of all admissible initial states (q, x) .
- $Inv(q) : Q \rightarrow 2^X$ is the invariant set in mode $q \in Q$.
- $E \subseteq Q \times Q$ is the set of events e .
- $G : E \rightarrow 2^X$ is the set of guard conditions.
- $R(e, x, \dot{x}, \omega) : E \times X \times X \times W \rightarrow 2^X$ is the reset map.

where 2^X denotes the set of all possible subsets of X .

For example the HA of Fig. 2.1 operates as follows, defining the possible evolutions for its hybrid states $(q, x) \in (Q, X)$. It starts in the initial state $(q_1, x_0) \in \text{Init}$, where the corresponding dynamics represented by the DAE $f_{q_1}(x, \dot{x}, \omega; x(0) = x_0) = 0$ is followed as long as $x \in \text{Inv}(q_1)$. As soon as the guard condition $\Delta \in G(q_1, q_2)$ is fulfilled, the event $e = (q_1, q_2) \in E$ occurs. This resets x to $\dot{x} \in R(e, x, \dot{x}, \omega)$, making a transition to state (q_2, x) where the corresponding dynamics $f_{q_2}(x, \dot{x}, \omega) = 0$ is followed as long as $x \in \text{Inv}(q_2)$, and so on.

In order to clearly describe the relation between the hybrid model of the system represented by equations (2.1a)-(2.1c), and the definition of an HA by the 9-ple above, one should notice that:

Assuming $z(T_e^-) = q_1$ and $(q_1, q_2) \in E$, then $z(T_e^+) = q_2$ is possible (thus the event set E defines function Z), also $f(\cdot, \cdot, z, \cdot) = f_q(\cdot, \cdot, \cdot)$, and the algebraic function g is defined by reset map R which simply assigns new values to some continuous state variables.

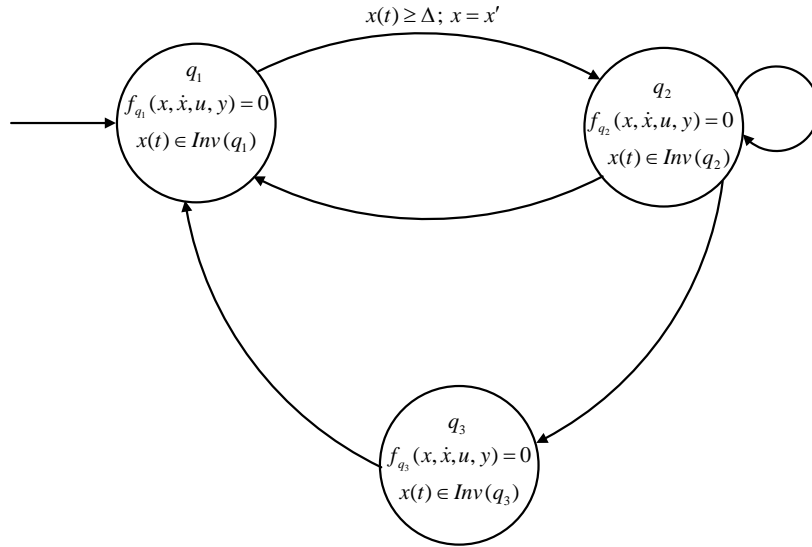


Figure 2.1: A simple hybrid automaton

2.4 Hybrid automaton component models for power system

In order to develop a sufficiently fast simulator, a power system is advantageously considered as a composition (or network) of interacting hybrid dynamical system

components. The formal HA modeling paradigm is then employed to model the underlying mixed continuous and discrete-event dynamics of the physical components. Every individual component is represented by an HA (or parallel composition of several HAs), where the continuous dynamics are expressed by DAEs, and discrete events are represented by the set of events of that HA (set E in § 2.3), using Modelica. The basic component models are briefly explained below.

2.4.1 ∞ -bus

By definition, an infinite bus refers to an infinitely strong rigid network with voltage and frequency unchanged under any load condition. Here it will be modeled as an ideal voltage source.

2.4.2 Transmission line

Transmission lines are often modeled as π -equivalent circuits but here for simplicity they will be modeled as series impedances. They are considered more inductive in transmission networks but more resistive in distribution networks.

2.4.3 Capacitor bank (CB)

A CB typically consists of a group of several identical capacitors, connected in parallel or in series with one another, which are switched on/off in steps. Automatic or manual switching of CBs can locally support the voltage in a connected bus, but also may cause some low/medium frequency oscillatory transients that affect power quality for nearby loads. Each switching step of a CB corresponds to the injection of some reactive power which is quadratically dependent on the voltage. This actually degrades the effectiveness of the CBs during voltage instability scenarios as it provides less reactive power support at low voltages [14].

2.4.4 Synchronous generator equipped with AVR and OXL

Synchronous generators are the primary source of active power and one of the main sources/sinks of reactive power in electrical power systems. Therefore, they are, to a great extent, responsible for maintaining a good voltage profile across a power system. The AVR controls the field current i_{fd} , which is proportional to field voltage E_{fd} in p.u., to keep the terminal voltage of the synchronous generator V close to the desired setpoint V_0 .

It is also standard practice for excitation systems to include an over excitation limit function to suppress the generator field current when the temperature of the field winding exceeds an allowable level [49]. The OXL protects the field winding

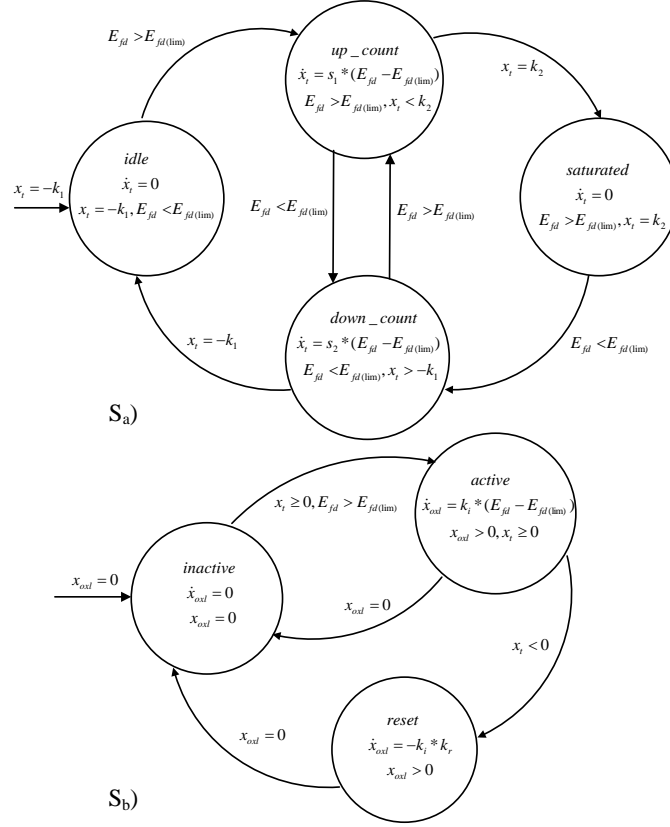


Figure 2.2: S_{OXL} : An HA representation of an OXL with inverse-time delay S_a and integral action S_b

from overheating when the generator is requested to provide too much field current [6]. This often occurs during voltage collapse incidents when generators are forced to produce some excessive reactive power beyond their capability. The OXL allows the full range of reactive power capability of a generator to be utilized, by keeping i_{fd} as close as possible to the limit $i_{fd(lim)}$ which is slightly larger than the permanent admissible field current. The OXL activation has a direct effect on voltage support provided by the generator, and thus its analysis is very important for enhancing voltage stability of a power system.

The HA representation of an integral-type OXL S_{OXL} , as a discrete-event part of the synchronous generator model, is shown in Fig. 2.2.

S_{OXL} implements a simple integral action with inverse-time characteristic to model OXL [25], and is composed of two synchronously executing machines S_a and S_b i.e. $S_{OXL} = S_a || S_b$. S_a and S_b implement inverse-time delay, and limit enforce-

ment by integral action respectively. If the generator field current i_{fd} , which is proportional to E_{fd} in p.u., exceeds the limit $i_{fd(lim)}$, the OXL intermediate state variable x_t starts increasing (approximately representing temperature increase in the field winding), and as soon as it becomes positive, the error integration initializes and produces an x_{oxl} signal that is subtracted from the AVR inputs causing i_{fd} to decrease.

Note that Armature Current Limiter (ACL) is also sometimes included in the excitation system of the generators (by providing an additional ACL feedback signal to the AVR inputs). The ACL, similar to OXL, prevents excessive current in the armature winding and thus protects it from overheating. However, the ACL is not primarily concerned in voltage control thanks to the larger thermal capability of the armature windings. Therefore, in this thesis a very simple fixed-current-pickup-value $I_{arm(lim)}$ (no deadband around $I_{arm(lim)}$) with fixed-time-delay T_{arm} (no inverse-time characteristic) is employed to model the ACL.

The HA representation of this ACL S_{ACL} , as another discrete-event part of the synchronous generator model, is shown in Fig. 2.3.

S_{ACL} consists of three simple discrete modes namely *ok*, *wait* and *limited*. If the generator armature current I_{arm} exceeds the limit $I_{arm(lim)}$ for longer than T_{arm} , the ACL becomes activated. This produces a feedback signal to be subtracted from the AVR main summing point that reduces the AVR voltage setpoint V_0 lowering the reactive power production of the generator.

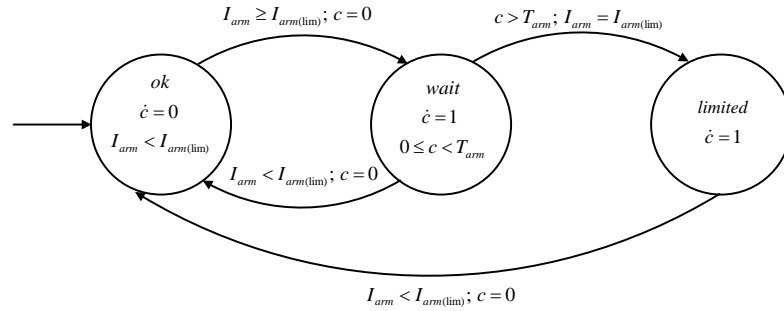


Figure 2.3: S_{ACL} : An HA representation of a simple ACL with fixed $I_{arm(lim)}$ and fixed T_{arm}

For the long-term voltage control studies, a 5rd order synchronous generator model (including AVR and OXL dynamics) can be employed, neglecting subtransients [6, 16]. By way of summary, the continuous part of this model is represented below:

$$\dot{x} = \begin{pmatrix} \Delta\omega \\ \frac{1}{2H}(P_m - P_e - D\Delta\omega) \\ \frac{-E'_q + E_{fd} - (X_d - X'_d)I_d}{T'_{do}} \\ k_i(E'_q + (X_d - X'_d)I_d - E_{fd(\text{lim})}) \\ \frac{-E_{fd} + G(V_0 - V - x_{\text{oxl}})}{T} \end{pmatrix} \quad (2.2)$$

where $x = (\delta \ \Delta\omega \ E'_q \ x_{\text{oxl}} \ E_{fd})^T$.

In the formulation above, the AVR is represented by the simple first-order transfer function with anti-windup limits on the field voltage, G being the steady-state open-loop gain of the AVR and T its time constant.

Note that since the overall system is assumed to successfully perform frequency regulation through a single slack bus, no governor system is considered in the model of the generator.

Under the control of AVR	$G(V_0 - V) = \frac{V^4 + V^2 Q X_d + V^2 Q X_q + Q^2 X_d X_q + P^2 X_d X_q}{V \sqrt{V^4 + P^2 X_q^2 + Q^2 X_q^2 + 2V^2 Q X_q}}$
Under the control of OXL	$E_{fd(\text{lim})} = \frac{V^4 + V^2 Q X_d + V^2 Q X_q + Q^2 X_d X_q + P^2 X_d X_q}{V \sqrt{V^4 + P^2 X_q^2 + Q^2 X_q^2 + 2V^2 Q X_q}}$
Under the control of armature current limiter	$Q = \sqrt{(VI_{\text{arm}(\text{lim})})^2 - P^2}$

Table 2.2: Different steady-state operating conditions of generator for voltage control

The voltage collapse in power systems is often a relatively slow phenomenon from several seconds to several minutes- and the long-term dynamics of interest thus can be advantageously captured by the well-known QSS approximation, assuming that short-term fast dynamics are infinitely fast and can be represented by their algebraic equilibrium equations instead of by their full dynamics [50]. QSS simulation allows obtaining much faster-than-real time simulators for reasonably sized systems.

Under steady-state operation, and for constant active power P , equation (2.3) describes the possible combinations of values of V and Q achievable for a typical unsaturated round-rotor generator with the field voltage E_{fd} :

$$E_{fd} = \frac{V^4 + V^2 Q X_d + V^2 Q X_q + Q^2 X_d X_q + P^2 X_d X_q}{V \sqrt{V^4 + P^2 X_q^2 + Q^2 X_q^2 + 2V^2 Q X_q}} \quad (2.3)$$

According to the well-known so-called VQ characteristic of a typical synchronous generator equipped with AVR, for any given active power (i.e. constant P), the over excitation limit and armature limit specify different operating conditions for voltage control.

In normal mode of operation, AVR controls the reactive power generation and maintains the terminal voltage (PV mode; constant terminal voltage).

For heavy load condition, the maximum reactive power generation limit may be reached, and from there on the generator terminal voltage is no longer controlled, but the machine will operate under OXL control (PQ mode; constant reactive power generation).

If the voltage degradation still persists, the armature limit may be reached and, as a result, the reactive power generation will be drastically reduced [6].

Different equations describing steady-state VQ characteristic of a synchronous generator is given in Table 2.2.

The discrete-event transition among these different operating modes of synchronous generator and the resulting interaction with its continuous nonlinear dynamics is being captured by concurrently running the underlying hybrid automata.

2.4.5 LTC

Among the available countermeasures against the long-term voltage instability in electrical power systems, LTC controls, as (one of) the most likely driving mechanisms for voltage control but also as a possible cause of voltage collapse in the long-term, is of special interest for the analysis presented in this thesis.

LTCs are slowly acting discrete devices. Under traditional deadband control of LTC, the transformer ratio r is changed by one step at a time if the voltage error ΔV at the designated side of the transformer (usually the distribution side) remains outside a deadband DB around a reference voltage V_{ref} longer than a specified time delay T_d [6,31]. The tap position n is then changed after a mechanical time delay T_m in order to control the voltage of the connected bus.

In addition to the standard deadband logic for the operation of LTCs in the normal control mode, some other control logics are often added as so to enable LTCs to more effectively contribute to the long-term voltage control in the emergency control mode. Most existing emergency/modified LTC control strategies are implemented in the following ways [51], where only local voltage measurements determine the actions, without coordination with other LTCs, and without anticipation of saturation of OXLs:

- Blocking: fixing tap positions at their current positions.
- Locking: moving to a specific tap position, and then blocking at this tap position.

- Reversing: changing the control logic to control the transmission side voltage instead of the distribution side [52].
- Voltage setpoint reduction: lowering the reference voltage.

The common drawback of all those rule-based logics is that they all first require to identify on which LTCs to act. This identification is not a trivial task as it can be realized in many different ways. Furthermore, blocking and locking logics “kill” the tap-changing functionality of LTCs (by simply changing them to fixed transformers), ignoring all the voltage support contribution they can have for voltage control. On the other hand, those local heuristic rules may not either suffice to face all possible scenarios in a large and complex power system. Thus there is, obviously, a need for automatic model-based coordination of LTCs. To the best of our knowledge there has been relatively little attention paid to devising a truly model-based anticipating and coordinating voltage control of LTCs.

In order to be able to design a model-based coordinating controller we need a dynamical model of an LTC. Here the LTC for simplicity is modeled as an ideal transformer with variable $1 : n$ tap ratio in series with a pure leakage reactance X . Figures 2.4 resp. 2.5 show the HA representation of an LTC in the classical uncoordinated fashion S_{LTC-DB} resp. in the distributed coordinating control fashion S_{LTC-C} (to be introduced later on in this thesis).

S_{LTC-DB} includes three discrete modes, namely *idle*, *count* and *action*. S_{LTC-DB} remains in the discrete mode *idle* as long as the local voltage deviation ΔV is less than a chosen deadband $DB/2$. This is a classical uncoordinated action. Upon exceeding this limit, a timer c is initialized and a transition to the discrete mode *count* occurs. Timer c runs until either it reaches the time delay T_d causing another transition to the discrete mode *action*, or until the voltage deviation ΔV becomes less than the deadband $DB/2$ returning the HA back to the mode *idle*. In mode *action*, the discrete state LTC tap position n is changed after the mechanical time delay T_m , returning the HA back to the mode *idle* [53].

S_{LTC-C} includes two discrete modes namely *idle* and *action*. S_{LTC-C} remains in the discrete mode *idle* until the corresponding CA requests, by an external signal, an upward $u = +1$ or downward $u = -1$ tap change. This external control input signal u can coordinate, and will be defined later on in chapter 4 of this thesis. When $u = \pm 1$, a transition to the mode *action* occurs, returning the HA back to the mode *idle* by changing discrete state LTC tap position n after T_{delay} seconds counted by a timer c , and updating the position n .

2.4.6 Load

Loads undoubtedly are one of the most important factors in voltage instability which is often also referred to as load instability [6, 19]. Loads in practice are an

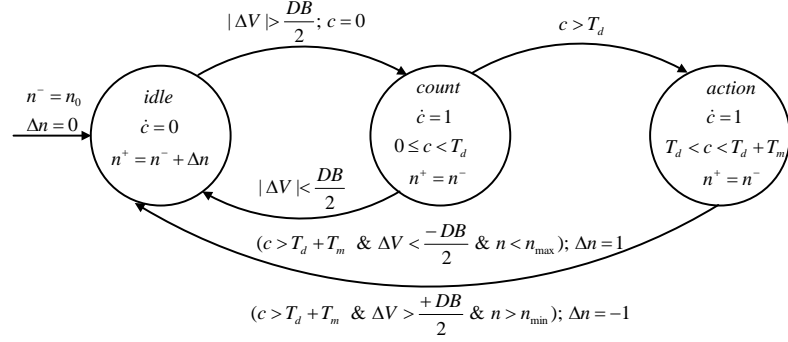


Figure 2.4: S_{LTC-DB} : An HA representation of an LTC in the classical uncoordinated fashion

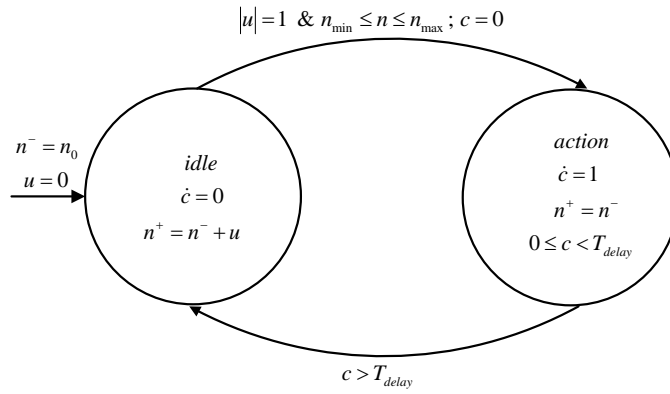


Figure 2.5: S_{LTC-C} : An HA representation of an LTC in the distributed operation fashion

aggregation of a large variety of many different individual load devices such as induction motors, thermostatic loads and household loads, and thus are often represented in a generic aggregated model. This eliminates the unrealistic/impractical need for identifying the voltage response of the individual loads.

Load models are traditionally classified into two broad categories namely *static* models and *dynamic* models, associated with steady-state and dynamic voltage instability analysis [54–56].

2.4.6.1 Static load models

The static load model is a set of algebraic equations to characterize the relationship between bus voltage and active and reactive power absorbed by the load, when

load voltage varies slowly. The consumed powers P, Q of static models are only a function of the load bus voltage. This model does not reflect the dynamic behavior of the load, and thus is mainly employed in steady-state load flow studies.

A common practice is to represent the voltage dependence of static loads in exponential form as below [6, 54]:

$$\begin{aligned} P &= P_0 \left(\frac{V}{V_0} \right)^\alpha = P_0 V_{\text{pu}}^\alpha \\ Q &= Q_0 \left(\frac{V}{V_0} \right)^\beta = Q_0 V_{\text{pu}}^\beta \end{aligned} \quad (2.4)$$

where P_0 and Q_0 are the active and reactive powers consumed at the reference voltage V_0 , and the exponents α and β represent the voltage dependence of the load. Three particular types of load namely constant impedance (Z), constant current (I) and constant power (P), are respectively obtained for values of $\alpha = \beta = 2, 1, 0$. The well-known *ZIP* load model is a special class of static load model which a composite of these three types:

$$\begin{aligned} P &= P_0 \left(a_P \left(\frac{V}{V_0} \right)^2 + b_P \left(\frac{V}{V_0} \right) + c_P \right) = P_0 (a_P V_{\text{pu}}^2 + b_P V_{\text{pu}} + c_P) \\ Q &= Q_0 \left(a_Q \left(\frac{V}{V_0} \right)^2 + b_Q \left(\frac{V}{V_0} \right) + c_Q \right) = Q_0 (a_Q V_{\text{pu}}^2 + b_Q V_{\text{pu}} + c_Q) \end{aligned} \quad (2.5)$$

where the coefficients a_P, b_P, c_P, a_Q, b_Q and c_Q determine the shares of Z, I and P loads, and satisfy $a_P + b_P + c_P = a_Q + b_Q + c_Q = 1$.

2.4.6.2 Dynamic load models

The dynamic load model includes differential equations in order to reflect the load dynamics, the consumed powers P, Q being a function of both time and bus voltage. This model is mainly employed in dynamic voltage stability studies, when the magnitude of the load voltage may vary over a large range, at the same time scale as the voltage dynamics in other buses in the network. Field test results indicate that the typical response of an aggregated load to a sudden step in load voltage can be characterized by an instantaneous change in the load power demand (the transient characteristic of the load), followed by a time span for the load to recover to steady-state (recovery time constant) [57]. During this restoration process, the dynamics of various load components (induction motors, thermostatic loads) and control mechanisms (including LTCs) tend to restore load powers at least to a certain extent. These characteristics are typically modeled by a so called generic

dynamic self-restoring load model as below [6, 54]:

$$\begin{aligned} \dot{x}_P &= -\frac{x_P}{T_P} + P_0\left(\left(\frac{V}{V_0}\right)^{\alpha_s} - \left(\frac{V}{V_0}\right)^{\alpha_t}\right) \\ P &= (1-k)\left(\frac{x_P}{T_P} + P_0\left(\frac{V}{V_0}\right)^{\alpha_t}\right) \\ \dot{x}_Q &= -\frac{x_Q}{T_Q} + Q_0\left(\left(\frac{V}{V_0}\right)^{\beta_s} - \left(\frac{V}{V_0}\right)^{\beta_t}\right) \\ Q &= (1-k)\left(\frac{x_Q}{T_Q} + Q_0\left(\frac{V}{V_0}\right)^{\beta_t}\right) \end{aligned} \quad (2.6)$$

where

P, Q : actual active resp. reactive power consumed by the load

P_0, Q_0 : nominal load powers consumption

V : actual load voltage

V_0 : reference voltage

T_P, T_Q : active resp. reactive power recovery time constants

x_P, x_Q : continuous state variable of load dynamics

α_s, β_s : steady-state active resp. reactive power voltage dependency

α_t, β_t : transient active resp. reactive power voltage dependency

The scale factor of $(1 - k)$ on the load powers has been introduced to model load shedding. No load shedding (full load) corresponds to $k = 0$, while complete load shedding is given by $k = 1$.

In case of any voltage drop on the load bus following a disturbance, the load restoration process will initially start responding with its transient characteristics, and the instantaneous power consumed will drop instantaneously. Following this, the load state variables x_P and x_Q will start to increase causing both actual active and reactive power to recover to their steady-state characteristics. This process will end when as soon as the steady-state characteristics are reached.

Note that the static load models (equations (2.4)) are just a special case of the dynamic load models (equations (2.6)), taking $T_P = T_Q = 0$ (infinitely fast response) and $\dot{x}_P = \dot{x}_Q = 0$ (no dynamics).

2.5 Conclusions

The two fundamental limitations of the block-oriented tools such Matlab/Simulink are causal modeling and very high probability for the occurrence of the algebraic loops. Modelica is a free object-oriented equation-based language which allows the development of simulation tools for modeling and simulation of the large-scale compositional systems such as electrical power networks. Modelica effectively

takes the hybrid nature of the power systems into account by allowing the composition of DAE components and DES/hybrid components.

In order to resolve the above-mentioned drawbacks of block-oriented simulation tools like Matlab/Simulink, and also to effectively capture the complicated interactions between continuous dynamics and discrete events in power systems, this chapter has developed a much-faster-than-real-time simulator, using Modelica. The simulator easily allows the reuse of the components' models, and implementation of the model-based predictive coordination control strategy.

3

The need for coordination

3.1 Introduction

The coordination of the control actions in a network of many interacting components, where each component is controlled by an independent CA, is a very challenging problem. Indeed coordination seems to be inevitable in any network of interacting components where a local perturbation can lead to global performance degradation. Some examples are:

- voltage control in multi-area power systems
- traffic lights in an urban traffic network
- on-ramp metering in control of freeway traffic, taking overflow into neighboring roads into account
- flood control, where controllable gates can regulate the flow of water

The case study of voltage control in large-scale multi-area power systems is an interesting application for coordination control, as the poorly coordinated operation of those areas (each operated by an independent TSO) may endanger the power system security, for example, by increasing the risk of blackouts. In the case of a simple and small interconnected power system, e.g. power systems consisting of at most two areas, or in the conventional radial distribution networks with the integration of distributed generation (DG) units, the coordination may be obtained by heuristic ad-hoc schemes based on off-line assessment of utilities [6, 53]. As

the size and heterogeneity of the network increases, or in the case of a complex meshed structure, coordination can become a very challenging or even infeasible problem. Local control actions in one area may have strong influence on the system variables of its neighboring utilities initiating further, possibly undesirable, control actions by those neighbors, leading to even more control actions in the local component as well as in all its neighbors.

Designing a possible coordination strategy is a major challenge involving many issues such as what information to communicate, how to avoid the need that each area knows the global model, and last but not least the choice of abstraction level of the models.

Coordination achieved in the control algorithm introduced in this thesis via exchanging messages on scheduled control actions among CAs, should be implemented in such a way that each area has its own voltage regulator. This TSO-wise coordinator determines the favorable combinations of control actions with respect to the voltage profile of its own area i.e. to maintain the voltage profile at the scheduled level while maintaining the net tie-line active/reactive power interchange from the given area at acceptable values.

The communication and information exchange must also be limited as electricity utilities tend to preserve some prerogative of their own system operation, and it may not be acceptable to reliably communicate all the necessary information about operational conditions, scheduled active/reactive power generation pattern, load demand, control actions, objective functions and constraints to neighbors.

Another challenge for TSOs is to approximate the dynamic model of their (possibly) complex-structured neighboring utilities. Standard abstraction algorithms e.g. Thévenin theorem calculate exact equivalence, while advanced predictive model-based control theory needs an approximated model. Obviously, the latter should be capable of reflecting the changes occurring in the neighboring areas as a reaction to the neighbor's control actions (communicated), and as a reaction to their own active/reactive power exchange with neighbors, but without requiring too much computation and without being too sensitive to inaccurately known and changing parameters of the approximated model of the neighbors.

To design a well-performing system-wide coordination control in large-scale multi-area power system, the afore-mentioned important issues need to be carefully addressed. As far as we know, little attention has been paid on devising a truly model-based coordinating feedback voltage control of complex interconnected power systems. This chapter is devoted to show the need of coordination for voltage control in electrical power systems, and to explain the principles of the coordination control, addressing some of the above-mentioned challenging issues.

3.2 Example illustrating the need for coordination

This example illustrates why coordination is necessary for voltage control in power systems, and how different local control actions can trigger each other. The 12-bus meshed test system, shown in Fig. 3.1, is adopted from [58]. LTCs 1, 2 and 3 respectively try to locally maintain the voltage of buses A , B and C within an upper and lower bound $[0.98, 1.02]$ p.u. by using deadband strategy modeled by S_{LTC-DB} in chapter 2. Two pairs of “bus voltage-LTC moves” namely (LTC 1, Bus A) and (LTC 2, Bus B) are shown in Fig. 3.2, following the outage of two parallel lines¹ in the location F at $t = 20$ s. Following the fault, both LTCs, after a delay of 10 s, try to restore the corresponding local voltages. As one can see, the voltage of Bus A is already within its safety limit around $t = 40$ s, but still one extra move around $t = 82$ s is observed. The reason is that the LTC 2 causes the voltage at Bus A to drop below its threshold, again causing LTC 1 to activate its local deadband strategy. Thus, this extra move is indeed attributed to the interaction between LTC 2 and Bus A (via LTC 3 and Bus C). A possible coordination scheme should aim at avoiding these kinds of interactions among local controllers.

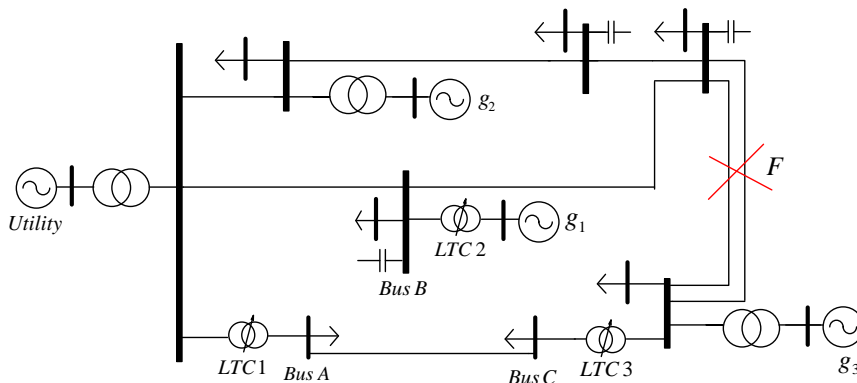


Figure 3.1: On-line diagram of a 12-bus power system

3.3 Trial and error coordination

In order to study the mechanisms involved in voltage instability, two case studies are considered. The attempt is to illustrate that the proper coordination among

¹The local deadband and fault are particularly chosen to illustrate the interaction among local controllers.

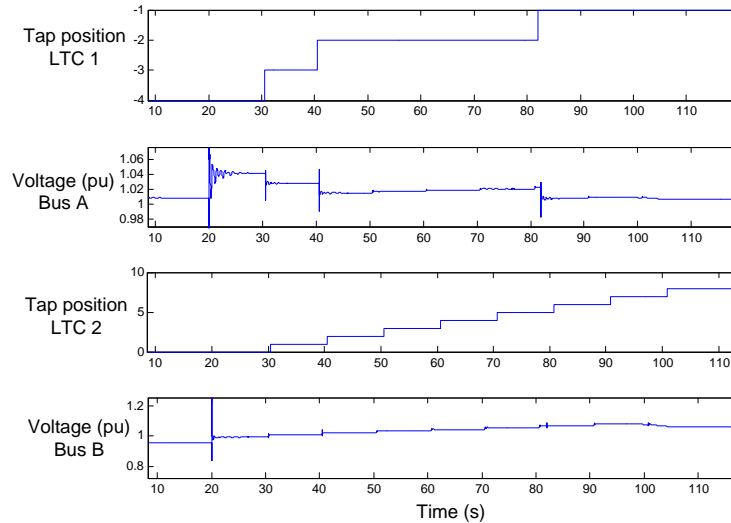


Figure 3.2: Bus voltages and the corresponding LTC actions

available control actions can stabilize system voltages in circumstances where uncoordinated control actions lead to a final collapse.

The primary control objective is to stabilize all bus voltages within the interval $[0.9, 1.1]$ p.u. by applying different countermeasures against voltage instability. The secondary objective is to minimize the amount of load to be shed by a properly coordinated voltage control.

The coordination, here in this chapter, is achieved by a manual, heuristic design approach, in a trial and error fashion, by carrying out many simulations. However, systematic search strategies, using the proposed Modelica simulation tool, will be presented in the following chapters.

The simulation results also show that the developed hybrid simulator is much faster-than-real-time, and can effectively capture the interactions between continuous dynamics and discrete events.

3.3.1 Case study 1

The first case study [59], is a small 4-bus meshed power system, as shown in Fig. 3.3. The system is composed of one slack bus ∞ , one generator G equipped with OXL, an LTC, a capacitor bank C and a dynamic recovery load L connected by 3 tie-lines $l1$, $l2$ and $l3$.

To have an idea about time scale values involved in the simulations in this chapter, note that $T'_{do} = 8$ s for the synchronous generators, $T = 0.1$ s for the AVRs, $T_d + T_m = 30$ s for LTCs and $T_P = T_Q = 60$ s for the loads have been considered.

3.3.1.1 Uncoordinated deadband control

The response of the system, following the tripping of only one circuit in *l3* at $t = 100$ s is illustrated in Fig. 3.4, where a standard uncoordinated deadband control strategy modeled by S_{LTC-DB} is applied. The bus voltages, LTC tap position, generator field current and x_t and x_{oxl} signals are shown in Fig. 3.4.

Instability occurs and the solver fails to solve the nonlinear equations of the system at $t = 262$ s when simulation stops because the system becomes unstable, leading to stopping the progress of simulation time due to unbounded (in practice extremely large) values of derivatives of state variables.

Directly following the fault, bus voltages drop. After this point the system dynamics is initially driven by the LTC trying to restore the distribution-side load voltage. Further drop in voltages initiates the inverse-time mechanism of the OXL, known as x_t signal, at $t = 179.2$ s. This leads, after approximately 45 s, to the activation of OXL at $t = 225.8$ s, and consequently the voltage support provided by generator *G* is withdrawn. The dynamic load restoration still deteriorates the voltage decline, and the final collapse occurs at $t = 262$ s. Note that the generator field current E_{fd} keeps rising up to the value 2.08 p.u., but activation of the integral-type OXL forces it to $E_{fd(lim)} = 1.85$ p.u. at $t = 225.8$ s.

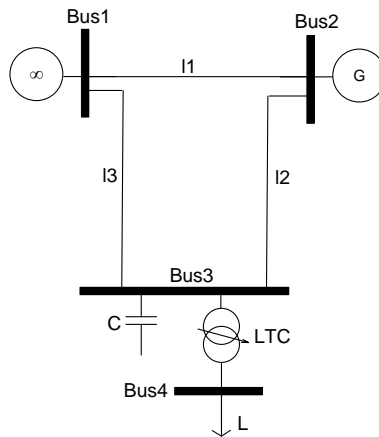


Figure 3.3: Case study 1: one-line diagram of a 4-bus power system

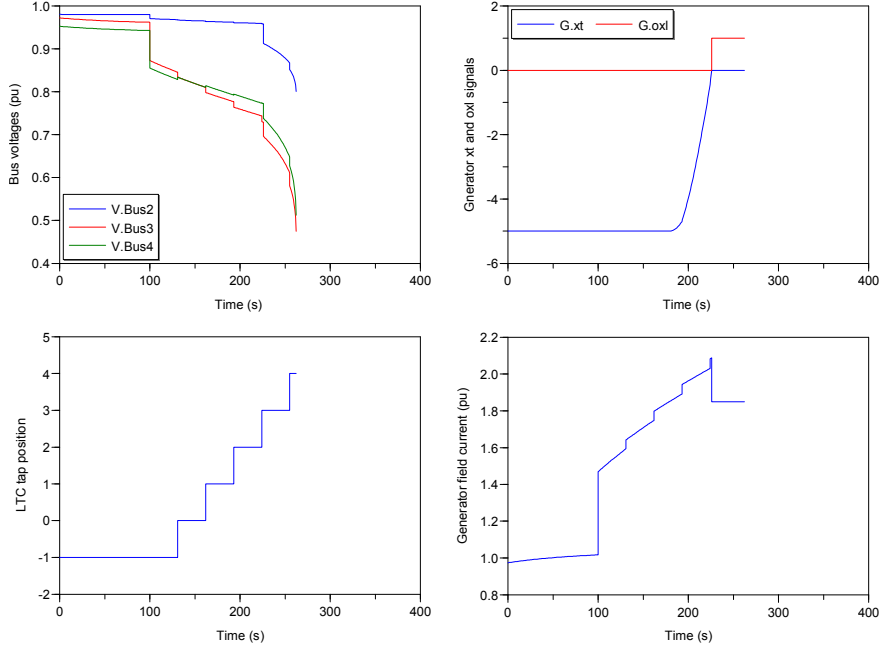


Figure 3.4: Case study 1: uncoordinated deadband control

3.3.1.2 CB switching

One CB, corresponding to 0.1 p.u. of reactive power support, is manually² switched on at $t = 110$ s to support the voltage at Bus3. This injects some additional reactive power to the system, and thus the reactive power limit of generator G is reached slightly later at $t = 284.5$ s. As shown in Fig. 3.5, the overall system response is quite similar to the former scenario with some time shift. x_t initiates at $t = 224$ s when the generator field current E_{fd} exceeds its limit $E_{fd(lim)} = 1.85$ p.u., and keeps rising up to the value 1.99 p.u. at $t = 284.5$ s when OXL become activated. After this point, the system evolves under the effect of the field-current-limited generator G and LTC moves, eventually leading to a voltage collapse $t = 348$ s. Clearly, this sole control action is not capable of stabilizing the system voltages.

3.3.1.3 Load shedding

The response of the system, when 25% of the load L is shed at $t = 110$ s, is shown in Fig. 3.6. This effectively stabilizes all system voltages above 0.9 p.u., OXL does not get activated at all, and generator field current E_{fd} remains far below the

²No feedback from measured local voltage or available VAR is used to decide upon CB switching. The switching time is chosen heuristically in order to illustrate the local voltage support provided by CB.

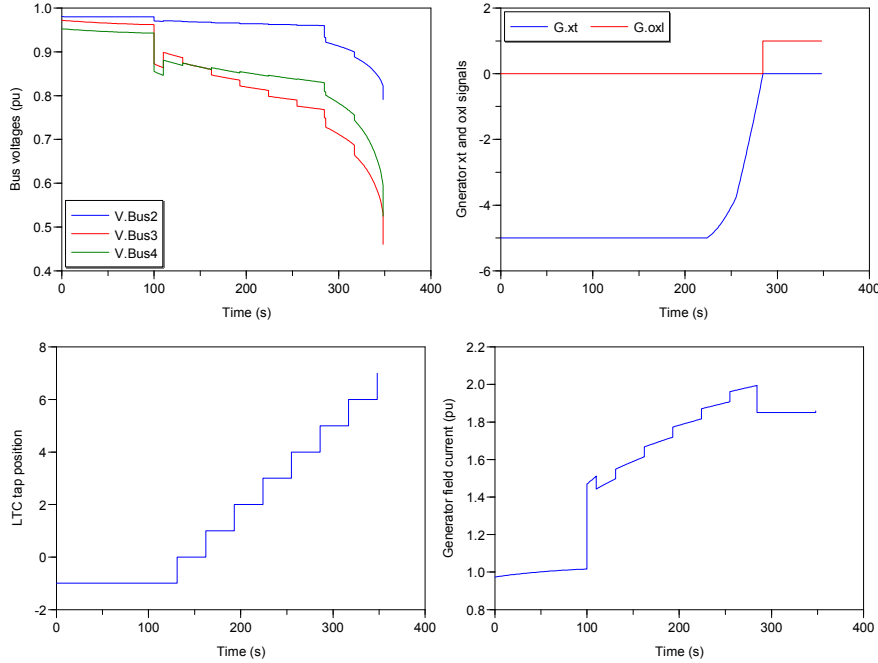


Figure 3.5: Case study 1: CB switching

limit $E_{fd(lim)} = 1.85$ p.u. Note that the system voltages, not shown here, are not stabilized even with 10% of load shedding.

It is noteworthy to mention that load shedding is an effective widely used countermeasure against voltage collapse but its use should be postponed as the last resort. Most existing load shedding schemes are activated manually by the system operator, and often are very expensive and undesirable from the customer's point of view [6]. However automatic under-voltage and/or under-frequency load shedding, and demand side management in the context of smart grids might provide better performance.

3.3.1.4 Coordinated action of LTC and CB

As stated before, single strategies such as one step CB switching, and 10% load shedding fail to arrest the voltage collapse. However, simulation results show that it is possible to stabilize all the bus voltages by a coordinated application of three steps of CB switching (corresponding to 0.3 p.u. of reactive power support) and LTC setpoint reduction, even without load shedding.

The system response is shown in Fig. 3.7, where the voltage setpoint V_{ref} for LTC deadband controller is reduced to 0.94 p.u. at $t = 110$ s, and the additional reactive power is injected by CB at $t = 130$ s. This manual coordination effectively

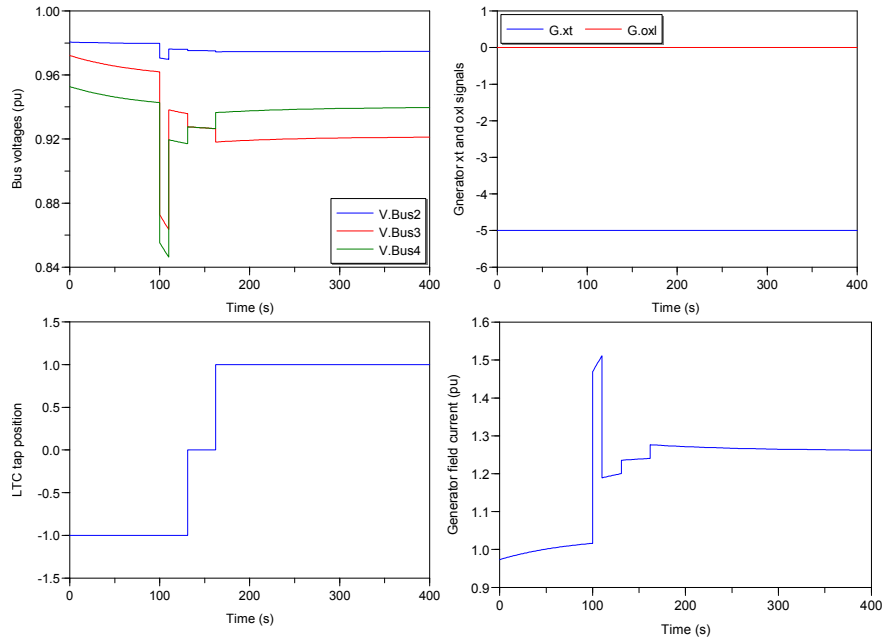


Figure 3.6: Case study 1: load shedding

stabilizes the system voltages, and no load is shed.

Note that this is not the optimal coordinated control strategy as no attempt was made to minimize the amount of CB switching, rather it shows that there exists some coordination strategy that stabilizes the system without load shedding.

This example clearly shows both need for anticipation and coordination features for voltage control in electric power networks. A (potential) “looking-ahead” voltage controller can anticipate the activation of OXLs in advance, and implements a local control action that does not lead to this constraint violation. Furthermore, by including an additional coordinating feedback signal among available local controllers, a multi-agent control system can be formed that aims to more effectively stabilize the voltages in the overall system.

3.3.2 Case study 2

The second case study is a 12-bus power system, as shown in Fig. 3.8, adopted from ABB [60]. It sets a control problem with around 20 control inputs, many measured disturbance inputs and up to 30 controlled outputs. This reasonably sized network is simulated to show the effectiveness of the proposed hybrid framework via some interesting experiments relating to coordinated voltage control.

This system is composed of three topologically almost identical areas connected

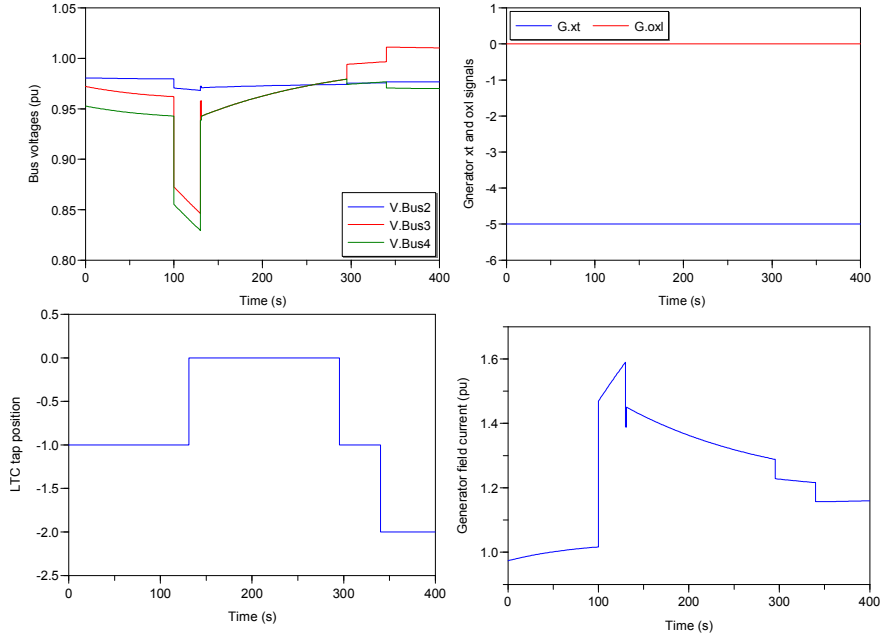


Figure 3.7: Case study 1: coordinated control actions

together via three double tie-lines as transmission system. The generators in *Area2* and *Area3* are equipped with OXL modeled as in § 2.4.4, while *Area1* is fed by an ∞ -bus. The distribution substation in each area is equipped with an LTC and a CB.

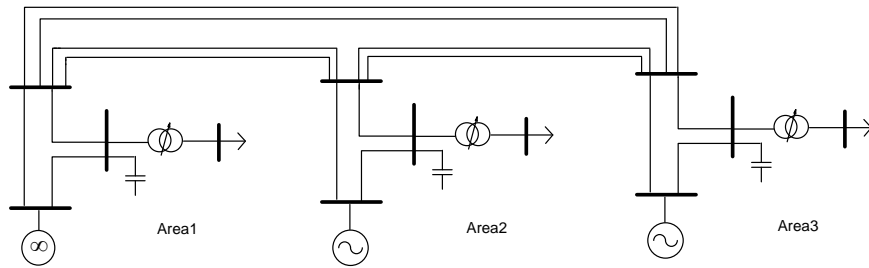


Figure 3.8: Case study 2: one-line diagram of a 12-bus power system

3.3.2.1 Uncoordinated deadband control

The load voltages, and the behavior of LTCs and OXLs are shown in Fig. 3.9, following the tripping of the double tie-line between *Area1* and *Area3* at $t = 100$ s where a standard uncoordinated deadband control strategy is applied. Instability occurs and the solver fails to solve the nonlinear equations of the system at $t = 652.3$ s when simulation stops corresponding (as explained above) to the system collapsing (instability). Directly following the fault, load voltages in each area drop, only slightly in *Area1* as compared to others, but soon afterwards a short-term equilibrium, with all load voltages apparently settling down close to 1 p.u., is established. After this point the mechanism driving the system response is LTC and OXL together with load dynamics.

Immediately after the fault the generator field current in *Area2* jumps to 2.13 p.u. exceeding $I_{fd(lim)} = 1.88$ p.u. for this generator. This initiates the inverse time characteristic of the OXL and eventually the OXL is activated at $t = 140.7$ s, meaning that the voltage support provided by this generator is withdrawn. This results in a further reduction of the load voltage causing the LTC to increase the tap position until the maximum tap limit is reached. Note that the integral type OXL forces the field current to $I_{fd(lim)}$, and subsequent tap changes result in a transient field current rise, which is quickly sensed and corrected by the OXL.

3.3.2.2 LTC setpoint reduction

The former experiment shows the LTC tap movements in *Area2* and *Area3* further aggravate the load voltage profiles and finally the load voltages drop below 0.9 p.u. Therefore, if the LTC tap movements can be somehow blocked or at least be slowed down, it intuitively seems that the voltage collapse could be possibly avoided or at least be delayed. Here, the load restoration process will be disabled by the reduction of the LTC setpoint voltage from 1 p.u. to 0.95 p.u. at $t = 150$ s in both *Area2* and *Area3*. As shown in Fig. 3.10, this results in two downward tap movements for LTCs in both areas which relieves generator in *Area3* of saturation, and its field current is kept slightly below the limit $I_{fd(lim)} = 1.75$ p.u., meaning that the corresponding OXL will not be activated in the long-term and, as a result, all load voltages are eventually stabilized above 0.95 p.u. This shows that coordinated actions by the LTCs in neighboring areas can avoid the voltage collapse.

3.3.2.3 A coordinated application of (one step) CB switching, LTC setpoint reduction and (one step) load shedding

Suppose that the fault considered earlier is followed by another line tripping, one of the circuits between *Area2* and *Area3* at $t = 110$ s. It happens frequently that voltage collapse initiates due to a cascade of events.

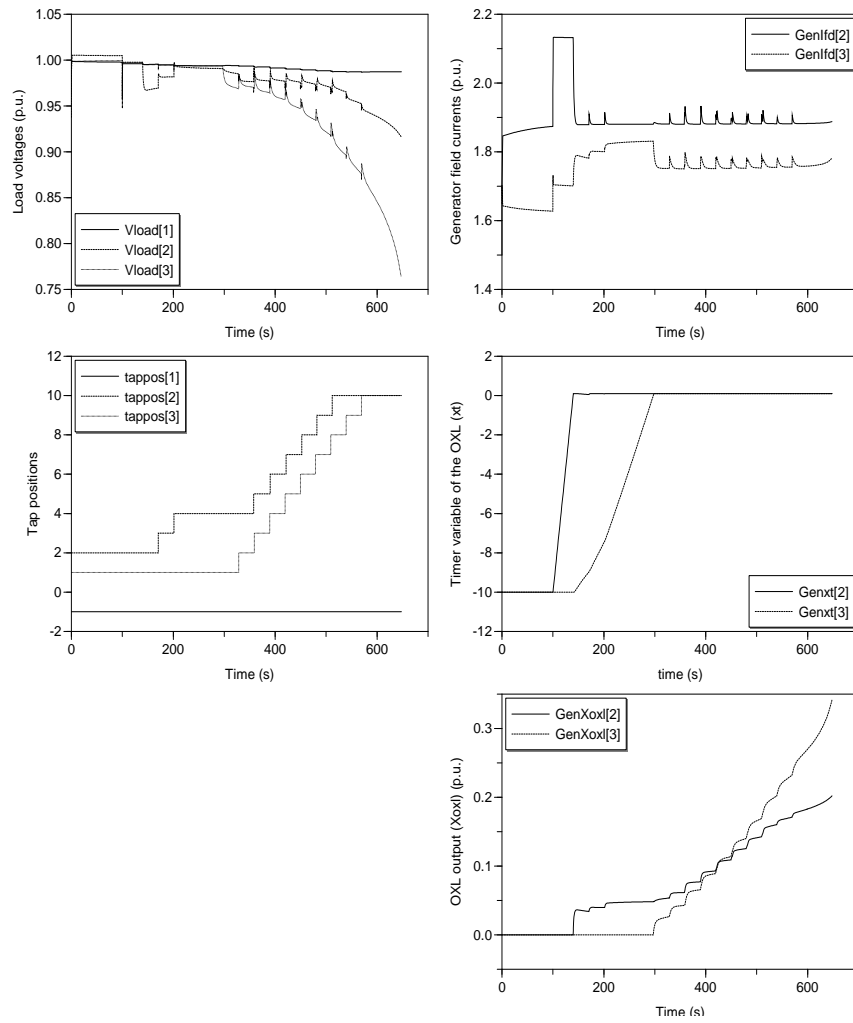


Figure 3.9: Case study 2: uncoordinated deadband control

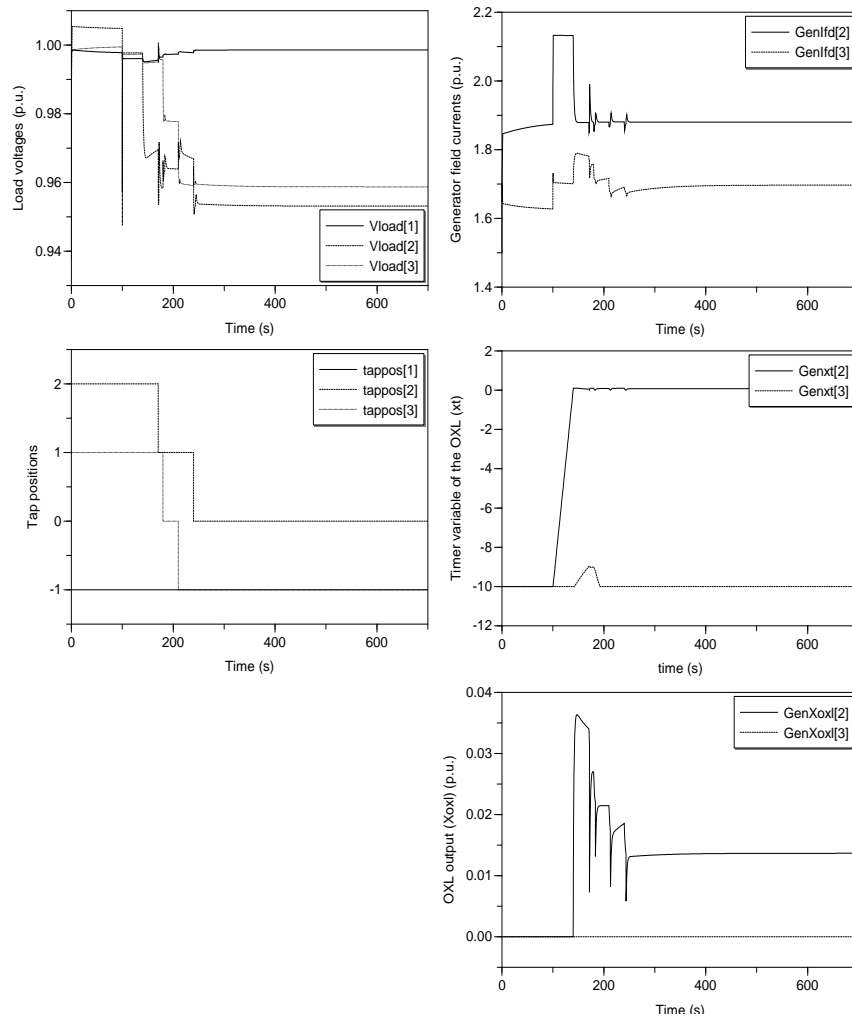


Figure 3.10: Case study 2: LTC setpoint reduction

Simulation results, not shown here to avoid repetition, show that single strategies such as LTC setpoint reduction, one step CB switching (corresponding to 0.1 p.u. of reactive compensation), one step load shedding (corresponding to disconnection of 10% of the load), and even a mixture of the LTC setpoint reduction and CB switching individually fail to arrest the voltage collapse. However, it is possible to stabilize all the load voltages by a coordinated application of (one step) CB switching, LTC setpoint reduction and (one step) load shedding in all areas at the right moment.

As shown in Fig. 3.11, switching of CB in *Area2* relieves the generator in this area of some reactive power, on the other hand, load shedding in both *Area2* and *Area3* relieves the generators in these areas of both active and reactive power, and, as a result, keeps the generator field currents for both generators well below their limits ($I_{fd(lim)} = 1.88$ p.u. for *Area2* and $I_{fd(lim)} = 1.75$ p.u. for *Area3*). Notice that neither of the OXLs are active in the long-term.

3.4 Main trends in development of coordination schemes

In the context of large-scale multi-area power systems, control areas are typically interconnected through power transmission corridors carrying often heavy power flows. The power flow in the tie-lines of these interconnected areas may be controlled to ensure economical benefits/constraints as well as to avoid possible voltage collapses [61]. The voltage and current values at boundary buses, and hence the flow of active and reactive power over the tie-lines depend on the control actions taken by different involved parties. It happens that a local initiating disturbance in one area triggers some undesirable control actions in the neighboring areas. A complex interaction among the CAs can eventually destabilize the whole system. Thus, secure operation of multi-area power systems requires appropriate coordination of the local control actions with those actions taken by (at least adjacent) CAs. Note that CA_i , associated to control area i , in practice only has local knowledge about its own model and may only know about active/reactive power flow or the voltage profile at interconnections.

Roughly speaking, coordination strategies can be classified into three different trends, described in the following three sub-sections:

3.4.1 Centralized coordination schemes

A centralized coordination unit at the top level of the hierarchy receives information from all CAs via communication links. All control actions to be taken by CAs are computed in one single multi-party (possibly multi-objective) optimiza-

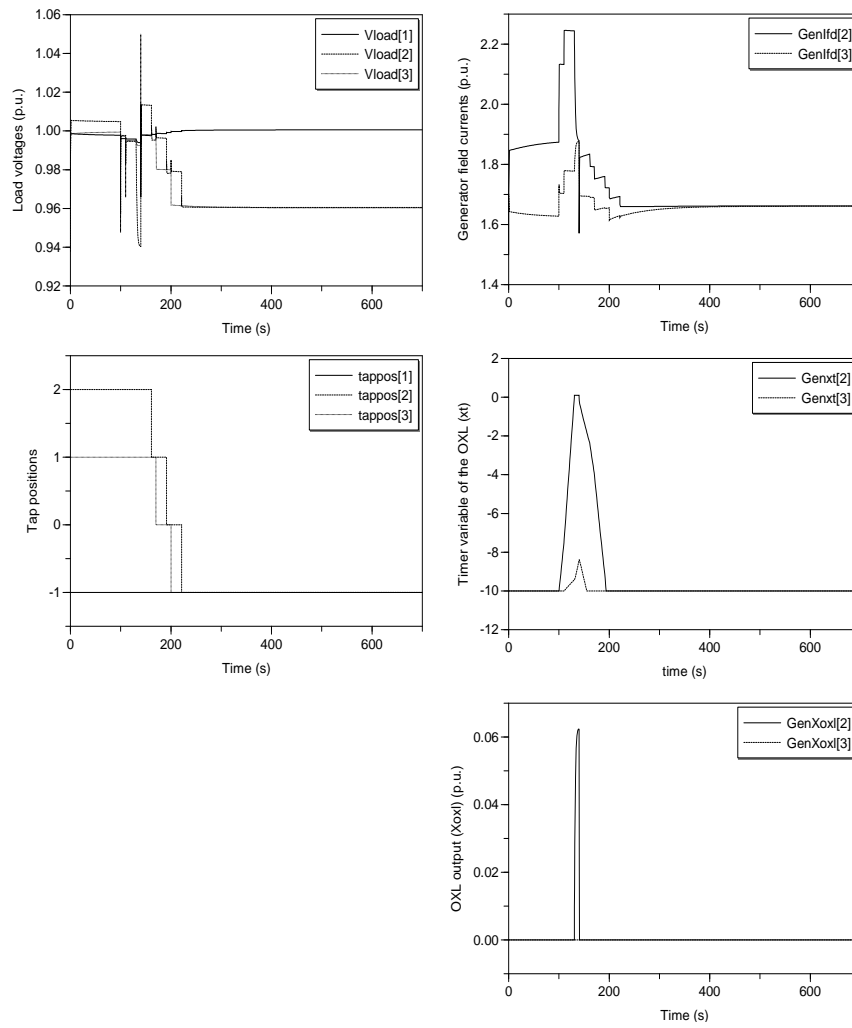


Figure 3.11: Case study 2: coordinated application of CB switching, LTC setpoint reduction and load shedding

tion problem, subject to individual constraints of each single party as well as the common constraints on the tie-line flows. Typical cost functions are, for example, minimization of the voltage deviation, active power losses/generation costs, switching of the discrete controllers, or maximization of the reactive power reserves. The centralized optimal solution, also called the Pareto optimal solution, assigns the least possible cost to every party so that there exists no other solution that reduces at least one cost without increasing any other costs (and no constraints are violated) [34, 62].

The main drawback of centralized coordination in large-scale multi-area power systems is the huge computational cost, the lack of robustness due to requiring global knowledge of the complete model of the overall system, and reliability problems due to possible communication failures. In addition, the decision made by the central coordination unit should be sufficiently “fair” to be accepted by each party. The concept of fairness in the sense of economics has been briefly studied in [63], where fairness criteria namely “free from envy”, “efficiency”, “accountability” and “altruism” have been defined using a centralized optimization of a multi-area power system. Successful centralized coordination has been reported only for rather small-scale power systems [35, 64, 65].

3.4.2 Decentralized schemes (no coordination)

On the other hand (purely) decentralized schemes with no information exchange have been proposed to overcome the above-mentioned drawbacks of centralized approaches. CAs are assumed to be non-overlapping. Each CA solves its own optimization problem without taking the objective and constraint of neighboring areas into account, and ignoring the interactions among CAs [27, 66–70]. In the context of large-scale multi-area power systems where the dynamics of the different areas are highly coupled, the decentralized approach may not lead to well-performing system-wide coordination control as has been illustrated in sections 3.2 and 3.3. The decentrally computed solutions will in general not converge to the (nearly) optimal global centralized performance. It may not even be stable in cases where a stabilizing centralized controller exists.

3.4.3 Distributed coordination schemes

A recently developed state-of-the-art approach [34, 71, 72], a so-called distributed coordination scheme, relies on partitioning of the large-scale power system into several areas, each area being possibly controlled by an independent TSO.

Each CA is assumed to have exact and detailed information on its own area (accurate dynamic model, and all the local on-line measurements including voltages and power flows at interconnections). Furthermore, the effect of the neighboring areas is taken into account only by representing them with an approximately equiv-

alent model. The parameters of this equivalent model must be updated on-line by appropriate parameter identification techniques as the system's dynamics evolves in time. Furthermore, each CA is assumed to agree on transmitting some of its on-line information to the neighboring CAs. Intuitively, the minimal information necessary for achieving acceptable performance includes the local control decisions (solutions of the local optimization problem) [73]. In this way, distributed coordination strategies combine the advantages of both centralized and decentralized approaches. CAs may further negotiate on what additional information should be exchanged. The performance of the distributed coordination schemes may be influenced by two key mechanisms of *a*) class of approximately equivalent models used by CA for its own area and the more abstracted models used for other areas, and *b*) parameter fitting for the approximated model. Every CA is assumed, in the approach we develop below, to adopt the same type of equivalent models, used to represent its neighboring areas as well as identical parameter identification algorithm to estimate the parameters of the equivalent [29]. Special cases where one (or several) CAs fail to find a solution for the local optimization problem, due to inevitable violation of the constraint for the set of all available control actions, must be handled by sending a request for additional reactive power to the supervisor.

3.5 Measurements and communication

The availability of on-line synchronized phasor measurement units (PMUs) as well as reliable high-speed communication networks enables Wide-Area Monitoring and Control (WAMC) systems [74, 75] which complement already existing classical SCADA/EMS Supervisory Control And Data Acquisition/Energy Management System) platforms. Traditional SCADA/EMS systems are based on steady-state power flow analysis, and have the industry standard resolution of 2 – 4 seconds. Therefore, this system cannot observe the faster dynamic variables of the power system. The newly developed WAMC/PMU platform ease the dynamic monitoring and control of the multi-area power systems by providing real-time “snapshots” of the state variables up to every millisecond. To emphasize this time resolution difference between PMU and SCADA/EMS technologies, they are often referred to as “MRI” resp. “X-ray” of the power systems.

For this thesis, a detailed local model of each area is assumed to be given to each corresponding CA. A sampling interval of 20 ms is fast enough to evaluate frequency (50 Hz), voltage and current phasors (magnitude and angle) and their correlation with time. The time scale of the long-term voltage control of interest for this research is typically in the period of several minutes after a disturbance. Thus the PMU updates of every 1 s (or 500 ms at best), for collecting the local area measurements, would be satisfactory for the practical implementation of the method. For example the (initial) tap positions of the LTCs and states of OXLs located

within the area can be provided - say every 1 s - by a local PMU. This local information collection might be even done via SCADA/EMS system in a lower time resolution (say every 2 – 4 s).

Each CA, beside collecting the local information, is assumed to communicate only its local control sequence (and no other data) over a prediction horizon to its immediate CAs. In all simulations in chapter 5, a control interval $T_c = 10$ s, is chosen to update the local controllers, and to communicate the local control actions among immediate neighboring CAs. This - only every 10 s - communication can be effectively done via existing SCADA/EMS system, requiring a rather small communication bandwidth. It is noteworthy to mention that the proposed control algorithm is currently implemented in this thesis in a synchronous fashion, where all CAs start acting at the same time instant and update their control actions after every fixed control interval (T_c), taking into account the exchanged information from immediate neighboring CAs which becomes available after one-step communication delay.³ However, a more realistic operation of CAs might be achieved by asynchronous implementation of the local MPCs, where the CAs (in general) can update their control actions whenever they want to. Since the control update interval of 10 s was selected taking the mechanical time delay of LTCs into account, the CAs would then still use the same control interval, but could start reacting at different times within each 10 s interval. It can, therefore, happen that two neighboring controllers act subsequently within - say - 1 – 2 s. The PMU is then needed to effectively capture these quick control updates. The asynchronous implementation might even lead to better performance for each local voltage controller as the local CAs can base their decisions on more recent control plans from their neighbors than previous synchronous time instant.

Substations typically include an Internet connection via fiber or cable, or a serial connection via a dial-up telephone line or radio link in order to communicate real-time data. Different communication protocols such as User Datagram Protocol (UDP) or Transmission Control Protocol (TCP) can be selected in the Internet connection, based on the bandwidth and performance implications.

3.6 Abstraction

Modern electrical power systems are typically very complex large-scale geographically wide-spread networks of the interconnected components. A full detailed model of such a system for on-line control, can not be reliably obtained due to its complexity, lack of full data from all available components (especially DGs), and excessive computational cost. Furthermore, this becomes practically impossible,

³Due to the mechanical time delay of LTCs $T_{\text{delay}} = 10$ s this (negligible) communication delay plays no longer an important role because the communicated sequence will be only taken into account to calculate the local solutions after the physical time delay of LTCs, anyway.

even with availability of powerful computational resources, in the context of multi-area power systems where competing TSOs cannot be expected to share detailed information, and hence cannot possibly have the full detailed dynamic model of the entire system, but only know the local model of their area of authority. Therefore, network equivalencing procedures, also called network reduction techniques, to properly represent static (steady-state) and dynamic characteristics of the power system models of an area controlled by a CA are of great importance. Obviously, the intuitive hypothesis behind the idea of a valid model reduction is that the equivalent (external/reduced) system model should reproduce a similar evolution in time of relevant variables (e.g. power flow in tie-lines connecting neighboring areas) on the study (internal/retained) system as the detailed system model does, following all disturbances that can occur in practice. Corresponding to the steady-state and transient performance of the power system following a disturbance, two different types of equivalents namely static and dynamic equivalents can be distinguished, respectively.

The classical static external network equivalents are Ward equivalents [76], and REI (Radial, Equivalent and Independent) equivalents [77]. They do not reflect the probable changes/contingencies occurring inside the external network, and thus the simulation of the new conditions requires the development of a new static equivalent model. The parameters of these equivalents are normally updated by using a measurement-based estimation (i.e. a recorded history of past observations at interconnections). Therefore, the changes in the external system can be taken into account only after new measurements become available. As static equivalents are generally obtained for a base/reference operating condition, the computed internal states for the other operating conditions (resulting from e.g. changes in the loading level, outage of some components, or control actions) will be inherently erroneous. This is especially important when the external area contains a considerable number of active DG units whose power generation pattern (switching status) varies regularly and unpredictably [78].

On the other hand, classical dynamic equivalent models update their parameters for representing real-time topology changes of the external system. In real-life on-line applications e.g. dynamic security assessment, stability analysis, fault detection, adaptive protection schemes and control design etc. a simple and fast dynamic equivalent is necessary. The parameters of such an equivalent model should be determined by using measurement data taken at interconnections of two sub-systems, if sufficient.

Roughly speaking, the construction of the dynamic equivalent can be accomplished using reduction-based and identification-based approaches [79].

3.6.1 Reduction-based approaches

In reduction-based approaches, the equivalent is typically determined after aggregation of generator terminal buses and the elimination of load buses. Modal techniques [80,81] and coherency analysis [82,83], as the two primary and mostly contemplated techniques, belong to this category. Since these approaches are based on an exact model of components, they are sufficiently accurate and reliable. Some synchronous generators are observed to tend to swing together after a particular disturbance. Coherency measures provide a grouping criterion to identify a group of coherent generators, which swing together, and have identical terminal voltage. However, identification of coherent groups and thus the resulting aggregation procedure, require a complete set of parameters of the individual components in the external system to estimate the parameters of equivalent aggregated component. This may be problematic in the framework of large-scale multi-area power systems where each TSO preferably should directly derive the equivalent model for its neighboring areas from a set of real-time measurements taken solely at boundary buses of interconnections. In this way, the equivalent model will be independent of the external network size and complexity, and the correct on-line information of the external areas will not be required. Furthermore, the coherency criterion seems to fail when applying it to the power systems with high penetration of converter-based DG units e.g. fuel cells and photovoltaic systems where their characteristic is not even determined by the classical electro-mechanical dynamic equations in § 2.4.4 [78].

3.6.2 Identification-based approaches

On the other hand, identification-based approaches determine the dynamic equivalent models by perturbing the internal system by natural/intentional disturbances, and monitoring the response of the assumed approximated system model variables by taking measurements at boundary buses. These real-time measurements will then be compared with the corresponding signals computed from computer simulations. Accordingly, the equivalent model will be adjusted so as to match those two signals (real-time measurement and corresponding computed value) with each other as well as possible. Identification-based approaches are more desirable in the context of multi-TSO systems with the limited access to only boundary information. However, since these approaches yield an approximated model determined by noisy measurements taken only at boundary buses, rather than exact physical model given by reduction-based approach, they seem to be less accurate. Another issue with employing identification-based approaches to the highly coupled multi-area power systems is that many input ports must be considered for each area. This means that each area requires information even from the neighbors of its neighbors in order to accurately identify the parameters of its own immediate neighbors. This

in turn needs again information exchange, this time even from distant CAs.

Note that the advanced control theories e.g. model predictive control etc. call for dynamic model-based equivalents whose parameters, to be determined with least required measurements data taken at interconnections, can reflect the changes in the external network (over the finite control/prediction horizons ahead) [84].

In the next chapters, we employ the same reduced-order QSS models for the local area as well as for the immediate neighboring areas. However, a simple PV approximation is used to represent the distant areas as buses with constant voltage magnitudes and constant active power consumptions over the prediction horizon H . Note that the reduced-order models for the immediate neighboring areas and for the distant areas are assumed to be given in the simulations in chapter 5 as we do not deal in this thesis with their estimation.

3.7 Conclusions

This chapter illustrates the need for real-time model-based coordination in complex meshed power systems, where a local perturbation can lead to global performance degradation. Using the hybrid simulation tool, developed in chapter 2, for time-domain simulations on two test systems the following observations are made:

- There is an intrinsic coupling between continuous dynamics and discrete events, and the proposed hybrid framework can effectively capture them.
- The proposed HA-based simulator is sufficiently fast to evaluate different coordinating control strategy, serving as a real-time countermeasure to arrest voltage collapse. During this research the author did not have access (due to budgetary constraints) to the commercial special-purpose time-domain simulation tools such as EUROSTAG[®], PSS[®]E, and DIgSILENT⁴. Using these tools could potentially have allowed treatment of larger case studies. However it is believed that the analysis based on Modelica[®] simulations, in this chapter and in the next chapters, illustrates clearly the advantages of using anticipation and coordination.
- The proper coordination control, achieved by a manual, heuristic design approach in this chapter, can stabilize the system voltages where a purely decentralized deadband approach leads to a collapse, and also can minimize (or even eliminate) the need for undesirable load shedding.

⁴EUROSTAG is a software tool developed by Tractebel Engineering GDF SUEZ and RTE (France TSO), PSS/E by SIEMENS, and DIgSILENT by a consultancy company DIgSILENT GmbH in Germany, for dynamic modeling, simulations and analysis of power systems.

4

Distributed neighbor-to-neighbor coordination control

4.1 Introduction

In the context of multi-area power systems, as discussed in § 3.4.2, specifying a particular ad-hoc fixed rule in advance for each CA, using only local information and local anticipation, without taking coordination with neighboring CAs into account, may increase the risk of blackouts.

In order to avoid such a collapse in large-scale multi-area power systems, it has been shown in § 3.4.3 that there is a need for designing an automatic model-based system-wide coordinating feedback controller, capable of properly coordinating local control actions taken by each independent CA, yet preserving each TSO's non-disclosable local information.

This chapter proposes a paradigm for properly coordinating local control actions, taken by many communicating CAs, in order to maintain multi-area power system voltages within acceptable bounds, and to guarantee that generators deliver enough reactive power to avoid voltage instability whenever sufficient reactive power is available in the overall system. The proposed control scheme is inspired by distributed model predictive control (DMPC), and relies on the communication of planned local control actions among neighboring CAs, each possibly operated by an independent TSO. Each CA, knowing a local model of its own area, as well as reduced-order QSS models of its immediate neighboring areas, and assuming a simpler equivalent PV model for the distant areas, performs a greedy local op-

timization over a finite window in time, communicating its planned control input sequence to its immediate neighbors only.

In this chapter, the principle of the proposed DCMPC¹ scheme, the mathematical formulation of the voltage control problem, and the proposed discrete optimization algorithm is elaborated. The good performance of the proposed real-time model-based feedback coordinating controller, will then, in the next chapter, be illustrated by simulating cases with major disturbances, for two well-known test systems, assuming worst case conditions.

4.2 Model Predictive Control (MPC)

A power system is a MIMO (multiple-input and multiple-output) control system with hybrid dynamics subject to many operational and control constraints. Voltage control specifications as well as economical factors in the newly liberalized competitive power market increase the need for explicit on-line optimization.

One of the most successful classes of closed-loop model-based schemes is the Model Predictive Control paradigm (MPC), also called receding/moving horizon control. MPC calculates the control action $u(t_k)$ at time $t_k = k * T_c$, $k \in \mathbb{Z}^+$ relying on an estimate of the current system states at discrete time instant t_k and on an explicit *model* of the system, in order to *predict* the future output behavior via simulation over a finite window $[t_k, \dots, t_{k+H}]$, for a given set of allowable control sequences $\mathbf{u} = \{u(t_k), u(t_{k+1}), \dots, u(t_{k+N-1})\}$, where $\mathbf{u} \in \mathcal{U}$, $0 < N \leq H$, calculating the corresponding performance criterion over horizon $[t_k, \dots, t_{k+H}]$. At the time instant t_k , the first element $u^*(t_k)$ of the selected best sequence \mathbf{u}^* at time t_k is then implemented as control input to the physical system during the interval $[t_k, \dots, t_{k+1})$. All these calculations are repeated, using new observations leading to a new state estimate at the next time instant t_{k+1} , each time predicting performance over a shifted window with the size of $H * T_c$, each time selecting the best control sequence over a new prediction window [30–38]. A schematic representation of MPC is shown in Fig. 4.1. At present, MPC is the most widely used algorithm to deal with multivariable constrained control problems in industry [30].

The requirement that a dynamical model must be known is certainly a limitation, especially for electrical power systems, where the loads are not known accurately and where frequent changes of the generation and transmission resources can be expected. However, the inherent feedback of an MPC provides robustness against modeling errors. Moreover, in our control design, we look for distributed controllers that require a detailed dynamic model only of the area close to the local CA under consideration, and not of the distant areas.

¹DCMPC stands for Distributed Communication-based Model Predictive Control, and will be introduced in § 4.4.

As shown in Fig. 4.2, in order to find the k^{th} control action $u(t_k)$, MPC operates in successive estimation and optimization steps:

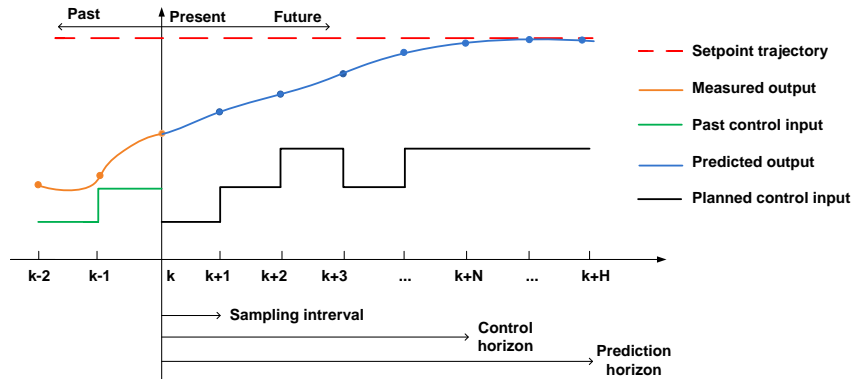


Figure 4.1: MPC concept

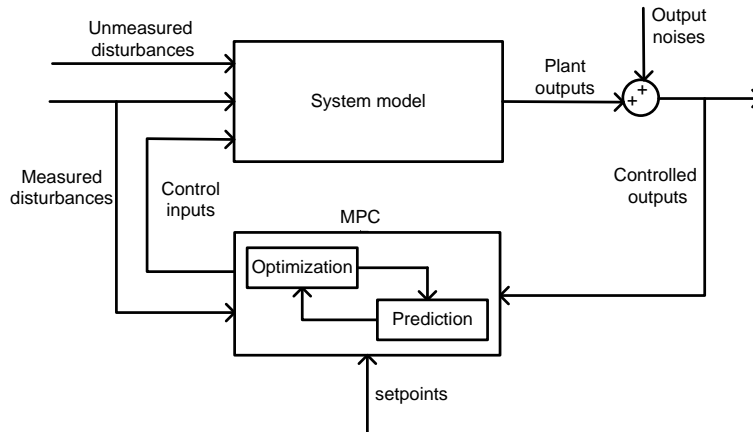


Figure 4.2: A system controlled by MPC

- MPC needs to know the current state $x(t_k)$ of the controlled system, including all internal variables that influence the future trend. However, in reality, not all system states can be measured or measurement of some state variables may be economically too expensive [30]. During the estimation step, a state observer uses all available measurements, up to the present time t_k , as well as the dynamic model, to obtain the best possible estimate of the present system state. This estimate will be used as initial condition for simulating trajectories in the next MPC optimization step.

- Values of setpoints, measured disturbances, and constraints are specified over a prediction horizon $H * T_c$ (i.e. for $t_k, t_{k+1}, \dots, t_{k+H}$). During the optimization step, MPC computes an open-loop optimal sequence of N control actions $u(t_k), u(t_{k+1}), \dots, u(t_{k+N-1})$, while $u(t_{k+N}), \dots, u(t_{k+H})$ are kept fixed, where $N(1 \leq N \leq H)$ is the control horizon. The system model is then used to evaluate the state evolution resulting over $t_k, t_{k+1}, \dots, t_{k+H}$ from these control actions. When a certain controllable input sequence is selected as the best one satisfying all constraints, MPC then only applies the first value of that sequence $u(t_k)$ to the system.

The system operates with this constant input until the next sampling instant $t_{k+1} = (k + 1) * T_c$, where the MPC uses newly obtained measurements, derives a new estimate of the state $x(t_{k+1})$, and calculates new optimal control input values $u(t_{k+1})$ by repeating the same steps for $t_{k+1}, \dots, t_{k+N}, \dots, t_{k+H+1}$, as were used to calculate $u(t_k)$.

H and N should be selected as the smallest values that lead to a good controller performance. Given sufficiently long horizon H , the controller may avoid violating the potential constraints by taking corrective actions immediately. The emergency voltage control in electrical power systems, was first formulated as an MPC problem in [10].

It is noteworthy that the concept of “looking ahead” is very useful for designing an on-line coordinating voltage control. The looking-ahead voltage controller can anticipate, within the prediction horizon window t_k, \dots, t_{k+H} , for example, the activation of OXLs, moving towards reaching the maximum physical tap limits for LTCs, and deviating too much from the prescribed voltage bounds for buses. The controller will then efficiently use this anticipation, by not selecting a control sequence that causes the above-mentioned constraint violations.

4.3 Networks of MPC-based voltage controllers

The traditional MPC-based voltage control has, over the past few years, received increasing interest, thanks to the flexibility of MPC on-line optimization in explicitly incorporating voltage control specifications, soft/hard operational constraints (on both control inputs and controlled outputs), and economical factors in the newly liberalized competitive electricity market.

However, the vast majority of the existing MPC-based voltage controllers in the literature are formulated in either a *centralized* or a completely *decentralized* fashion. These two distinct approaches are briefly explained below. In § 4.4 we introduce our proposed distributed neighbor-to-neighbor communicating controller (DCMPC).

4.3.1 Decentralized MPC

Large-scale power systems are often composed of many non-overlapping interacting areas. Decentralized local area-based control approaches ignore the interactions among adjacent areas. The MPC optimization only considers the local model and the local state evolution, using local anticipation. This certainly leads to inefficient uncoordinated design of a system-wide controller, and often unnecessarily causes voltage collapse [34, 70], and § 3.4.2.

In this thesis in order to illustrate the performance improvement via distinct contribution of local anticipation and feedback coordination, the proposed DCMPC approach is compared with a decentralized MPC approach. The identical models for the local, immediate and distant areas are considered for both DCMPC and the decentralized MPC approaches, allowing them to enjoy the local anticipation. However, the existing communication among neighbors in the DCMPC approach is removed when applying the decentralized MPC to the multi-area system. Therefore, each CA, assuming that its neighboring CAs will take no control actions (no LTC tap moves) over the prediction horizon, optimizes the controls for its own area regardless of what the neighbors are actually planning to do. The limitation of this decentralized approach can effectively illustrate the contribution of coordination in the improved performance of the DCMPC. Experiments discussed in chapter 5 will also illustrate the limitations of using anticipation only without coordination. Load frequency control in interconnected power systems is tackled in [37] by using a decentralized MPC formulation. A so called “almost” decentralized Lyapunov-based MPC algorithm is used in [38] for asymptotic stabilization of the network frequency.

4.3.2 Centralized MPC

Centralized MPC requires global knowledge of the complete model of the overall system, and all control actions are computed in a single optimization problem. Designing such a full-scale control structure for the large-scale systems, based on the dynamic models of very many components, is very difficult due to the computational complexity.² The fact that the global model is usually not known completely by the global control agent, moreover, makes this approach non-robust. Bandwidth limitation and the risk of failures of communication channels for a large geographically widespread power system make centralized control unreliable [71, 72]. On the other hand, a centralized formulation of the voltage control problem is not

²A recently completed FP7 EC (European Commission) project PEGASE (Pan European Grid Advanced Simulation and state Estimation) was devoted to develop the first simulation engine allowing the time-domain simulation with good accuracy of very large-scale systems such as European Transmission Network.

necessary either, because in power systems only areas that are electrically close together interact with each other for voltage, and there is no need to involve remote areas with negligible common interest in solving a local optimization problem. Note that in the deregulated competitive power markets the CAs often cannot divulge all information about their local models and cost functions. Thus the MPC cannot be effectively formulated as a centralized global optimization problem anyway, and a distributed MPC scheme with limited information exchange fits better the requirements of multi-area power systems.

In [31], a centralized MPC formulation is performed, using a linearized global system model around an equilibrium, and the underlying optimization problem is solved by a heuristic tree search technique to coordinate generator voltage setpoints, LTC moves and load shedding. A centralized MPC optimization, using a single-stage Euler state predictor, and a pseudo-gradient evolutionary programming algorithm is solved in [32], to select an optimal combination of the available control inputs. MPC is used in [33] to design a central supervisor which provides setpoints for each local controller, using a pattern search optimization method. A centralized MPC optimization in [35] is solved in a distributed fashion using a classic Lagrangian decomposition algorithm to select optimal combinations of generator voltage setpoints and load shedding. Reference [36] employs a centralized MPC formulation, using an explicit model for time evolution of the load power, to select a combination of generator voltage setpoints, shunt capacitors and load shedding to correct non-viable transmission voltages.

4.4 Distributed Communication-based Model Predictive Control (DCMPC)

As mentioned before, the main drawbacks in the centralized formulation are the huge computational cost, the lack of robustness due to requiring global knowledge of the complete model of the overall system, and the reliability problems due to possible communication failures. Purely decentralized approaches, ignoring interactions among areas, may not lead to a well-performing controller in highly-coupled power systems, leading to suboptimal or even non-convergent performance. On the other hand, the commercial availability of synchronized wide-area measurement units and resilient high-speed communication, as well as the development of distributed computation techniques, suggests the use of distributed wide-area communication-based control approaches. These enabling technologies may allow the local optimizations to be computationally solved in a distributed manner, while still accounting for the interactions among CAs and preserving the TSO's non-disclosable local information e.g. the local economical cost functions.

A cooperative distributed MPC, using a linear time-invariant model of the system, is applied in [34] to automatic generation control aiming at frequency and tie-line interchange regulation. In the approach of [34] each subsystem requires the full knowledge of all other subsystems.

4.4.1 Basic assumptions

We assume that all system buses are locally observable and the installed phasor measurement units (PMUs) hardware provides real-time “snapshots” of the required local power system state variables. The system is assumed to successfully perform frequency regulation through a single slack bus.

This thesis deals with long-term voltage control, and assumes that short-term voltage control provided by the available fast-reacting countermeasures (e.g. the AVRs of generators) acts perfectly. The tap position changes of the LTCs are considered as the only available countermeasure against the long-term voltage instability of interest in the following simulations in this thesis. However, additional discrete controls such as switched CBs and load shedding can be easily accommodated in the formulation.

The control objective of each CA is twofold. The main objective of $CA_i, i \in \{1, \dots, M\}$ is to maintain at time t its B_i voltage magnitudes $v_B^i(t)$ at buses $B \in \{1, \dots, B_i\}$ within prescribed bounds $v_{min}^i \leq v_B^i(t) \leq v_{max}^i$ close to the nominal bus voltages. This thesis does not consider the physical thermal limits of the interconnecting tie-lines that limits the maximum power transfer capacity among TSOs, however, these additional constraints could also be included in the DCMPC formulation. In the simulations in the next chapter, we consider $v_{min}^i = 0.9$ p.u. and $v_{max}^i = 1.05$ p.u. for all CAs.

A simple quadratic cost, as shown in Fig. 4.3, is employed to penalize the voltage deviations for the buses. The secondary objective is to minimize the number of changes of tap positions n_L^i in its L_i LTCs $L \in \{1, \dots, L_i\}$, as they cause transients on the system voltages as well as mechanical wear of the LTCs themselves. The optimal economical operation of individual areas, for example, minimization of the active power losses or maximization of the reactive power reserves, will not be considered in this study, as it has to be studied in an even slower time scale than that of our interest (the time scale of tertiary voltage control).

The time scale of the secondary voltage control of interest for this study is in the period of several minutes after a disturbance. Thus, the long-term dynamics of interest, driven typically by LTCs, by OXLs of synchronous generators, and by exponential recovery loads, are advantageously captured by the well-known QSS approximation, assuming that short-term fast dynamics (including effects of CBs and FACTS devices) are infinitely fast and can be represented by their algebraic equilibrium equations instead of by their full dynamics [50]. QSS simula-

tion allows obtaining much faster-than-real time simulators for reasonably sized networks. Chapter 3 of this thesis provides more details on the QSS models for components used in the time-domain simulations.

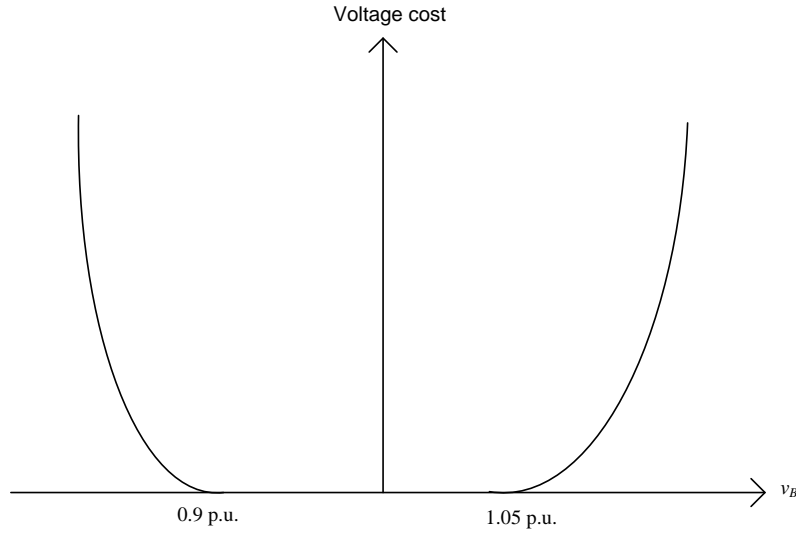


Figure 4.3: A simple quadratic cost function

4.4.2 Decomposition criterion

We define the overall multi-area power system, as shown in Fig. 4.4, as a graph $\mathcal{G} = (\mathcal{V}, \mathcal{E})$ of M interacting areas A_i , $i \in \mathcal{A} = \{1, \dots, M\}$, where each corresponding control agent CA_i , $i \in \mathcal{I} = \{1, \dots, M\}$, is assigned to a vertex $\nu_i \in \mathcal{V} = \{\nu_1, \dots, \nu_M\}$, and the interconnecting power transmission lines (and also the communication links as will be shown later) among CAs are represented by a set of edges $\mathcal{E} \subseteq \{(\nu_i, \nu_j) \in \mathcal{V} \times \mathcal{V} \mid i \neq j\}$.

For each CA_i , $i \in \mathcal{I}$, associated to vertex $\nu_i \in \mathcal{V}$, consider the sets of indices $\mathcal{N}_i = \{j \mid (\nu_i, \nu_j) \in \mathcal{E}, j \neq i\}$ corresponding to the immediate neighbors (directly interconnected through tie-lines), and $\mathcal{R}_i = \{r \mid (\nu_i, \nu_r) \notin \mathcal{E}, r \neq i \neq j\}$ representing the remote/distant areas (indirectly interconnected), where $i \cup \mathcal{N}_i \cup \mathcal{R}_i = \mathcal{A} = \mathcal{I}$. For example, for CA_4 in Fig. 4.4, $\mathcal{N}_4 = \{1, 3, 5\}$ and $\mathcal{R}_4 = \{2, 6, 7\}$.

This decomposition of the overall system, from a power system point of view, may be realized in several ways. In the most common practice, also adopted in this the-

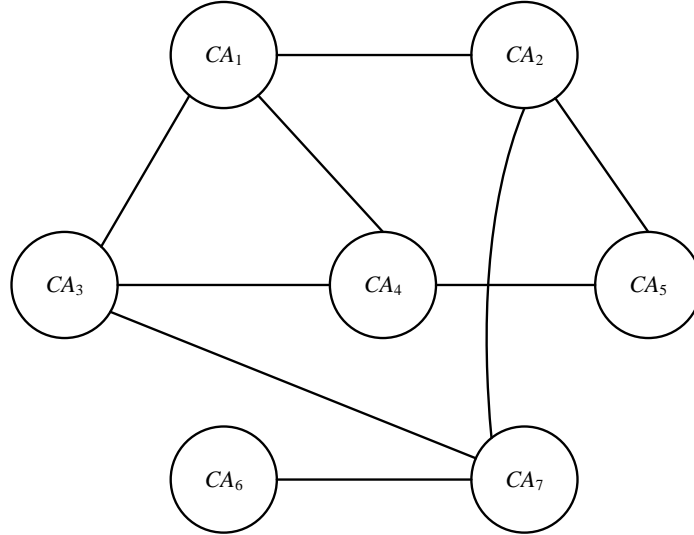


Figure 4.4: A multi-area power system

sis, depending on the geographical structure of the system, a set of buses located at a relatively short electrical distance from each other, are considered as one particular area. The advantage is that because the electrical distances are proportional to the physical lengths of the interconnecting transmission lines, the voltage control areas (zones), as a result, are identified in advance, and are assumed to remain unchanged during the real-time dynamic operation of the system. In other words, the areas are not affected by, for example, loading/generation conditions and/or faults, and need not be re-identified after possible changes in the system operating conditions. However, areas may also be adequately determined by sensitivity analysis of the overall system with respect to the influence of the available controls. In this case the boundaries of areas change dynamically during real-time system operation, and areas must be redefined periodically in order to better reflect the system topology and dynamic changes in the operating conditions. [27].

The decomposition based on electrical distance, allows us to collect the neighboring LTCs that move in a relatively coherent way as well as the neighboring generators with almost identical terminal voltage profile, all in one individual area. We will then assign one representative LTC for areas which contain several LTCs. This approach seems to be an effective decomposition criterion that determines the size of areas, based on the topology of the system, such that areas are not too large (thus computationally feasible) neither too small (containing at least one LTC and/or generator).

4.4.3 Modeling framework

Each area $A_i, i \in \mathcal{A} = \{1, \dots, M\}$ in this thesis is modeled as a hybrid dynamical system, using DAEs to describe piecewise continuous dynamics as well as a set of events in hybrid automata representing the discrete logical controllers, capturing the complex interactions between continuous and discrete dynamics, as explained in chapter 2. The QSS approximation of the hybrid behavior of each area $A_i, i \in \mathcal{A} = \{1, \dots, M\}$ is expressed by mixed discrete-event continuous differential-algebraic equations, subject to some local constraints. In order to implement the DCMPC approach for each area, we need to take a discrete-time approximation of the nonlinear system equations, in § 2.2.2, as the following form:

$$x_i(k+1) = f_i(x_i(k), z_i(k), y_i(k)), k \in \mathbb{Z}^+ \quad (4.1a)$$

$$z_i(T_e^+) = Z_i(x_i(T_e^-), z_i(T_e^-), y_i(T_e^-), u_i(T_e^-)) \quad (4.1b)$$

$$z_i(k) = z_i(T_e^+), T_e \leq k < T_{e+1}$$

$$g_i(x_i(k), z_i(k), y_i(k), \phi_i(y_{\mathcal{N}_i}(k), u_{\mathcal{N}_i}^*(k-1))) = 0 \quad (4.1c)$$

$$h_i(x_i(k), z_i(k), y_i(k)) \leq 0 \quad (4.1d)$$

where x_i denotes the local dynamic continuous states of the generators, AVRs, OXLS and load dynamics in area $A_i, i \in \mathcal{A} = \{1, \dots, M\}$, z_i the discrete-event state variables typically arising from discrete control logic such as thresholds reached by OXLS, LTC tap positions, switched CBs and disturbances, T_e the time at which a discrete event e occurs, $T_e^- = \lim_{\epsilon \rightarrow 0} T_e - \epsilon$ the pre-event time, $T_e^+ = \lim_{\epsilon \rightarrow 0} T_e + \epsilon$ the post-event time, y_i the local algebraic state variables e.g. network voltages and currents, u_i the discrete local control inputs. LTC tap position changes are considered as the control actions in this thesis. The equality constraint $g_i(\cdot)$ in (4.1c) corresponds to the algebraic power flow equations. The inequality constraint $h_i(\cdot)$ in (4.1d) includes physical unviolatable limits (hard constraints) e.g. limits on the tap positions of the LTCs, and/or penalized operational limits (soft constraints) e.g. predefined voltage bounds. The inequality constraint $h_i(\cdot)$ could also represent power-flow limitations along tie-lines, however, this is not included in this thesis.

Note that $\phi_i(\cdot, \cdot)$ has been included into g_i in (4.1c) to represent the interaction with the directly connected neighboring areas $A_j, j \in \mathcal{N}_i$. This means that the effect of the dynamic states and the control actions taken by the immediate neighbors on the state evolution of area $A_i, i \in \{1, \dots, M\}$ is implicitly reflected through the instantaneously changing algebraic variables (among which are the boundary bus voltages). Moreover, the distant areas $A_r, r \in \mathcal{R}_i$ (the neighbors of neighbors) do not even explicitly appear in (4.1c), instead their possible effect is incorporated

in the nonlinear function $\phi_i(\cdot, \cdot)$ of the immediate neighboring areas $A_j, j \in \mathcal{N}_i$. A discrete time model of the overall control problem can be readily obtained by aggregation of all the discrete time models for individual areas (as represented by equations (4.1a)–(4.1d)).

One should clearly distinguish between the local control models and the physical model of the overall system. There exist several local discrete time control models, one for each area, in order to be able to implement the MPC scheme for each CA. These local control models obviously differ from one CA to another. However, on top of this, there also exist one continuous model for the overall physical power system (with information available from all areas) in order to simulate the dynamic response of the physical power system after applying the control actions calculated by the local MPCs. In other words, all the local MPCs concurrently calculate the local control actions for each time instant, say t_k , by using the distinct discrete time local control models of their own area, reduced-order models of their immediate neighbors and for the distant areas, and by establishing the proposed communication protocol. We then apply all these calculated control actions to the physical system in continuous real-time, and let the power system evolve until next time instant, in this case, t_{k+1} . At t_{k+1} all the state variables will be collected by performing new (noisy) measurements in the real physical power system, which will indeed be used as initial conditions for solving the local optimization problems by the local MPCs at t_{k+1} . This procedure is identically repeated for all the following time instants.

4.4.4 Notation

Each CA $i, i \in \{1, \dots, M\}$ is implemented in this section as a local controller MPC $_i, i \in \{1, \dots, M\}$. Letting N be the control horizon and H the prediction horizon, the sequence of predicted state and control values at time $k + \ell, \ell \in \{1, \dots, H\}$ for MPC $_i, i \in \{1, \dots, M\}$, based on the information available at time instant k is denoted, respectively, by \mathbf{x}_i and \mathbf{u}_i , where

$$\mathbf{x}_i(k) = \{x_i(k+1|k), \dots, x_i(k+H|k)\}$$

$$\mathbf{u}_i(k) = \underbrace{\{u_i(k|k), \dots, u_i(k+N-1|k)\}}_N \underbrace{\{0, \dots, 0\}}_{H-N+1}$$

4.4.5 Principle of the proposed coordination scheme

For each MPC $_i, i \in \{1, \dots, M\}$ with the identical prediction horizon H and control horizon N , let $\mathbf{u}_i \in \mathcal{U}_i$ denote a candidate control sequence of LTC tap position changes, where $\mathcal{U}_i = \{0, +1, -1\}^N \times \{0\}^{H-N+1}$ is the corresponding

finite set of all admissible control sequences, with 0, +1 and -1 referring resp. to having no tap movement, an upward tap movement, and a downward tap movement. Note that no tap movement is considered in the interval $[t_{k+N}, \dots, t_{k+H}]$. Furthermore, for the sake of simplicity in the formulation and without loss of generality, we only consider one single LTC in each area A_i , $i \in \{1, \dots, M\}$ resp. controlled by MPC_i , $i \in \{1, \dots, M\}$. The cardinality of \mathcal{U}_i is then $|\mathcal{U}_i| = 3^N$.

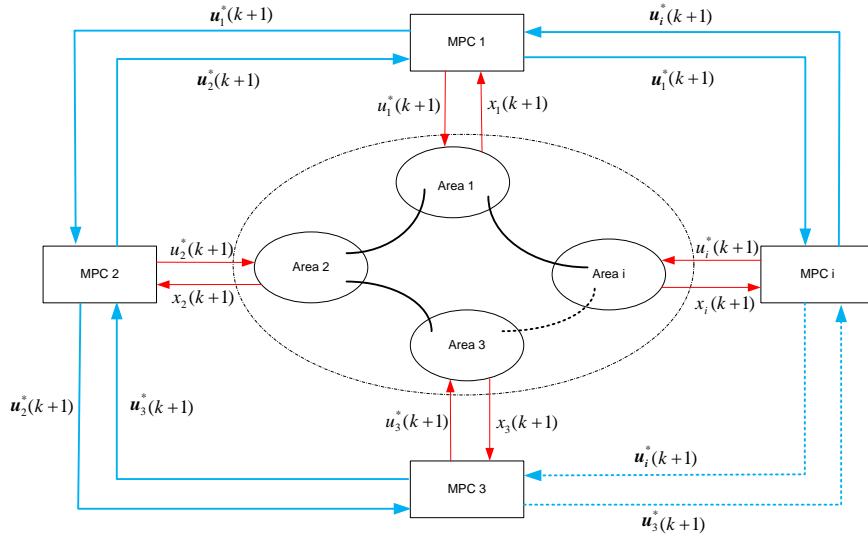


Figure 4.5: Distributed MPC with neighbor-to-neighbor communication

In order to design a wide-area well-performing coordinating feedback controller, we propose a coordination scheme where each local MPC_i , $i \in \{1, \dots, M\}$ is required to have some way of anticipating how the control actions taken by the immediate neighboring MPC_j , $j \in \mathcal{N}_i$ will evolve in the future. This is effectively achieved, in this study, by mutual exchange of information about local future control actions among neighboring MPCs, and assuming that each MPC_i , $i \in \{1, \dots, M\}$ approximately knows the model of its immediate neighboring areas A_j , $j \in \mathcal{N}_i$ in order to predict how these future plans will approximately influence the evolution of its own state variables in the future.

In the next chapter, the same reduced-order QSS models for the local area as well as for the immediate neighboring areas will be employed to perform the simulation experiments.

Note that thanks to the physical nature of voltage, being a local quantity, distributed MPC application make sense for voltage control, not for frequency control. Thus, considering voltage control, only electrically close areas (immediate neighbors)

may interact for voltage, and it is acceptable to exclude the electrically distant areas with negligible influence on the local behavior, and thus negligible impact on the local optimization.

In this thesis, in order to obtain the discrete time control model for the local anticipation for MPC_i , each $CA_i, i \in \mathcal{I}$ uses a simple PV approximation [29] to represent the distant areas $A_r, r \in \mathcal{R}_i$ as buses with constant voltage magnitudes and constant active power consumptions over the prediction horizon H .

Using information on the input signals from the immediate neighbors, and knowing a local model of its own area as well as reduced-order models of its immediate neighboring MPCs, and assuming a simpler PV equivalent model for distant areas, each local $MPC_i, i \in \{1, \dots, M\}$, solves, at each time step k , a finite-horizon open-loop optimal control problem, minimizing a greedy local performance criterion J_i satisfying all the local constraints.

One very important feature of the proposed DCMPC scheme is its “scalability”, which makes it suitable to deal with large-scale multi-area power systems containing many distinct identified voltage control areas. This is thanks to the fact that each CA in order to perform the local optimization requires the QSS reduced-order models only of its few immediate neighboring areas (as well as limited information exchange only with them), and replaces the remaining distant areas by much simpler PV models without any information exchange. Thus no matter how large the power system is, the computational complexity of the local calculations at each CA remains the same. Fig. 4.5 illustrates a schematic representation of the proposed control scheme.

4.4.6 Control problem formulation

The distributed non-cooperative MPC-based control algorithm with neighbor-to-neighbor communication for each $MPC_i, i \in \{1, \dots, M\}$ at time instant k can be formulated as the following optimization problem:

$$\min_{\mathbf{u}_i(k) \in \mathcal{U}_i} J_i(\mathbf{x}_i(k), \mathbf{u}_i(k); x_i(k)) \quad (4.2)$$

where

$$J_i = \sum_{t_k}^{t_k+H} \Delta u_i^T \Gamma_i \Delta u_i + \int_{t_k}^{t_k+H} (\rho_i^T \Lambda_i \rho_i) dt$$

subject to for all $k \leq \ell \leq k + H - 1$

$$\begin{aligned} x_i(\ell + 1|k) &= f_i(x_i(\ell|k), z_i(\ell|k), y_i(\ell|k)) \\ z_i(T_e^+) &= Z(x_i(T_e^-), z_i(T_e^-), y_i(T_e^-), u_i(T_e^-)) \\ z_i(\ell) &= z_i(T_e^+), T_e \leq \ell < T_{e+1} \\ g_i(x_i(\ell), z_i(\ell), y_i(\ell), \phi_i(y_{\mathcal{N}_i}(\ell), u_{\mathcal{N}_i}^*(\ell - 1))) &= 0 \\ n_{min}^i &\leq n_L^i(z_i(\ell)) \leq n_{max}^i, L \in \{1, \dots, L_i\} \end{aligned}$$

$\Gamma_i = \text{diag}(\gamma_1, \dots, \gamma_{L_i})$ and $\Lambda_i = \text{diag}(\lambda_1, \dots, \lambda_{B_i})$ are the non-negative diagonal weighting matrices for MPC $_i$, $i \in \mathcal{I}$, to penalize the amount of tap position changes Δu_i in its L_i LTCs, and the voltage magnitude deviations in its B_i buses, respectively. Note that the soft constraints on the B_i bus voltage magnitudes v_B^i are mathematically relaxed by introducing the slack variable³ $\rho_B = \max\{(v_B^i - v_{max}^i), (v_{min}^i - v_B^i), 0\} \geq 0$, $B = \{1, \dots, B_i\}$, and $\rho_i = [\rho_1 \ \rho_2 \ \dots \ \rho_{B_i}]$ penalizing the potential violation of the voltage constraint due to e.g. an unavoidable large disturbance, while the hard constraint on the physical tap positions n_L^i can never be violated.

4.4.7 Optimization algorithm

The following algorithm is employed by CA $_i$ to solve the DCMPC optimization problem for MPC $_i$, $i \in \{1, \dots, M\}$:

1. $k = 0$
2. Initialize with $u_i^*(k - 1)$, $\mathbf{u}_{\mathcal{N}_i}^*(k - 1)$, $\mathbf{u}_{\mathcal{R}_i}^*(k - 1)$, $x_i(k)$, $\tilde{x}_{\mathcal{N}_i}(k)$
3. Enumerate the discrete set of possible sequences \mathcal{U}_i and compute the corresponding costs $J_i(\mathbf{x}_i(k), \mathbf{u}_i(k); x_i(k))$
4. Select the best sequence $\mathbf{u}_i^*(k)$ and obtain its first element $u_i^*(k)$
5. Apply $u_i^*(k)$ to CA $_i$ until next time instant $k + 1$
6. Obtain the state estimate $x_i(k + 1)$ at time $k + 1$
7. Communicate $\mathbf{u}_i^*(k)$ to the immediate neighboring MPC $_j$, $j \in \mathcal{N}_i$
8. $k := k + 1$; go back to step 3.

³In an optimization problem, a slack variable is a non-negative variable that is added to an inequality constraint to convert it into an equality constraint. For example $h_i(\mathbf{x}) \leq 0$ is equivalent to $h_i(\mathbf{x}) + s_i^2 = 0$

Note that the DCMPC approach requires no information exchange on the local state trajectories. However $\tilde{x}_{\mathcal{N}_i}(k)$ is the state estimate at time t_k of the neighbors that MPC_i uses, based on the QSS reduced-order models of its neighbors, in order to compute its own solutions.

In general MPCs may have different local objectives expressed by different cost functions. Here all MPCs utilize a local cost function maintaining the local voltages within the limits, and minimizing the amount of local LTC moves.

This optimization leads in some sense to a dynamic Nash-like game, where each CA_i at each decision moment assumes that the other players will stick to their announced control plans, and the solutions, if they converge, will converge to the Nash equilibrium (NE). Under this assumption one cannot expect that the system will in general perform as well as would be the case if some global supervisor would apply a centralized global feedback control law, known as Pareto optimal in game theory, where the least possible global cost is achieved by cooperation of all agents so that there exists no other solution that reduces at least one cost without increasing any other costs (and no constraints are violated). However in the next chapter, we show that, under certain conditions, the DCMPC strategy can stabilize a system in cases when a completely decentralized strategy, without any communications, leads to collapse.

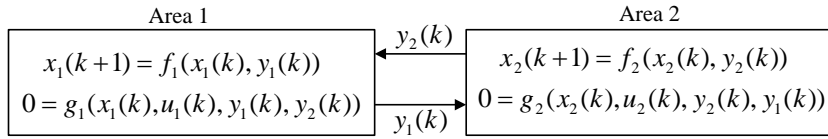


Figure 4.6: A simple 2-area interacting power system

4.4.8 On the choice of signal to communicate

The Fig. 4.6 shows a simple but prototypical multi-area power network composed of only two interacting areas. The dynamic of each area is effectively represented by the difference-algebraic equations, ignoring the discrete-event state variables, for simplicity. The areas physically interact via infinitely fast-changing algebraic state variables i.e. y_1 and y_2 (voltage/current or active/reactive powers over the tie-lines). Considering Area 1 as example, and assuming that the Jacobian of g_1 with respect to u_1 (i.e. $\frac{\partial g_1}{\partial u_1}$) is non-singular, one can obtain the control action u_1 at time t_k as a function of the other variables:

$$u_1(k) = G_1(x_1(k), y_1(k), y_2(k)) \quad (4.3)$$

Equation (4.3) shows the effect of interaction variable from Area 2 (y_2) on the control action of Area 1 (u_1). Similarly for y_2 :

$$y_2(k) = G_2(x_2(k), u_2(k), y_1(k)) \quad (4.4)$$

Substituting equation (4.4) in the equation (4.3) clearly shows how u_2 can affect u_1 .

In the current implementation of the DCMPC approach in this thesis, we have taken this effect into account by providing to CA₁ (corresponding to Area 1) the optimal control sequence of CA₂ (corresponding to Area 2) \mathbf{u}_2^* over a prediction horizon H . i.e.;

$$u_1(k) = \mathcal{G}_1(x_1(k), y_1(k), y_2(k), \mathbf{u}_2^*(k-1)) \quad (4.5)$$

This seems to be an effective signal to be communicated as the simulation results show that the uncoordinated local control actions can lead to voltage collapse. The exchange of the information of the planned control sequences allows each CA to “actively/directly” take its own coordinated local control actions knowing what the neighbors have planned to do. One other possible signal to be exchanged, instead of exchanging the planned control sequences, might be the exchange of the planned output trajectories of interacting variables directly (e.g. the expected values in future for voltages over the tie-lines). i.e.;

$$u_1(k) = \mathfrak{G}_1(x_1(k), y_1(k), \mathbf{y}_2^*(k)) \quad (4.6)$$

where $\mathbf{y}_2^*(k) = \{y_2(k+1|k), \dots, x_i(k+H|k)\}$.

However, this seems to be much too complex as the neighbors will “passively/indirectly” coordinate. Each CA is then expected to try to respect the voltage profile of its neighbors by taking some local control actions and without knowing what the neighbors themselves will do in the future in order to correct their (potential) voltage violation. This might mislead the neighbors and stop them from reacting. This in turn can at least lead to a slower correction of a low voltage condition if, at best, we assume that the potential misunderstandings among neighbors can be resolved after some iteration of information exchange.

As mentioned before, the DCMPC approach is generally applicable to many large networks of interacting dynamic components. It is useful whenever both anticipation (implemented via the analysis of the effects of a local control action over a sufficiently long window of time) and coordination (avoiding that the overall system is destabilized by unintended interactions between local control actions) are needed. Other potential applications of DCMPC include the coordination/synchronization of the traffic lights for alleviating urban traffic congestion, where the “smart” traffic lights may exchange their dynamic switching times, based on the inflow and outflow of platoons of vehicles, to their neighboring traffic lights.

4.5 Conclusions

This chapter proposes a distributed neighbor-to-neighbor coordination paradigm for properly coordinating local control actions, taken by many interacting CAs, in large-scale multi-area power systems. The overall aim is to stabilize all area-wise bus voltage within prescribed bounds, and to minimize the number of LTC moves. TSOs are assumed to have agreed on exchanging their control actions, LTC moves in this thesis, with the neighbors. Each CA only communicates with its immediate neighbors and not with the distant areas. The proposed coordinating control does not require TSOs to exchange information that they are not often willing to disclose such as local economical cost functions. The concepts of “looking-ahead” and “communication” are mathematically reflected in the formulation of the control problem, and in its underlying optimization algorithm.

5

Simulation Results

The good performance of the proposed DCMPC control scheme of chapter 4 will be demonstrated, in this chapter, on two well-known test systems, the ABB 12-bus and Nordic32 systems, by simulating several different scenarios, and demonstrating the improved behavior achieved by combining coordination and anticipation.

5.1 ABB 12-bus test system

The first case study is the small ABB 3-area 12-bus test system [60], shown in Fig. 3.8. The response of this system is illustrated following two disturbances at $t = 98$ s, as follows:

- Case 1: Tripping of the double tie-line between Area1 and Area3
- Case 2: Load variations in Area2 and Area3

The uncertainty in the amount of available load in power system, as well as measurement inaccuracies may in general cause robustness issues for the controller. This is taken into account, in the first case study, by stochastically perturbing the consumed active/reactive power of the loads by some small values at each time instant, when predicting the state of the system. The feedback structure of the local MPCs provides enough robustness to deal with those errors.

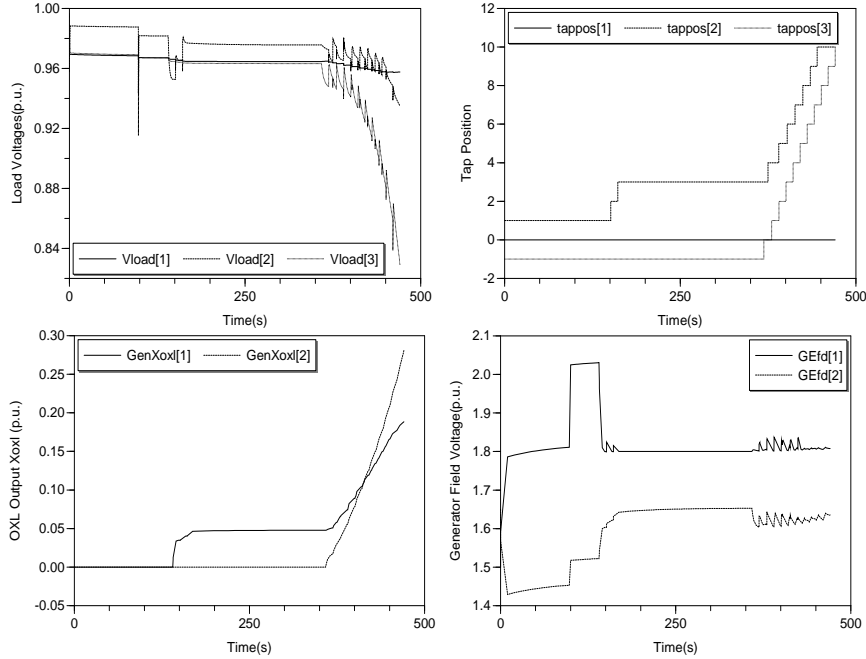


Figure 5.1: ABB 12-bus, case 1: response with the decentralized deadband control

5.1.1 Case 1: response with the decentralized deadband control

Fig. 5.1 shows the load voltage, LTC and OXL behavior following the tripping of the double tie-line between Area1 and Area3 at $t = 98$ s with decentralized deadband control.

In this case, LTCs operate based on only the local measurements, using a simple rule. The LTC is actuated if the voltage at the load bus remains outside a deadband for more than 1 s, and then the tap position is changed after a mechanical time delay, according to § 2.4.5. Instability occurs and the solver fails to solve the nonlinear equations of the system at $t = 470.54$ s when the simulation stops. Directly following the fault, load voltages in each area drop, but soon after a short-term equilibrium, with all load voltages settling down close to the respective reference voltages, is established. After this point the mechanism driving the system response is OXL and LTC together with the load dynamics. After the fault the generator field voltage in Area2 jumps to 2.02 p.u. which exceeds $i_{fd(lim)} = 1.88$ p.u. for this generator. This initiates the inverse time characteristic of the OXL, and eventually the OXL of the generator in Area2 gets activated at $t = 139$ s. At that time the voltage support provided by this generator is withdrawn. This results in a further reduction of the load voltage causing the LTC to increase the tap

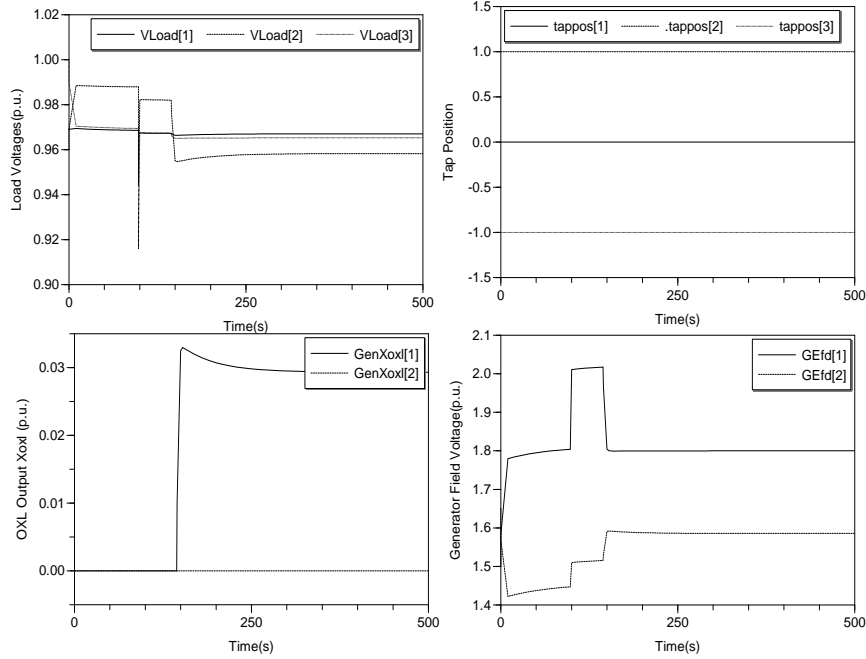


Figure 5.2: ABB 12-bus, case 1: response with the DCMPC

position until its maximum tap limit is reached, and the voltage drops suddenly at $t = 470.54$ s, when the generator can no longer deliver the consumed reactive power. In this case OXL activation occurs before saturation of the LTCs, and in fact it acts as a pushing force for LTCs to move towards their physical tap limits. Thus one can easily conclude that if there were a way of anticipating OXL activation in advance, some different (coordinated) LTC moves could have been taken, and the final collapse could be avoided.

5.1.2 Case 1: response with the DCMPC

Now, for exactly the same system conditions with all parameters the same as for the previous simulation, but with the LTCs controlled by the distributed communication-based MPC approach, the simulations are repeated. For the first initialization of the controller, each CA takes the initial tap positions of its neighbor(s) into account. The MPC_{*i*} at each area A_i , $i = 1, 2, 3$, with a sampling time $T_c = 10$ s, control horizon of 30 s ($N=3$), and the prediction horizon of 90 s ($H=9$), calculates the optimal control action at $t = 100$ s by simulating the system until $t = 190$ s. After solving local optimization problem for each area (one LTC in each CA), all LTCs select “no tap movement” as the local optimal control action at $t = 100$ s.

The procedure is repeated at next sampling instant $t = 110$ s simulating the system until $t = 200$ s, again “no tap movement” for all LTCs offers the lowest local cost. The controller is updated every 10 s, until $t = 500$ s and all CAs, subject to local cost and local constraints, always prefer having “no tap movement”. At $t = 500$ s, the load voltages are close to their reference values, as shown in Fig. 5.2. The OXL for generator in Area3 is not activated at all, while the one for the generator in Area2 gets activated at $t = 144.4$ s, OXL output signal rises up to the value 0.033 p.u., and then stays saturated at 0.029 p.u. Thus one can conclude that the distributed coordinating voltage control avoids the voltage collapse, by predicting the future behavior of the system and communicating among CAs.

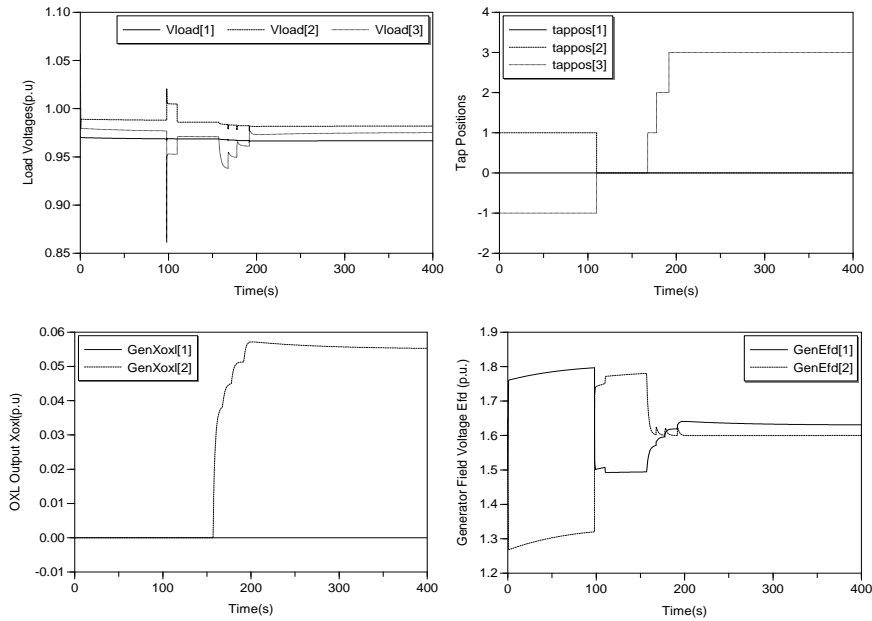


Figure 5.3: ABB 12-bus, case 2: response with the decentralized deadband control

5.1.3 Case 2: response with the decentralized deadband control

Load variation is simply considered by suddenly increasing some reactive load in Area2, and decreasing it in Area3 at $t = 100$ s. Figures 5.3 resp. 5.4 show the system response to this sudden change of reactive load with decentralized deadband control resp. distributed MPC approach.

Here the first tap change for LTC in Area2 occurs at $t = 110$ s, as it moves one tap down, while at the same time the LTC in Area3 moves one tap up. At $t = 154.5$ s the OXL of generator in Area3 gets activated, acting as a driving force for 3 sub-

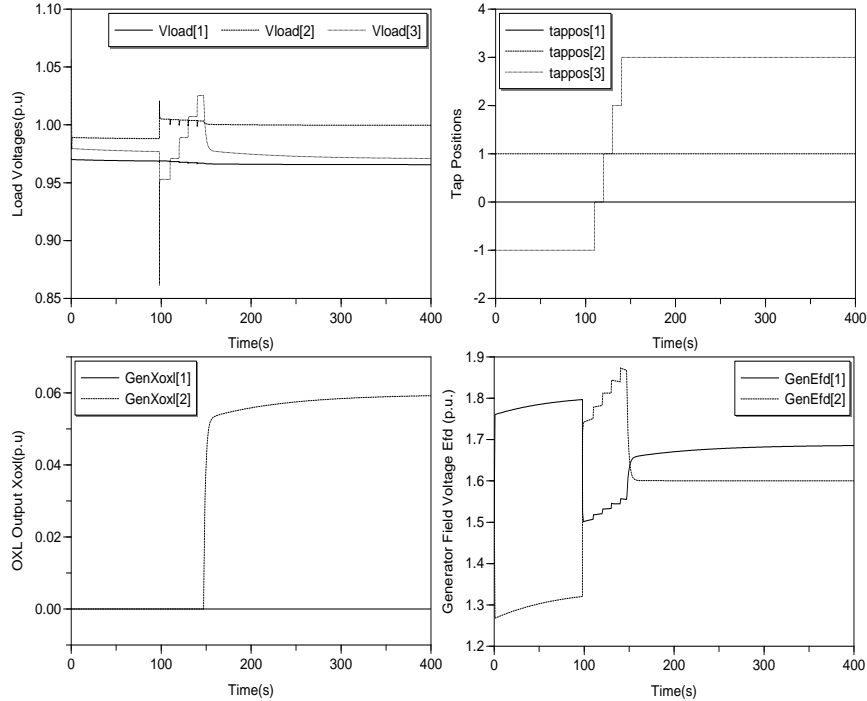


Figure 5.4: ABB 12-bus, case 2: response with the DCMPC

sequent upward tap movements of LTC in Area3 starting at $t = 167$ s. This OXL output signal at $t = 400$ s reaches the value 0.0552 p.u.

5.1.4 Case 2: response with the DCMPC

For exactly the same system conditions, the optimal control actions for LTC in Area3, suggested by the distributed coordinating MPC, asks for 4 subsequent upward tap movements at $t = 110, 120, 130$ and 140 s. At $t = 400$ s all voltages are close to their reference voltage, being within the prescribed deadband. The OXL output signal value at $t = 400$ s is 0.0592 p.u. Therefore, it is observed that one fewer tap movement, compared to the local deadband control approach, is employed by the distributed coordinating MPC. Note that in the deadband approach, LTC in Area3 initially acts on the local voltage at $t = 110$ s, and stays in this position until $t = 167$ s. At $t = 154.5$ s the OXL in Area2 gets activated, and consequently LTC in Area3 again acts on the OXL activation, while distributed MPC does in advance at $t = 110$ s advantageously anticipate the activation of OXL (in this case, $t = 150$ s), and thus start acting early at $t = 110$ s. This means that system voltages, with the distributed coordinating MPC, settle down to their

reference values about 50 s earlier than in the case of a local deadband approach.

5.2 Nordic32 test system

The second case study in this chapter, is a slightly modified version of the CIGRE Nordic32 test system, with one-line diagram shown in Fig. 5.5. This test system describes the complex meshed transmission system of the Nordel grid consisting of Sweden, Norway, Finland and (eastern) Denmark [85], where the corresponding grids are nowadays deregulated (in slightly different ways in each country), establishing a common competitive electricity market NordPool which dispatches the power generation among areas, on an hourly basis. Some operational information is shared, from time to time, by the market participants in the NordPool's information system (called Urgent Market Message (UMM)) [86]. The model includes 71 buses, 20 synchronous generator units equipped by OXL (including 1 slack generator), 22 dynamic loads, 52 transmission lines (including 15 tie-lines), 48 transformers (including 2 parallel-transformers and 13 LTCs) and 11 switched capacitor bank (including 2 reactors).

We illustrate the performance of the distributed coordinating controller considering two distinct disturbances, both occurring at $t = 10$ s, as follow:

- Case 1: outage of line 4032 – 4044
- Case 2: outage of line 4011 – 4021

The Nordic32 test system consists of four major areas namely *External*, *North*, *Central*, and *South West*. The generating units are mainly located in the *North* area. The power flows from *North* to the *Central* area (the main load center containing 13 LTCs). The *Central* area is further decomposed for computational purposes into six sub-areas, as shown in Fig. 5.6, namely $\text{Central}_1, \dots, \text{Central}_6$, each containing one (or a few coordinated) LTCs. This decomposition is based on electrical distance between buses, which is also proportional to physical lengths of interconnecting lines. Therefore, depending on the geographical structure of the system, a set of buses located at a relatively short electrical distance from each other have been considered as one particular area. Considering the operational time delay of LTCs $T_{\text{delay}} = 10$ s, and the slowest dominant time constant of the entire system which is that of the dynamic recovery loads (say 60 s), the sampling time of $T_c = 10$ s and the prediction horizon of 90 s ($H = 9$), is chosen to design the controller. Given this sufficiently long horizon, the controller can “see” at time t_k a potential constraint violation in the interval $[t_k, t_{k+H}]$, leading the controller to move in the right direction towards a long-term equilibrium by avoiding to react to the short-term dynamics. The control horizon of 30 s ($N = 3$), turned out to be

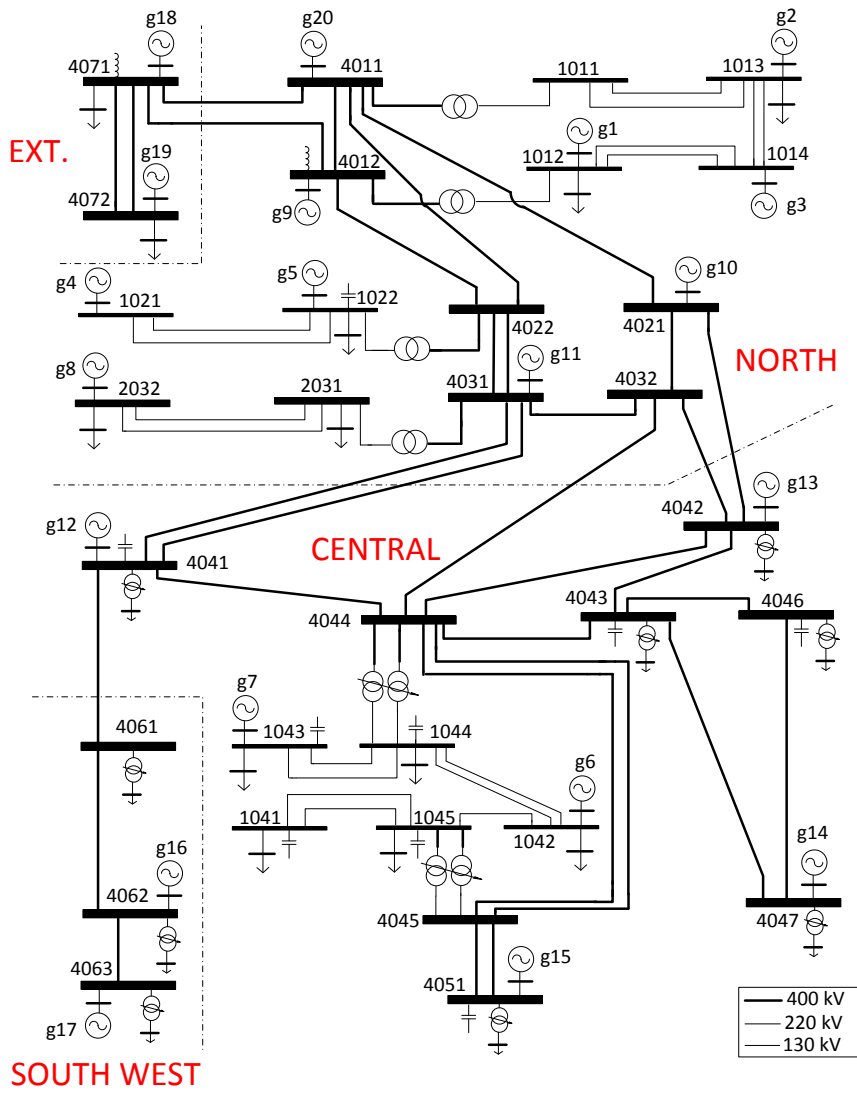


Figure 5.5: One-line digram of Nordic32 test system

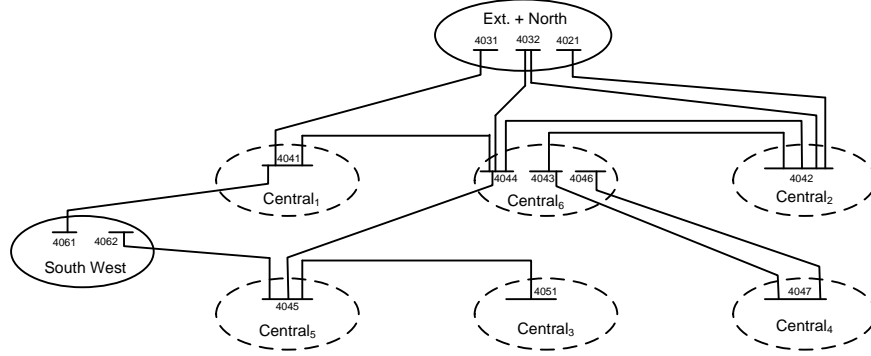


Figure 5.6: Nordic32 partitioned interconnected test system

a good compromise between computational complexity and the closed-loop controller performance.

5.2.1 Case 1: Outage of Line 4032-4044

The long-term time evolution of the transmission voltage magnitudes at the four most affected buses 1041, 1042, 1043 and 1044 as well as the coordinated LTC moves are shown in Fig. 5.7. The voltage decline is due to the effect of LTCs trying to restore the distribution side voltages of the LTC-controlled buses as well as OXLs activation of field-current-limited generators restricting their reactive power generation. This proposed set of controls successfully maintains the voltages within the limits, leading to no activation of OXLs for any of the generators. This is thanks to the anticipation of the activation of OXLs, and taking coordinated local control actions with the neighbors, that do not force LTCs to move towards reaching their maximum physical tap limits. As an example the inverse-characteristic timer signal x_t of OXL over $g7$ within Central₅ is shown in Fig. 5.8, which initiates twice at $t = 8$ and 67 s. This is initially “seen” by the local MPC for Central₅ in advance, and in an effort to correct this, the local LTC $Tr40451045$, takes an upward tap move at $t = 20$. Furthermore, at $t = 80$ s, the local LTC coordinates its upward move with its immediate neighbors, and as a result $g7$ does never become limited.

This is a significant improvement over the uncoordinated deadband operation of LTCs that leads to a final collapse, as shown in Fig. 5.9. Here LTCs use only local voltage measurements, and act on the basis of a local deadband $db = 0.02$ p.u., and tap positions are changed accordingly after a time delay $T_{\text{delay}} = 10$ s. This uncoordinated set of LTC moves trigger the activation of OXLs over five genera-

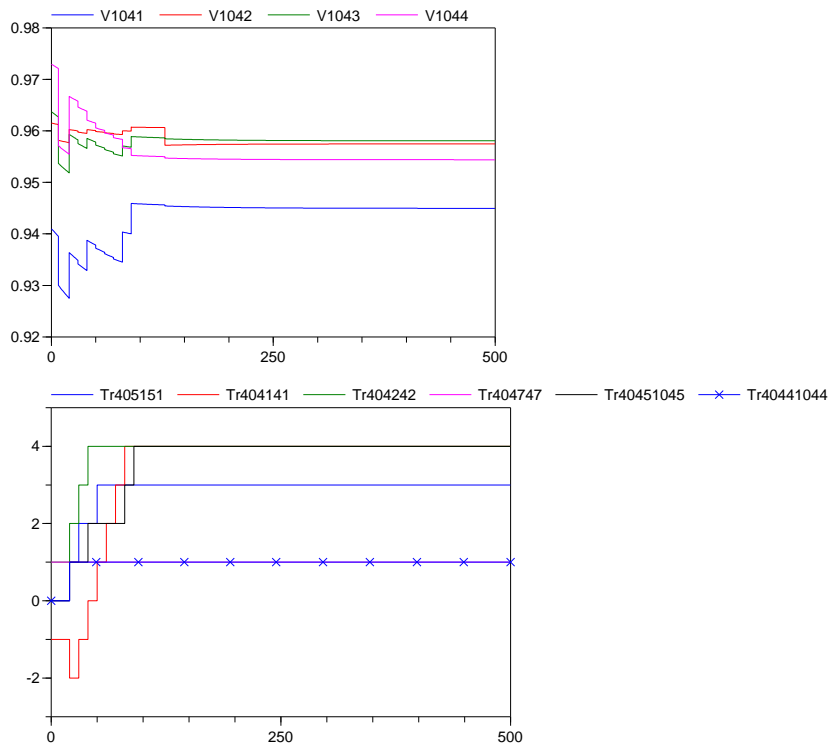


Figure 5.7: Case 1: Transmission bus voltages, and distributed coordinated LTC moves

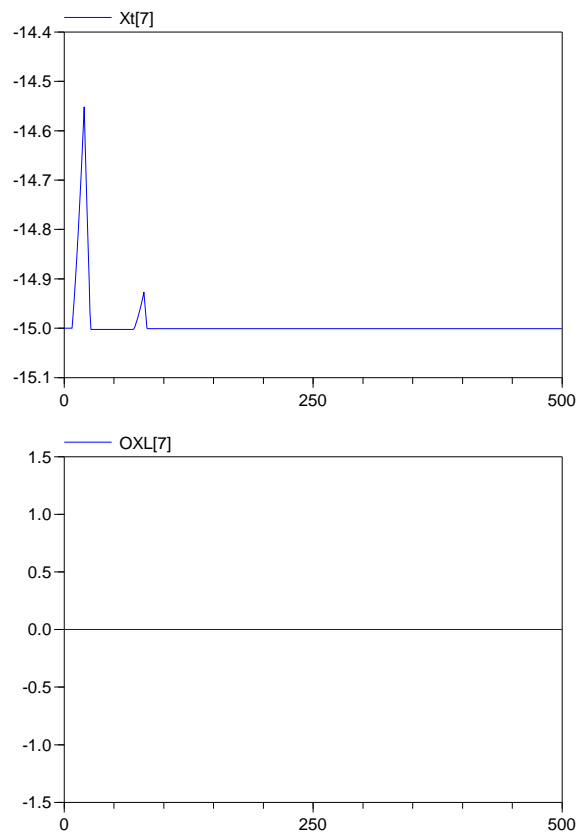


Figure 5.8: Case 1: Inverse-characteristic timer x_t and OXL signal of $g7$

tors g_{13} , g_{14} , g_{15} , g_{16} , and g_{17} at $t = 102.1, 106.8, 139.8, 152.4$ and 215.4 s, respectively, as shown in Fig. 5.10, and final collapse occurs soon after g_{17} becomes limited. The LTCs $Tr405151$ in $Central_3$, $Tr404242$ in $Central_2$, $Tr404747$ in $Central_4$ and $Tr404141$ in $Central_1$ reach their maximum limits at times around $t = 110, 120, 120$ and 130 s.

As explained before, the proposed DCMPC approach combines two concepts of “looking-ahead” in time and “communication” with the neighbors.

We further compare the performance of the DCMPC with the decentralized MPC approach to illustrate what is the contribution of combining communication and anticipation to improved performance. Fig. 5.11 shows the voltage evolution at buses 4046, 4047 and 4043 which, controlled according to decentralized MPC, experience the largest drop, when the local MPCs receive no information from their neighbors, and assume the neighbors will take no control action. The overall system survives until $t = 461$ s, when simulations stop, lasting some 245 s longer than that with decentralized deadband control. This uncoordinated decentralized MPC approach, as shown in Fig. 5.12, leads to the activation of OXLs over three machines; g_{13} , g_{15} and g_{17} at $t = 170, 274$ and 459.8 s, respectively. In comparison to the decentralized deadband control, only one LTC ($Tr404242$) reaches its maximum tap limit, while three other LTCs, namely $Tr404141$, $Tr405151$ and $Tr404747$, have not moved toward reaching their limits, thanks to the local MPC’s anticipation. Furthermore, at $t = 50$ s, the local MPC for $Central_2$ successfully anticipates the moving towards activation of OXL for g_{13} , and therefore freezes the upward tap movements of the local LTC $Tr404242$ for three subsequent steps. However, due to the lack of coordination with the actions of the neighbors, eventually g_{13} becomes limited. Likewise $Central_4$ fails at preventing the activation of OXL over g_{15} .

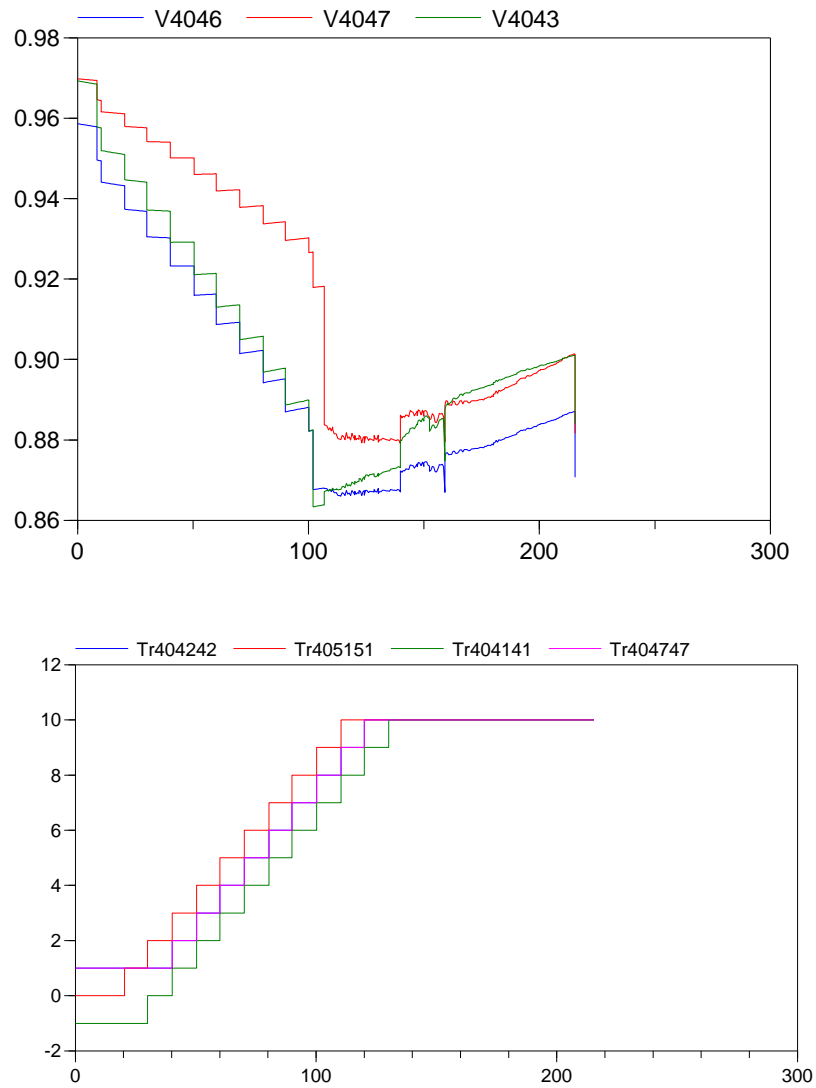


Figure 5.9: Case 1: Bus voltages and uncoordinated deadband LTC moves

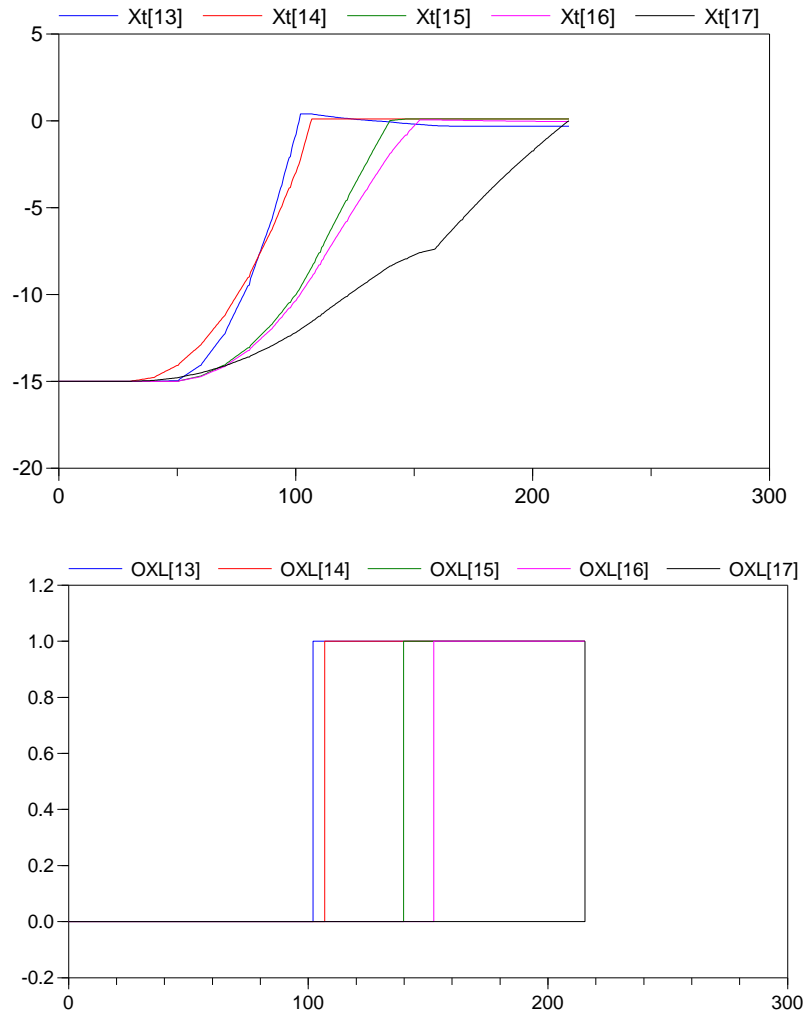


Figure 5.10: Case 1: Timer signals x_t and OXL signals in the deadband control approach

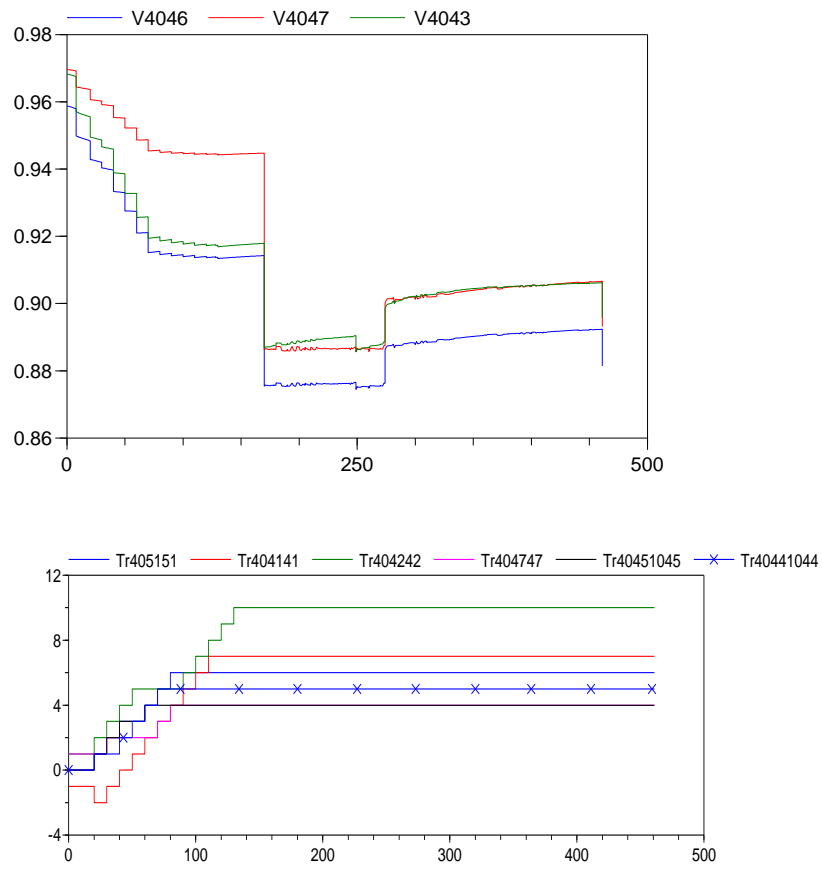


Figure 5.11: Case 1: Bus voltages and uncoordinated LTC moves in the decentralized MPC approach

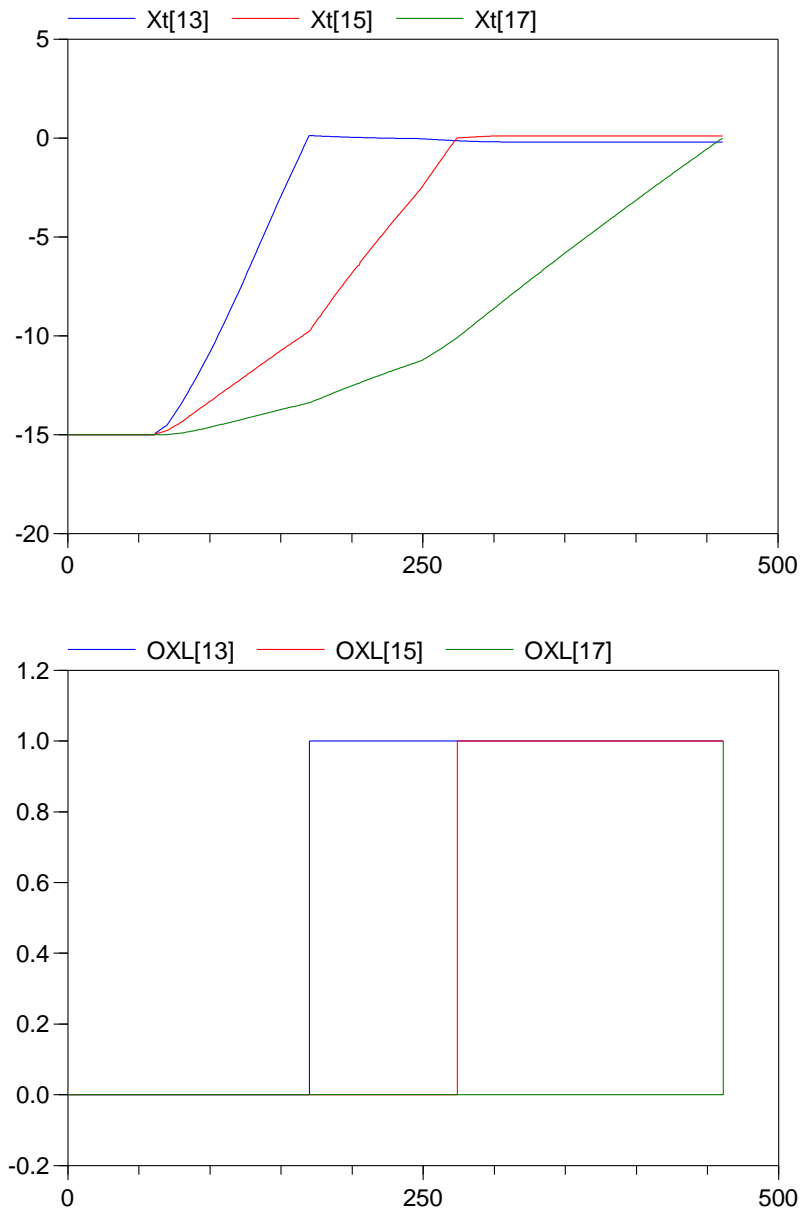


Figure 5.12: Case 1: timer signals x_t and OXL signals in the decentralized MPC approach

5.2.2 Case 2: Outage of Line 4011-4021

Fig. 5.13 shows the voltage evolution at buses 4046, 4047 and 4043, experiencing the largest drop, as well as the uncoordinated deadband operation of LTCs. The maximum tap limits for LTCs $Tr404242$, $Tr404343$, $Tr404747$ and $Tr405151$ are reached either before or after the activation of OXLs over four machines; $g14$, $g13$, $g4$ and $g15$ at $t = 178.1$, 182.7 , 187.3 and 224.2 s, respectively, as shown in Fig. 5.14. This leads to a non-convergent AC power flow at $t = 290.1$ s when the system voltages diverge (collapse) and simulation stops.

The proposed DCMPC algorithm, as shown in Fig. 5.15, looking ahead in time, freezes the uncoordinated upward moves of LTCs. This together with the coordination of the local LTC moves with the neighbors, effectively stabilizes the system voltages, leaving only one generator $g4$ limited at $t = 233.3$ s.

It is of interest to illustrate the response of the system with the decentralized local MPCs exchanging no information. Fig. 5.16 shows the voltage at buses 4046, 4047 and 4043, as well as the decentrally calculated uncoordinated local control actions. The system manages to survive the disturbance until $t = 410$ s, when the numerical integration cannot proceed further, lasting some 120 s longer than under the deadband control of the LTCs. As shown in Fig. 5.17, only three OXLs are activated over machines; $g9$, $g4$ and $g13$ at $t = 95$, 150 and 258 s. This is thanks to the local anticipating feature of the MPCs in solving their own greedy local optimization problem. Note that only one LTC, namely $Tr404242$ in $Central_2$, still reaches its limit at $t = 100$ s, withdrawing voltage support that could relieve the local generator $g13$ of final saturation.

5.2.3 Computational Burden

The hybrid system model is implemented in Modelica [24], a free object-oriented language for modeling complex physical systems, and is simulated using commercial tool Dymola [23]. All component models used for simulations are detailed in chapter 3.

The CPU time required to complete a simulation experiment consists of two distinct terms; the time that the local MPCs take to calculate their optimal control actions at each discrete time instant, plus the time needed to simulate the physical system after applying those calculated control actions in order to obtain the state variables at the end of that control interval. In order to determine whether or not the DCMPC algorithm is suitable for the real-time applications, what matters is the time needed for computing the local control actions for each CA (and not for

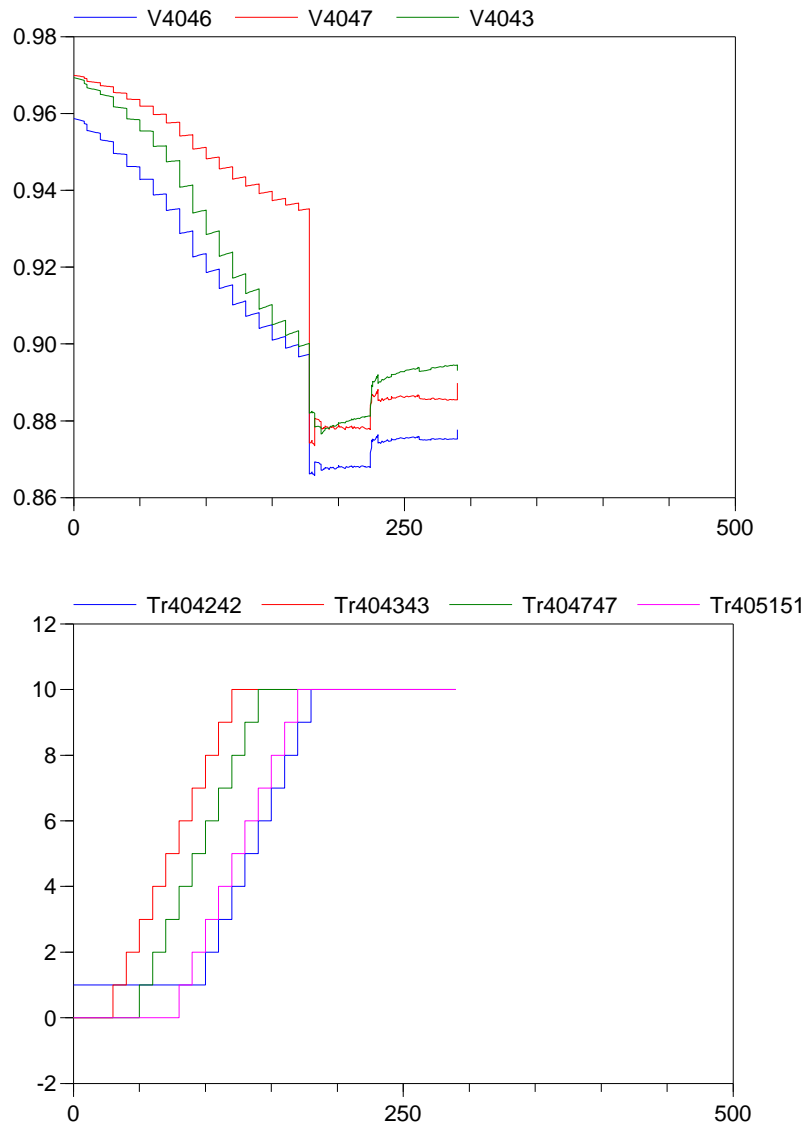


Figure 5.13: Case 2: Bus voltages and uncoordinated deadband LTC moves

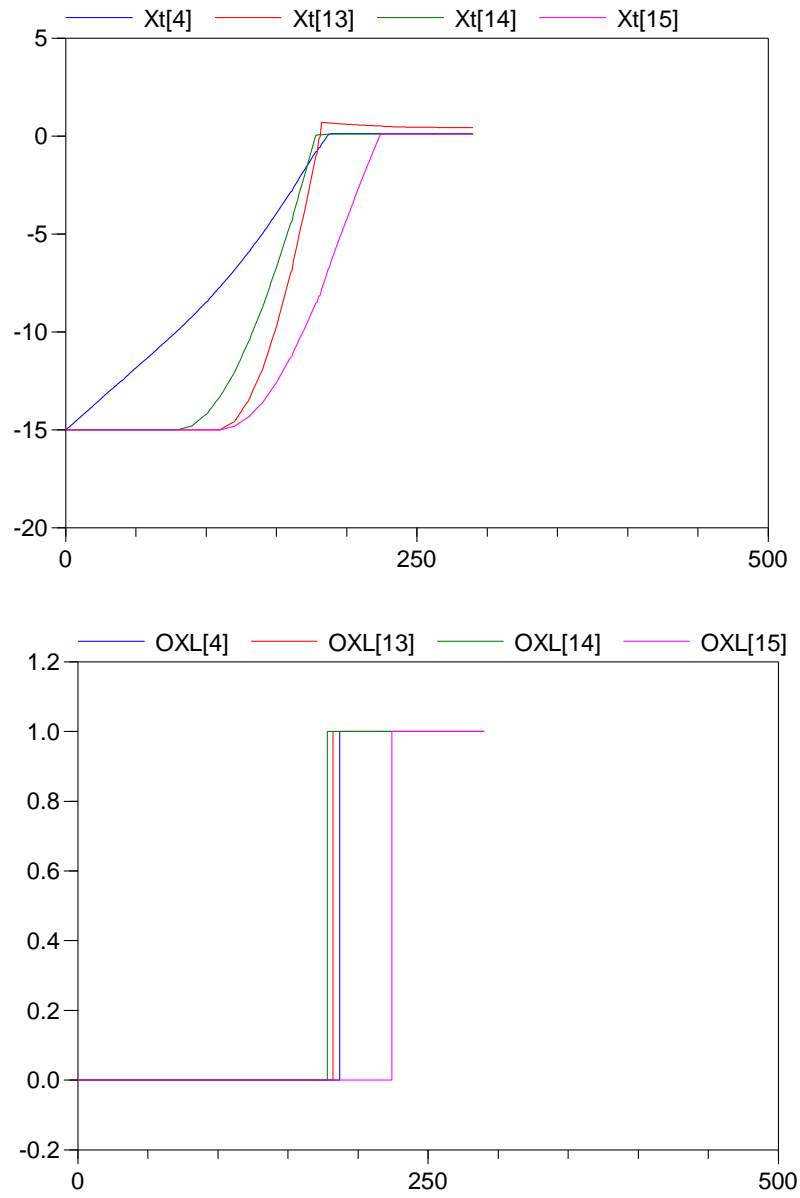


Figure 5.14: Case 2: timer signals x_t and OXL signals in the deadband control approach

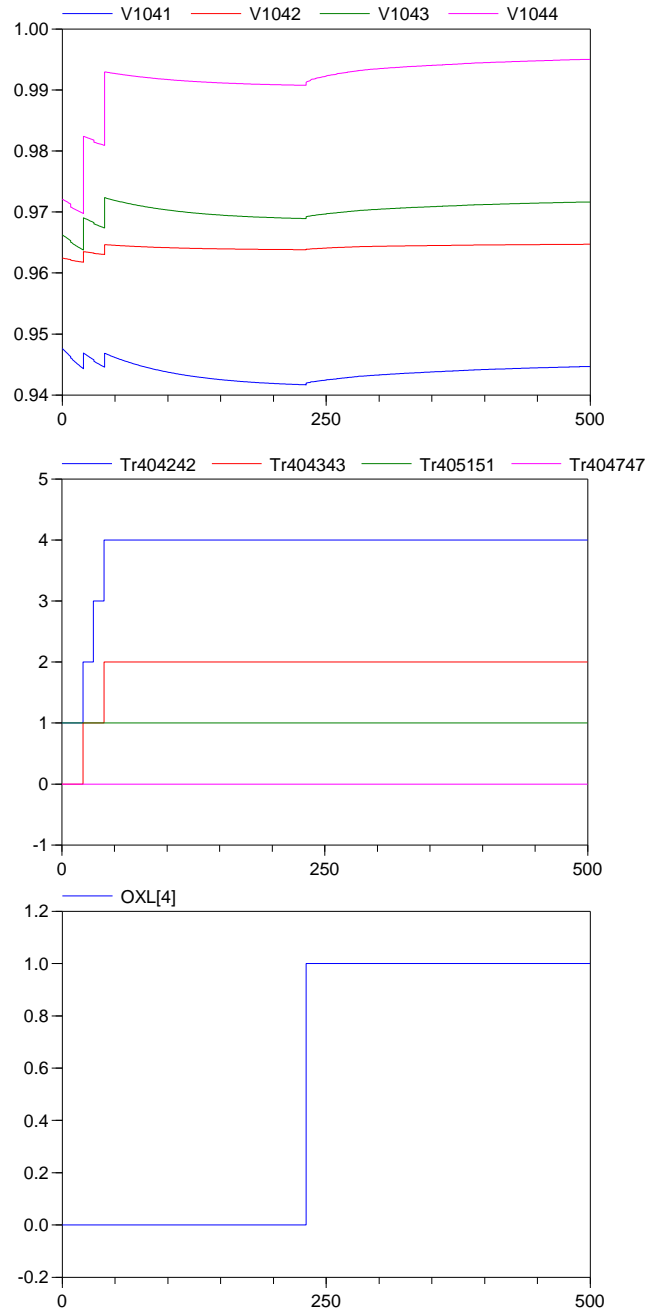


Figure 5.15: Case 2: Bus voltages, coordinated LTC moves, and OXL signals

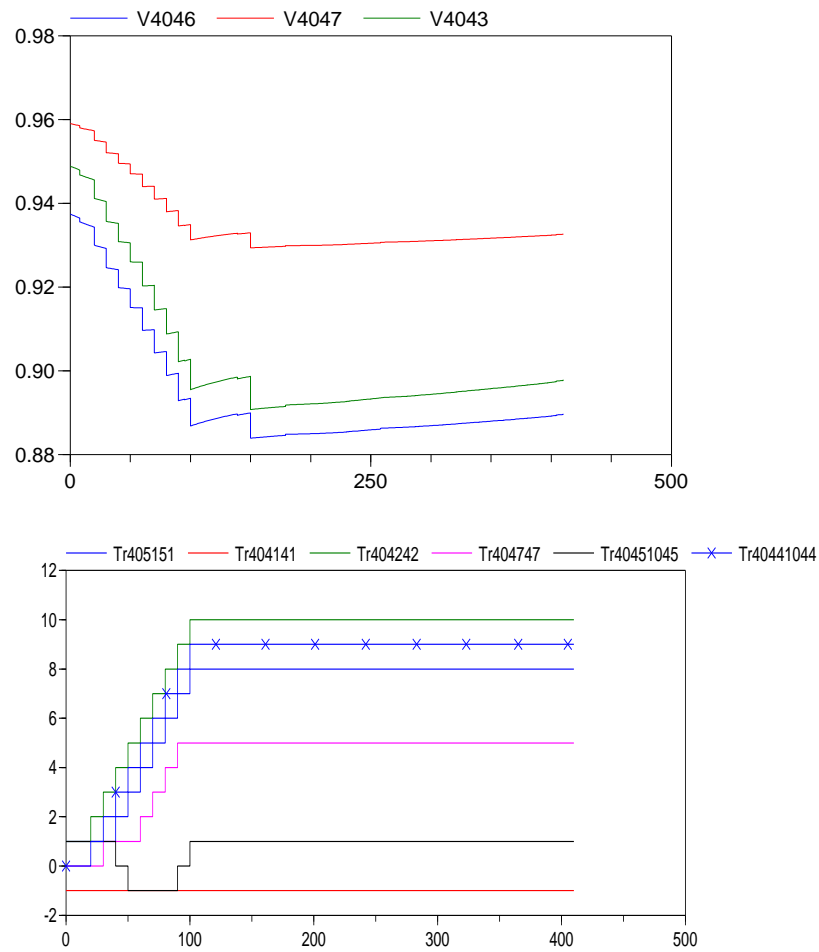


Figure 5.16: Case 2: Bus voltages and uncoordinated LTC moves in the decentralized MPC approach

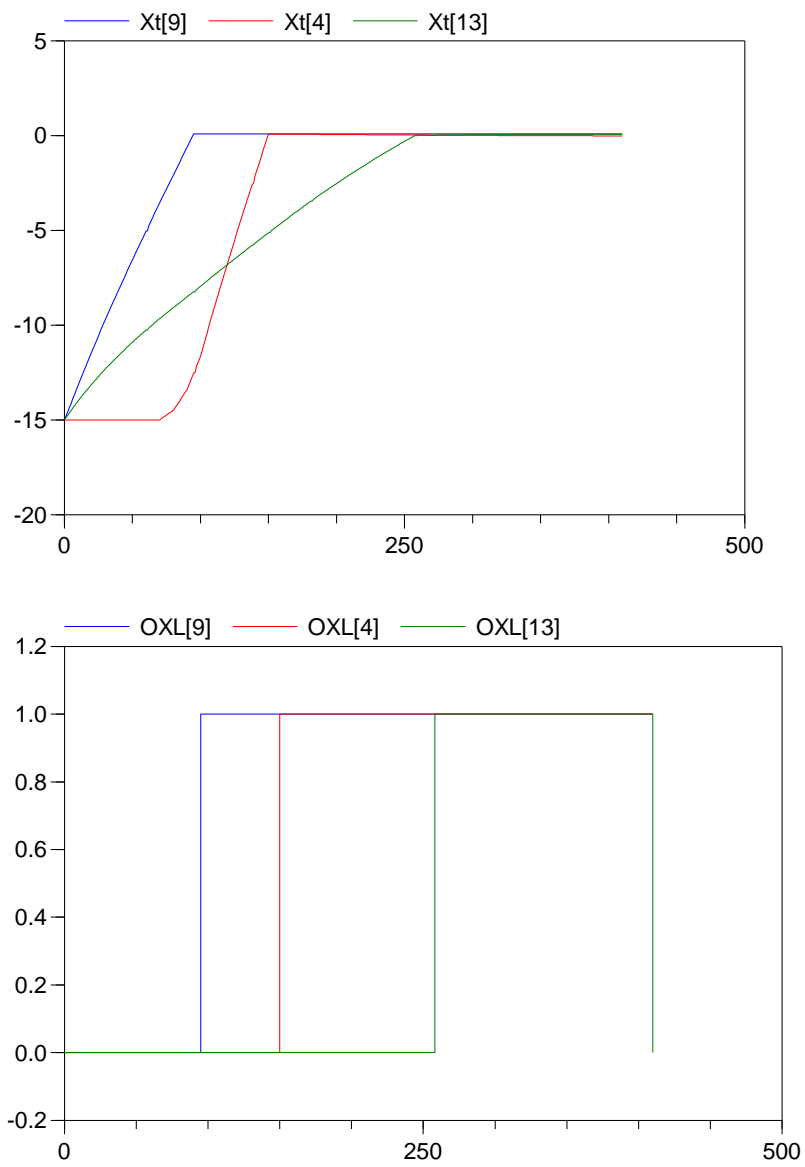


Figure 5.17: Case 2: x_t and OXL signals in the decentralized MPC approach

all CAs), and obviously not for the simulation of the physical system.¹ The local optimization problems are solved sequentially for the existing CAs in this thesis. However in practice in the real-time multi-area power systems, one independent computer is assigned to every CA to find solutions for the local optimization problem. Thus the rule of thumb for the feasibility of the DCMPC for the real-time applications is that every CA must finish computing its own local controls sooner than the duration of time interval for control updates (every $T_c = 10$ s in our simulations). For the test systems considered in this chapter, each CA performs a number of simulation runs, i.e. one simulation run per each possible control sequence, and selects the best sequences in a reasonably short CPU time. For the case study of Nordic32, the slowest agent-wise simulator integration time including local optimization, using a fixed step size solver e.g. Euler, when running on a Windows PC with 3.154 GHz Intel Core 2 Duo CPU and 4 GB of RAM, takes less than 3 s. Taking into account that each CA takes decisions at every 10 s, this ensures that the approach can meet the requirement for on-line voltage control.

5.2.4 Robustness analysis

In the simulations presented so far for the Nordic32 test system, the reduced-order models for the immediate neighboring areas and for the distant areas are assumed to be given for each local area. It was of interest to perform additional experiments to assess the robustness of the DCMPC against modeling errors, and to test the impact of the unmodeled dynamics of the neighbors. To this end, the consumed active power of the LTC-controlled load at bus 4043 in Central₆, the most critical area with the most immediate neighbors containing three LTCs represented by a single equivalent one, is increased by 10% at $t = 0$ s for the simulation of the physical system. However the models used by neighboring CAs (Central₁, Central₂, Central₄ and Central₅) for anticipating the power flows along the transmission lines connecting them to Central₆ are not updated at $t = 0$ s. Fig. 5.18 shows the evolution of voltages at buses under the effect of the same disturbance as in Case 1 (i.e. outage of line 4032 – 4044 at $t = 10$ s, and in addition all other neighbors assuming wrong parameter value for load at bus 4043 in Central₆ at $t = 0$ s). The bus voltages are quite similar to (but lower than) those of base disturbance in Case 1, all stabilized within the limits in long-term. However, in response to initiating (at $t = 0$ s) “disturbance-like” load change in Central₆, the local LTC *Tr40441044* advances its upward tap move (from $t = 20$ s in base disturbance) to $t = 10$ s, continued by another upward tap move at $t = 20$ s in response to the line outage at $t = 10$ s. Furthermore, the neighboring LTC *Tr4047* in Central₄ reacts to the nearby load change by taking a downward tap move at $t = 20$ s, and

¹The computer model of the physical system will be replaced by the physical system itself in real-time no matter how long its simulation takes for the computer.

LTC $Tr4042$ in $Central_2$ changes its (original base disturbance) LTC moves by freezing its upward moves at $t = 30$ s (instead of $t = 40$ s). The other neighbors do not change their LTC moves at all by properly coordinating them with this new set of control actions taken by the CAs in $Central_6$, $Central_4$ and $Central_2$. As shown in Fig. 5.19, the OXL at g_7 does not yet become activated and the triggered x_t signal dies out at $t = 13$ s by the LTC moves taken at $t = 10$ s.

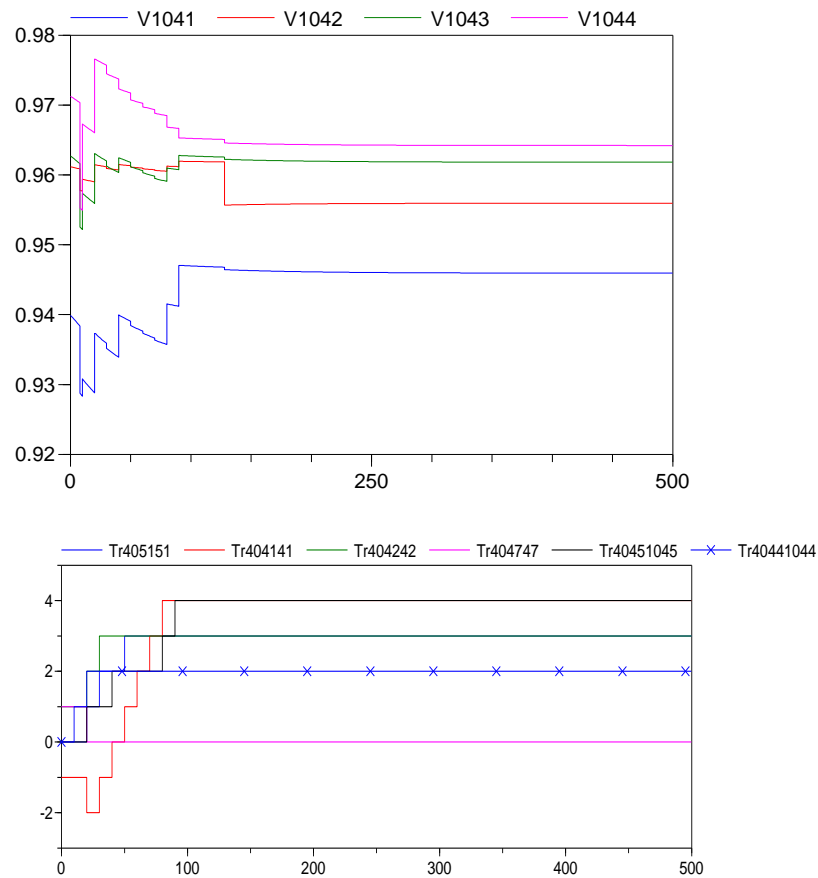


Figure 5.18: Case 1: Bus voltages and coordinated LTC moves, with 10% increase in the load at bus 4043

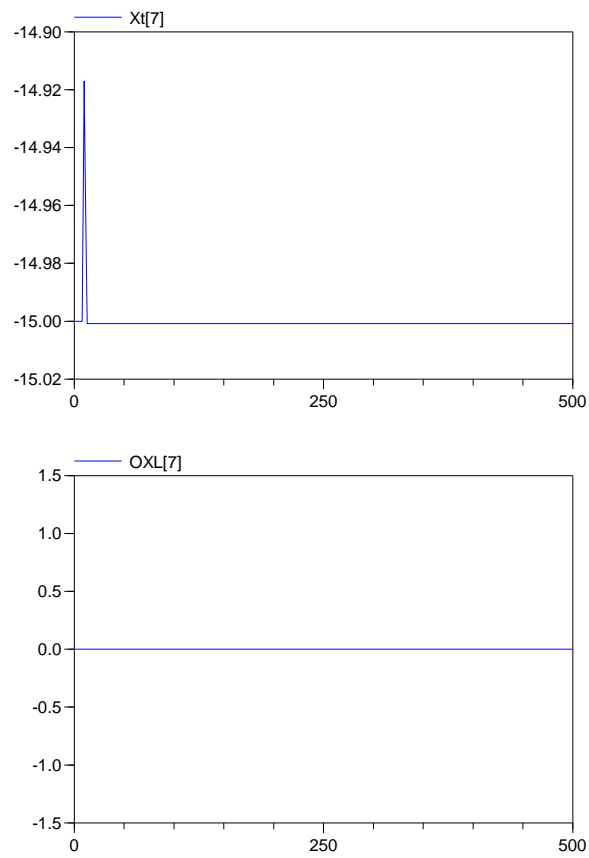


Figure 5.19: Case 1: Timer x_i and OXL signal of g_7 , with 10% increase in the load at bus 4043

5.3 Conclusions

This chapter presents the time-domain simulation results on two well-known test systems, illustrating the improved performance of the multi-area power system when the DCMPC is applied. In the ABB 12-Bus test system, it is assumed that the complete model of the overall system is given to each local CA. while, in the Nordic32 system, the local CAs are only assumed to be given the reduced-order QSS models for immediate neighbors, and a simpler equivalent PV model for the distant areas. In order to identify the distinct contribution of anticipation and communication to improved performance of the DCMPC, further experiments are made to compare the results with the uncoordinated decentralized deadband approach, and also with the uncoordinated decentralized MPC approach. Moreover, the robustness of the DCMPC against measurement noises and modeling errors has been shown, concluding that the feedback behavior of the MPCs provides enough robustness against those errors.

6

Conclusions and future work

Logical controllers of devices such as LTCs and CBs as well as discrete control logics such as threshold reached by OXLs introduce discrete events into power system continuous dynamics. The resulting dynamic behavior often leads to complicated interactions between continuous dynamics and discrete events, particularly during voltage collapse phenomena when many discrete devices (either controllers or thresholds) switch on and off. The ordering of these events is very important for the stability analysis, particularly for voltage control. This has been, in this thesis, modeled using concurrent execution of many hybrid automata.

This thesis presents an efficient framework to capture the hybrid behavior of power system using Modelica as an object-oriented equation-based modeling and simulation language for the different components of the power system. Toward our ultimate goal of designing a model-based coordinating voltage control, the Modelica models for transmission lines, LTC, OXL, CB, and dynamic exponential recovery loads have been presented in the hybrid dynamical systems framework, where all component models are transparent and can easily be modified or extended.

Simulation results show that the interaction between local controllers and continuous dynamics of power system as well as nonlinear behavior of load dynamics can easily be studied in the proposed hybrid framework. This enables effective analysis of different candidate coordinating control actions in order to avoid voltage collapse. The proposed simulator is much-faster-than real-time for reasonably-sized networks, and provides a flexible environment for modeling and simulation of large-scale power systems, and allows (possibly via further abstraction to speed up the on-line calculations) the implementation and fast verification of different

MPC control strategies. For example, for the case study 2 considered in chapter 3, the simulator integration time when running on a 3.15 GHz Intel Core 2 Duo CPU with 4 GB of RAM takes less than 1 s, i.e. about 700 times faster than real time. Initially in chapter 3, the timing of the control actions was obtained by carrying out many simulations. In chapters 4 and 5, this timing of control actions are obtained automatically by an MPC, selecting the best scenarios among a small number of possible scenarios. The fact that these scenarios can be simulated faster than real-time over a sufficiently long time window allows efficient and automatic comparison of their performance.

The main trends in the development of coordination schemes in large-scale multi-area electrical power systems particularly for voltage control problem are also presented in this thesis. The issues of communication, abstraction and optimization, which are highly linked to coordination control, have been briefly addressed in this thesis. By way of summary, the following conclusions can be drawn and must be taken into account when applying distributed model-based coordination schemes to the voltage control problem in large-scale multi-area power systems.

- Distributed cooperative-based coordination schemes fit best the requirements of multi-area large-scale power systems where each TSO (or each CA of an area) optimizes its own utility in a greedy way without taking the cost and constraints of the neighbors into account.
- The inherent feedback structure of the DCMPC provides enough robustness against modeling errors e.g. uncertainties in the load modeling as well as measurement inaccuracies.
- The minimum exchange of information among neighboring TSOs necessary for achieving acceptable coordination includes the local control decisions.
- Time-varying nature of the power system calls for dynamic equivalents whose parameters can be estimated via identification using measurements taken solely at boundary buses of interconnections. In order to obtain an equivalent model for neighboring areas in the multi-area power systems, identification-based approaches are more desirable than reduction-based approaches since they may be utilized with limited amount of information at boundary buses.

This thesis has developed a design methodology for voltage control based on distributed MPC as a tool for coordinating LTCs in adjacent control areas. More specifically, using a non-linear hybrid model of the system, a distributed non-cooperative MPC formulation with neighbor-to-neighbor communication is proposed for long-term voltage control of large-scale multi-area power systems. Each CA knows a local model of its own area as well as reduced-order models of its immediate neighboring CAs, assuming simpler equivalent models for its distant

areas. Local decisions are taken by solving a finite-horizon greedy local optimization, using only local measurements and the latest selected control sequences received from the immediate neighboring CA. The planned local control sequence is then communicated to the immediate neighboring CAs to be taken into account in their next optimization iteration.

The limited amount of exchanged information makes the approach more resilient to communication failures. Furthermore, the fact of not requiring knowledge of the overall system model provides enough robustness against lack of some system information. Via simulation on a reasonably sized 12-bus 3-area power system in chapter 5, the thesis shows that this coordination control can avoid voltage collapse in cases where traditional uncoordinated decentralized controllers fail. This first case study deals with a network that is small enough so that each local simulator knows and implements the hybrid dynamical model of the complete system.

However for realistic applications such as the well-known Nordic32 test system in chapter 5, the local simulator only knows and implement a detailed model of its own CA, and will need to represent the dynamics of the adjacent areas via more abstract models. Simulations on the Nordic32 test system show that, even in this case, the proposed control strategy can stabilize the system for fault scenarios where a completely decentralized strategy (deadband or MPC), without any communications, leads to collapse.

6.1 Future work

6.1.1 Extension of the DCMPC

In this thesis, we have applied the proposed DCMPC scheme to the transmission systems, where the distribution systems are represented as an aggregated dynamic loads connected by LTCs to the rest of the system. The LTCs are considered as the available countermeasure for long-term voltage control. At most one LTC (except area Central_6 containing three LTCs) is considered in each area. A control horizon of 30 s ($N = 3$) is chosen to perform the simulations. Given the LTC operational time delay $T_{\text{delay}} = 10$ s, this 30 s control horizon enables each LTC to perform three subsequent moves either *no move*, an *upward* or a *downward* move. Each MPC, corresponding to each CA, enumerates the number of all possible LTC move sequences, in this case $3^3 = 27$, without excluding those that the designer knows in advance will almost certainly not be optimal. This may be an issue, in terms of computational complexity and simulation time, when the size of the system grows, or when the longer control horizons are considered. Therefore, future research is required to reduce the number of possible input sequences, based on some heuristics and on physical intuition.

In the current implementation, each CA knows a local model of its own area as well as reduced-order QSS models of its immediate neighboring areas, assuming simpler equivalent PV model for the distant areas. However, we have assumed the same reduced-order QSS models for the local area as well as for the immediate neighboring areas. Future works can be devoted to devising abstraction methods to dynamically represent a more abstract model of the neighboring areas. The abstract models should not have the same degree of accuracy and details compared to that of local areas.

This thesis does not consider the power-flow constraints of interconnecting tie-lines. These constraint are due to the thermal limits of tie-lines which can in turn limit the maximum cross-border power interchange among areas. This additional constraint can be also taken into account in the future implementations of the DCMPC.

6.1.2 Application to microgrids

The DCMPC coordination scheme may also be applied as a tool for designing controllers for medium voltage (MV) microgrids (μ -grids) including distributed generations (DGs) and storage devices.

A microgrid is a cluster of local distributed energy resources (DERs) and optionally storage units such as batteries, ultra-capacitors, and flywheels that locally supply controllable (curtailable/sheddable) loads such as plug-in hybrid or electric vehicles (EVs), in a more economic and reliable fashion.

The DERs can be either in the form of non-controllable renewable sources such as wind and solar energy, or dispatchable (controllable) non-renewable sources such as microturbines, combined heat and cooling power (CHCP) units, and fuel cells whose output instantaneous active/reactive powers are controllable for a pre-specified time interval.

Microgrids are typically designed to act as a single controllable entity with respect to the main grid such that it can operate in both grid-connected (on-grid) and islanded (off-grid, autonomous) modes. Microgrids are often viewed as the key building blocks of the future “smart grids”, where information and communications technology (ICT) is used to gather and act on information, for example on the behaviors of DGs, storage devices, and loads, in an automated fashion to improve the efficiency, reliability, economics, and sustainability of the production and distribution of electricity. A typical configuration of a microgrid is shown in Fig. 6.1, where the main grid is connected, at the point of common coupling (PCC), to a microgrid composed of three radial feeders operating as a single controllable entity. Analogous to the proposed concept, a multi-area small-scale power system can be determined, within the microgrid, by considering, for example, each feeder as an area, and assigning a local MPC to it. These decomposed areas, or feeders,

are sometimes referred to as “active cells”. However, there is a fundamental difference between X/R ratio for transmission systems, being $X \gg R$, and distribution networks, being $X \ll R$. This is due to the predominant inductive nature of overhead lines in transmission systems, and resistive nature of (underground) cables in distribution networks. This means that, when considering distribution networks, the voltage can not be effectively controlled through adjusting only reactive power, and it is necessary to adjust active power as well. Therefore voltage control for a smart grid will not only involve LTC controls but also control of storage and of deferrable loads.

Smart grid (several interconnected μ -grids) control in long time scale is an economic dispatch problem which determines the optimal output active/reactive power from DERs to be allocated to various loads and storage devices (including auxiliary energy storage by EVs). The solution ensures the realization of the several objective functions such as minimization of the overall active/reactive power generation cost and/or minimization of active power losses. The extended economic dispatch problem (including the optimal timing for on/off switching of controllable loads, scheduling (postponing/advancing the charge/discharge timing of storage devices even including batteries in EVs, or adjusting the power to heat ratio of CHCP units) can be effectively tackled by the proposed coordination paradigm. In this case, the communication may include the variable import/export electricity pricing among cells, over a prediction horizon in future. The DERs within each cell will contribute to the coordination problem through their power electronic interfaces e.g. voltage source inverter (VSI).

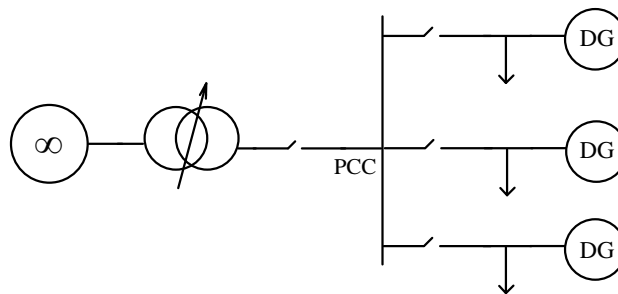


Figure 6.1: A basic microgrid architecture

6.1.3 Towards the practical implementation

The DCMPC approach is a novel communication-based control architecture for LTCs in order to improve the coordination among the corresponding CAs. This

coordinating feedback controller acts in the time scale of 10 s, and thus is suitable for mitigating the long-term voltage decays. This thesis has shown that the DCMPC is a feasible approach to reduce the risk of voltage collapse in a real system by studying some well-known case studies. One should notice that the DCMPC scheme complements (and does not replace) the existing secondary control layer of a generic voltage control hierarchy. It essentially equips each CA with an anticipation feature, and provides an additional feedback coordinating signal among LTCs. This makes the DCMPC approach to be incrementally implementable in practice, meaning that considering ENTSO-E grid for example, the entire 41 TSOs (and their underlying CAs) do not necessarily need to change their current voltage control strategy for LTCs at once. The fact that the DCMPC implementation can, rather, begin from one single TSO, would then make it possible to have a configuration in which a DCMPC-controlled CA might have some neighbors using another strategy, e.g. deadband-controlled neighboring CAs. This will not cause any problem because as long as the DCMPC-controlled CA is informed of, by some limited amount of communication, about the (one-step-ahead) control actions of its (even still possibly deadband-controlled) CAs, it will effectively take this information into account for calculating its own coordinated control actions.

A (potential) improvement for realizing practical applications might be achieved by the asynchronous implementation of the DCMPC. This may possibly provide an even more realistic operation of CAs by allowing them (in general) to update their control actions whenever they want to. However, due to the mechanical time delay of LTCs, the CAs would then still use the same control interval of 10 s, but could start reacting at different times within each 10 s interval.

It is also important to mention that the multi-area power systems are often heterogeneous networks stretching out over many independent TSOs (and their corresponding CAs) in different countries. Thus a possible non-cooperative behavior of some CAs (or even preventing a malicious operator from actually damaging the overall system) must be rewarded enforcing cooperation in practice. However, this thesis does not deal with this issue, assuming that the TSOs adhere to their contract which forces them to cooperate for the proposed DCMPC scheme.



Steady-state voltage characteristic of a synchronous generator

According to [16] in dq framework:

$$V_d = -RI_d - X'_q I_q \quad (\text{A.1})$$

$$V_q = -RI_q - X'_d I_d + E'_q \quad (\text{A.2})$$

Under steady-state conditions $E'_q = E_q$, $X'_d = X_d$ and $X'_q = X_q$, and ignoring armature resistance $R = 0$, one gets:

$$V_d = -X_q I_q \quad (\text{A.3})$$

$$V_q = -X_d I_d + E_q \quad (\text{A.4})$$

Generator output active P and reactive Q powers are given by:

$$P = V_d I_d + V_q I_q \quad (\text{A.5})$$

$$Q = V_d I_q - V_q I_d \quad (\text{A.6})$$

Solving (A.5) and (A.6) with respect to I_d and I_q yields:

$$I_d = \frac{PV_d - QV_q}{V_d^2 + V_q^2} \quad (\text{A.7})$$

$$I_q = \frac{QV_d + PV_q}{V_d^2 + V_q^2} \quad (\text{A.8})$$

Substituting (A.7) and (A.8) in (A.3) and (A.4) gives:

$$V_d = \frac{-QX_q V_d - PX_q V_q}{V_d^2 + V_q^2} \quad (\text{A.9})$$

$$V_q = \frac{PX_d V_d - QX_d V_q}{V_d^2 + V_q^2} + E_q \quad (\text{A.10})$$

Rearranging (A.9) and (A.10) gives:

$$((V_d^2 + V_q^2) + QX_q)V_d + PX_q V_q = 0 \quad (\text{A.11})$$

$$-PX_d V_d + ((V_d^2 + V_q^2) + QX_d)V_q = E_q(V_d^2 + V_q^2) \quad (\text{A.12})$$

Solving systems of Equations (A.11) and (A.12) with respect to V_d and V_q , and substituting the generator terminal voltage with $V = V_d^2 + V_q^2$ yields to:

$$V_d = \frac{-E_q V^2 P X_q}{(V^2 + Q X_q)(V^2 + Q X_d) + P^2 X_d X_q} \quad (\text{A.13})$$

$$V_q = \frac{(V^2 + Q X_q) E_q V^2}{(V^2 + Q X_q)(V^2 + Q X_d) + P^2 X_d X_q} \quad (\text{A.14})$$

Substituting (A.13) and (A.14) in $V^2 = V_d^2 + V_q^2$ gives:

$$V^2 = \frac{E_q^2 V^4 P^2 X_q^2 + V^8 E_q^2 + V^4 Q^2 E_q^2 X_q^2 + 2V^6 E_q^2 Q X_q}{(V^4 + V^2 Q X_d + V^2 Q X_q + Q^2 X_d X_q + P^2 X_d X_q)^2} \quad (\text{A.15})$$

Solving (A.15) with respect to E_q , one gets:

$$E_q^2 = \frac{(V^4 + V^2 Q X_d + V^2 Q X_q + Q^2 X_d X_q + P^2 X_d X_q)^2}{(V^2 P^2 X_q^2 + V^6 + V^2 Q^2 X_q^2 + 2V^4 Q X_q)} \quad (\text{A.16})$$

or

$$E_q = \frac{(V^4 + V^2 Q X_d + V^2 Q X_q + Q^2 X_d X_q + P^2 X_d X_q)}{V \sqrt{P^2 X_q^2 + V^4 + Q^2 X_q^2 + 2V^2 Q X_q}} \quad (\text{A.17})$$

Under steady-state conditions, and in per unit

$$E'_q = E_q = E_f = E_{fd} = i_{fd} \quad (\text{A.18})$$

Therefore

$$E_{fd} = \frac{(V^4 + V^2 Q X_d + V^2 Q X_q + Q^2 X_d X_q + P^2 X_d X_q)}{V \sqrt{V^4 + P^2 X_q^2 + Q^2 X_q^2 + 2V^2 Q X_q}} \quad (\text{A.19})$$

B

An example of Modelica code

The following Modelica code implements an LTC operating in a distributed MPC fashion.

```
model DisLTC

discrete input Integer u "UpDownMove";
Integer TapPos(start=0, fixed=true);
Real c(start=0, fixed=true) "timer";
Boolean idle(start=true, fixed=true);
Boolean action(start=false, fixed=true);
parameter Real T_delay=10;
parameter Real MaxTapPos=10;
parameter Real MinTapPos=-10;
parameter Real TapStepSize=0.02;
output Integer LTCTapPos;
output Real LTCTapRatio;

equation

idle = ((pre(idle) and u=0) or ((pre(action) and c>T_delay);
action = (pre(action) and c<T_delay)) or (pre(idle) and u<>0);
```

```
when idle and not pre(idle) and not initial() then
c=time;
end when;
```

```
when pre(action) and not action then
  if u==+1 and (pre(TapPos) < MaxTapPos) then
    TapPos = pre(TapPos) + 1;
  elseif u== -1 and (pre(TapPos) > MinTapPos) then
    TapPos = pre(TapPos) - 1;
  else
    TapPos = pre(TapPos);
  end if;
end when;
```

```
TrTapPos = TapPos;
LTCTapRatio=1+(TapStepSize* TapPos);
```

```
end DisLTC;
```

Bibliography

- [1] M. Amin, “North American electricity infrastructure: System security, quality, reliability, availability, and efficiency challenges and their societal impacts,” June 2004.
- [2] U.-C. power system outage task force, “Final report on the august 14, 2003 blackout in the United States and Canada: Causes and recommendations,” Apr. 2004.
- [3] P. Kundur, J. Paserba, V. Ajjarapu, G. Andersson, A. Bose, C. Canizares, N. Hatziaargyriou, D. Hill, A. Stankovic, C. Taylor, T. Van Cutsem, and V. Vittal, “Definition and classification of power system stability; IEEE/CIGRE joint task force on stability terms and definitions,” *IEEE Trans. on Power Syst.*, vol. 19, no. 3, pp. 1387 – 1401, Aug. 2004.
- [4] P. Kundur, *Power system stability and control*. McGraw-Hill publishing company, 1994.
- [5] C. W. Taylor, *Power system voltage stability*. McGraw-Hill publishing company, 1994.
- [6] T. Van Cutsem and C. Vournas, *Voltage stability of electric power systems*. Kluwer Academic Publishers, 1998.
- [7] I. A. Hiskens, “Power system modeling for inverse problems,” *IEEE Trans. on Circuits and Systems*, vol. 51, no. 3, pp. 539 – 551, March 2004.
- [8] S. Talukdar, D. Jia, P. Hines, and B. Krogh, “Distributed model predictive control for the mitigation of cascading failures,” in *Proc. of the 44th IEEE Conference on Decision and Control (CDC), and European Control Conference (ECC)*, Dec. 2005, pp. 4440 – 4445.
- [9] S. Chakrabarti, “Notes on power system voltage stability.”
- [10] M. Larsson, D. Hill, and G. Olsson, “Emergency voltage control using search and predictive control,” *International Journal of Electrical Power and Energy Systems*, vol. 24, no. 2, pp. 121–130, 2002.

- [11] H. Wang, "Multi-agent co-ordination for the secondary voltage control in power-system contingencies," *IEE Proceedings-Generation, Transmission and Distribution*, vol. 148, no. 1, pp. 61–66, Jan 2001.
- [12] A. Mehrizi-Sani and R. Iravani, "Potential-function based control of a microgrid in islanded and grid-connected modes," *IEEE Trans. on Power Syst.*, vol. 25, no. 4, pp. 1883–1891, Nov. 2010.
- [13] "Union for the Coordination of Transmission of Electricity (UCTE)," *UCTE Operation Handbook*, 2009.
- [14] O. Mousavi and R. Cherkaoui, "Literature survey on fundamental issues of voltage and reactive power control," 2011.
- [15] G. Morison, B. Gao, and P. Kundur, "Voltage stability analysis using static and dynamic approaches," *IEEE Trans. on Power Syst.*, vol. 8, no. 3, pp. 1159–1171, Aug 1993.
- [16] J. Machowski, J. Bialek, and J. Bumby, *Power system dynamics and stability*. Wiley, 1993.
- [17] Western Electricity Coordinating Council, "Guide to WECC/NERC planning standards I.D: Voltage support and reactive power," Mar. 2006.
- [18] P. Kundur, "Power system stability-overview," in *Power System Dynamics and Stability*, R. G. Farmer, Ed. CRC Press LLC, 2001.
- [19] Y. Mansour, "Voltage stability," in *Power System Dynamics and Stability*, R. G. Farmer, Ed. CRC Press LLC, 2001.
- [20] G. Andersson, P. Donalek, R. Farmer, N. Hatziaargyriou, I. Kamwa, P. Kundur, N. Martins, J. Paserba, P. Pourbeik, J. Sanchez-Gasca, R. Schulz, A. Stankovic, C. Taylor, and V. Vittal, "Causes of the 2003 major grid blackouts in North America and Europe, and recommended means to improve system dynamic performance," *IEEE Trans. on Power Syst.*, vol. 20, no. 4, pp. 1922–1928, Nov. 2005.
- [21] Union for the Co-ordination of Transmission of Electricity (UCTE), "Final report on system disturbance on 4 november 2006," Jan. 2007.
- [22] I. R. Navarro, M. Larsson, and G. Olsson, "Object-oriented modeling and simulation of power systems using Modelica," in *IEEE Power Engineering Society Winter Meeting*, 2000, pp. 790–795.
- [23] Dassault Systèmes AB, "Dymola user manual volume 1." [Online]. Available: <http://www.3ds.com/products/catia/portfolio/dymola>

-
- [24] Modelica association, “Modelica® - A unified object-oriented language for systems modeling.” [Online]. Available: <https://modelica.org/>
- [25] M. Moradzadeh and R. Boel, “A hybrid framework for coordinated voltage control of power systems,” in *Proc. IPEC*, Oct. 2010, pp. 304–309.
- [26] B. Fardanesh, “Future trends in power system control,” *IEEE Computer Applications in Power*, vol. 15, no. 3, pp. 24–31, July 2002.
- [27] G. Hug-Glanzmann and G. Andersson, “Decentralized optimal power flow control for overlapping areas in power systems,” *IEEE Trans. on Power Syst.*, vol. 24, no. 1, pp. 327–336, Feb. 2009.
- [28] P. Hines, J. Apt, and S. Talukdar, “Trends in the history of large blackouts in the United States,” in *Proc. IEEE Power Eng. Soc. General Meeting*, July 2008, pp. 1–8.
- [29] Y. Phulpin, M. Begovic, M. Petit, J.-B. Heyberger, and D. Ernst, “Evaluation of network equivalents for voltage optimization in multi-area power systems,” *IEEE Trans. on Power Syst.*, vol. 24, no. 2, pp. 729–743, May 2009.
- [30] J. M. Maciejowski, *Predictive control with constraints*. Pearson Education POD, 2002.
- [31] M. Larsson and D. Karlsson, “Coordinated system protection scheme against voltage collapse using heuristic search and predictive control,” *IEEE Trans. on Power Syst.*, vol. 18, no. 3, pp. 1001–1006, Aug. 2003.
- [32] J. Wen, Q. Wu, D. Turner, S. Cheng, and J. Fitch, “Optimal coordinated voltage control for power system voltage stability,” *IEEE Trans. on Power Syst.*, vol. 19, no. 2, pp. 1115–1122, May 2004.
- [33] R. R. Negenborn, S. Leirens, B. D. Schutter, and J. Hellendoorn, “Supervisory nonlinear MPC for emergency voltage control using pattern search,” *Control Engineering Practice*, vol. 17, no. 7, pp. 841–848, 2009.
- [34] A. N. Venkat, I. A. Hiskens, J. B. Rawlings, and S. J. Wright, “Distributed MPC strategies with application to power system automatic generation control,” *IEEE transactions on control systems technology*, vol. 16, no. 6, pp. 1192–1206, Nov. 2008.
- [35] A. Beccuti, T. Demiray, G. Andersson, and M. Morari, “A lagrangian decomposition algorithm for optimal emergency voltage control,” *IEEE Trans. on Power Syst.*, vol. 25, no. 4, pp. 1769–1779, Nov. 2010.

- [36] M. Glavic, M. Hajian, W. Rosehart, and T. Van Cutsem, "Receding-horizon multi-step optimization to correct nonviable or unstable transmission voltages," *IEEE Trans. on Power Syst.*, vol. 26, no. 3, pp. 1641–1650, Aug. 2011.
- [37] T. Mohamed, H. Bevrani, A. Hassan, and T. Hiyama, "Decentralized model predictive based load frequency control in an interconnected power system," *Energy Conversion and Management*, vol. 52, pp. 1208–1214, Feb. 2011.
- [38] R. M. Hermans, M. Lazar, A. Jokić, and P. van den Bosch, "Almost decentralized model predictive control of power networks," in *Proc. MELECON 2010*, Apr. 2010, pp. 1551–1556.
- [39] M. Moradzadeh, R. Boel, and L. Vandeveld, "Voltage coordination in multi-area power systems via distributed model predictive control," *IEEE Trans. on Power Syst.*, vol. PP, no. 99, pp. 1–9, 2012.
- [40] M. Moradzadeh, L. Bhojwani, and R. Boel, "Coordinated voltage control via distributed model predictive control," in *Proc. CCDC*, May 2011, pp. 1612–1618.
- [41] F. Milano, *Power system modelling and scripting*. Springer, 2010.
- [42] G. Andersson, *Modelling and analysis of electric power systems*. ITET ETH Zürich, 2008.
- [43] P. E. Wellstead, *Introduction to physical system modelling*. Control systems principles, 2000.
- [44] P. Fritzson, "Modelica tutorial - Introduction to object-oriented modeling and simulation with OpenModelica," 2006.
- [45] A. G. Beccuti, T. Geyer, and M. Morari, "A hybrid system approach to power systems voltage control," in *Proc. of the 44th IEEE Conference on Decision and Control (CDC), and European Control Conference (ECC)*, Dec. 2005, pp. 6774 – 6779.
- [46] S. Leirens, J. Buisson, P. Bastard, and J.-L. Coullon, "A hybrid approach for voltage stability of power systems," in *Proc. of the 15th Power Systems Computation Conference*, 2005.
- [47] A. van der Schaft and H. Schumacher, *Introduction to hybrid dynamical systems*. Springer, 1999.
- [48] T. Pulecchi and F. Casella, "Hyaulib: Modelling hybrid automata in Modelica," in *Proc. of the 6th International Modelica Conference*, Mar. 2008, pp. 239–246.

- [49] M. Shimomura, Y. Xia, M. Wakabayashi, and J. Paserba, "A new advanced over excitation limiter for enhancing the voltage stability of power systems," in *Proc. IEEE Power Engineering Society Winter Meeting*, Jan 2001, pp. 221–227.
- [50] T. V. Cutsem, M.-E. Grenier, and D. Lefebvre, "Combined detailed and quasi steady-state time simulations for large-disturbance analysis," *International Journal of Electrical Power & Energy Systems*, vol. 28, no. 9, pp. 634–642, 2006.
- [51] F. Capitanescu, B. Otomega, H. Lefebvre, V. Sermanson, and T. Van Cutsem, "Decentralized tap changer blocking and load shedding against voltage instability: Prospective tests on the RTE system," *International Journal of Electrical Power & Energy Systems*, vol. 31, no. 9, pp. 570–576, Oct. 2009.
- [52] B. Otomega, V. Sermanson, and T. Van Cutsem, "Reverse-logic control of load tap changers in emergency voltage conditions," in *Proc. IEEE Bologna Power Tech Conference*, June 2003.
- [53] M. Larsson and D. Karlsson, "Coordinated control of cascaded tap changers in a radial distribution network," in *Proc. IEEE Stockholm Power Tech Conference*, June 1995, pp. 686–691.
- [54] D. Karlsson and D. Hill, "Modelling and identification of nonlinear dynamic loads in power systems," *IEEE Trans. on Power Syst.*, vol. 9, no. 1, pp. 157–166, Feb. 1994.
- [55] IEEE Task Force on load representation for dynamic performance, "Standard load models for power flow and dynamic performance simulation," *IEEE Trans. on Power Syst.*, vol. 10, no. 3, pp. 1302–1313, Aug. 1995.
- [56] W. Xu and Y. Mansour, "Voltage stability analysis using generic dynamic load models," *IEEE Trans. on Power Syst.*, vol. 9, no. 1, pp. 479–493, Feb. 1994.
- [57] D. J. Hill, "Nonlinear dynamic load models with recovery for voltage stability studies," *IEEE Trans. on Power Syst.*, vol. 8, no. 1, pp. 166–176, Feb. 1993.
- [58] J. Shan, U. D. Annakkage, and A. M. Gole, "A platform for validation of facts models," *IEEE Trans. on Power Delivery*, vol. 21, no. 1, pp. 484–491, Jan. 2006.
- [59] M. Larsson, "The ABB power transmission test case," Feb. 2002.

- [60] M. Larsson, "The ABB medium scale power transmission test case," Feb. 2004.
- [61] A. M. Azmy, "Optimal power flow to manage voltage profiles in interconnected networks using expert systems," *IEEE Trans. on Power Syst.*, vol. 22, no. 4, pp. 1622–1628, Nov. 2007.
- [62] Y. Phulpin, M. Begovic, and D. Ernst, "Coordination of voltage control in a power system operated by multiple transmission utilities," in *IREP Symposium-Bulk Power System Dynamics and Control*, Aug. 2010, pp. 1–8.
- [63] Y. Phulpin, M. Begovic, M. Petit, and D. Ernst, "A fair method for centralized optimization of multi-TSO power systems," *International Journal of Electrical Power & Energy Systems*, vol. 31, pp. 482–488, Oct. 2009.
- [64] H. Seyedi and M. Sanaye-Pasand, "New centralised adaptive load-shedding algorithms to mitigate power system blackouts," *IET Generation, Transmission & Distribution*, vol. 3, no. 1, pp. 99–114, Jan. 2009.
- [65] N. Nimpitiwan and C. Chaiyabut, "Centralized control of system voltage/reactive power using genetic algorithm," in *Proc. International Conference on Intelligent Systems Applications to Power Systems*, Nov. 2007, pp. 1–6.
- [66] W. R. Wagner, A. Keyhani, S. Hao, and T. C. Wong, "A rule-based approach to decentralized voltage control," *IEEE Trans. on Power Syst.*, vol. 5, no. 2, pp. 643–651, May 1990.
- [67] F. A. Okou, O. Akhrif, and L.-A. Dessaint, "A novel modelling approach for decentralized voltage and speed control of multi-machine power systems," *International Journal of Control*, vol. 76, no. 8, pp. 845–857, 2003.
- [68] N. Iwase, K. Okada, K. Yasuda, and R. Yokoyama, "Decentralized voltage control in multiarea power system," *Electrical Engineering in Japan*, vol. 113, no. 1, pp. 43–51, 1993.
- [69] B. Tyagi and S. C. Srivastava, "A decentralized automatic generation control scheme for competitive electricity markets," *IEEE Trans. on Power Syst.*, vol. 21, no. 1, pp. 312–320, Feb. 2006.
- [70] A. N. Venkat, I. A. Hiskens, J. B. Rawlings, and S. J. Wright, "Distributed output feedback MPC for power system control," in *Proc. of the 45th IEEE Conference on Decision and Control*, Dec. 2006, pp. 4038–4045.
- [71] E. Camponogara, D. Jia, B. Krogh, and S. Talukdar, "Distributed model predictive control," *IEEE Control Systems*, vol. 22, no. 1, pp. 44–52, Feb. 2002.

- [72] R. Scattolini, "Architectures for distributed and hierarchical model predictive control - A review," *Journal of Process Control*, vol. 19, no. 5, pp. 723 – 731, 2009.
- [73] S. Mitter and A. Sahai, "Information and control: Witsenhausen revisited," *Learning, control and hybrid systems*, pp. 281–293, 1999.
- [74] M. Zima, M. Larsson, P. Korba, C. Rehtanz, and G. Andersson, "Design aspects for wide-area monitoring and control systems," *Proceedings of the IEEE*, vol. 93, no. 5, pp. 980 –996, May 2005.
- [75] J. De La Ree, V. Centeno, J. Thorp, and A. Phadke, "Synchronized phasor measurement applications in power systems," *IEEE Trans. on Smart Grid*, vol. 1, no. 1, pp. 20 –27, June 2010.
- [76] J. B. Ward, "Equivalent circuits for power-flow studies," *Transactions of the American Institute of Electrical Engineers*, vol. 68, no. 1, pp. 373 –382, July 1949.
- [77] P. Dimeo, *Nodal Analysis of Power Systems*. Taylor & Francis, 1975.
- [78] A. M. Azmy and I. Erlich, "Identification of dynamic equivalents for distribution power networks using recurrent ANNs," in *Proc. IEEE PES Power Systems Conference and Exposition*, Oct. 2004, pp. 348–353.
- [79] T. Singhavilai, O. Anaya-Lara, and K. Lo, "Identification of the dynamic equivalent of a power system," in *Proc. of the 44th International Universities Power Engineering Conference (UPEC)*, Sept. 2009, pp. 1–5.
- [80] J. M. Undrill and A. E. Turner, "Construction of power system electromechanical equivalents by modal analysis," *IEEE Trans. on Power Apparatus and Systems*, no. 90, pp. 2049–2059, 1971.
- [81] J. M. R. Arredondo and R. G. Valle, "An optimal power system model order reduction technique," *International Journal of Electrical Power & Energy Systems*, vol. 26, no. 7, pp. 493 – 500, 2004.
- [82] R. Podmore, "Identification of coherent generators for dynamic equivalents," *IEEE Trans. on Power Apparatus and Systems*, vol. PAS-97, no. 4, pp. 1344 –1354, July 1978.
- [83] F. Wu and N. Narasimhamurthi, "Coherency identification for power system dynamic equivalents," *IEEE Trans. on Circuits and Systems*, vol. 30, no. 3, pp. 140 – 147, Mar. 1983.

- [84] A. M. Stankovic, A. T. Saric, and M. Milosevic, "Identification of nonparametric dynamic power system equivalents with artificial neural networks," *IEEE Trans. on Power Syst.*, vol. 18, no. 4, pp. 1478 – 1486, Nov. 2003.
- [85] CIGRE Task Force 38.02.08, "Long-term dynamics-phase II," 1995.
- [86] S. Karkkainen and E. Lakervi, "Liberalisation of electricity market in Finland as a part of Nordic market," *IEE Proceedings- Generation, Transmission and Distribution*, vol. 148, no. 2, pp. 194–199, Mar. 2001.